
**The *Arabidopsis elch* mutant reveals functions of an ESCRT
component in cytokinesis**

Inaugural-Dissertation

Zur

Erlangung des Doktorgrades

der Mathematisch-Naturwissenschaftlichen Fakultät

der Universität zu Köln

vorgelegt von

Christoph Spitzer

aus Lünen

2007

Berichterstatter: Prof. Dr. Martin Hülskamp

Priv. Doz. Dr. Thomas Klein

Prüfungsvorsitzende: Prof. Dr. Maria Leptin

Tag der mündlichen Prüfung: 10. Januar 2007

DANKSAGUNG

Ich möchte mich bei Prof. Martin Hülskamp für die Freiheit und Unabhängigkeit bedanken, die es mir ermöglicht hat mit viel Spaß am Elch Projekt zu arbeiten.

Norman Zielke hat ein riesiges Danke verdient für sein Interesse an meiner Arbeit, seinen Ideen und viel Unterstützung. Ulli Herrmann hat durch seine Freundschaft und Hilfe in den letzten Jahren sehr dazu beigetragen, dass die Arbeit in Lehrstuhl III Spaß gemacht hat.

Vielen Dank an Norman, Moola, Ulli, Iris, Klaus, Cordula, Kenneth, Dierk und Marcel, die das schlimmste beim Niederschreiben verhindert haben. Ihr habt Struktur und Wissenschaft eingebaut, Unsinn und peinliche Schnitzer vertrieben. Besonders die letzten drei haben sich sehr reingehängt – Danke!

Viktor war eine grosse Hilfe im Umgang mit Pflanzen und hat mir viel beigebracht – Danke.

Katja, Birgit und Irene haben beide Augen zuge drückt wenn ich wieder einmal zwischen 25 und 75% des kleinen Büros blockierte und mich nett in meine Ecke verwiesen. Die ruhige Arbeitsatmosphäre wurde ab und zu durch unser Geschnatter aufgelockert – eine prima Mischung die ich vermissen werde.

Lange dachte ich meine kurze Schulzeit in London ließe sich nicht toppen. Das schöne Köln konnte das Gegenteil zeigen- Vieles werde ich vermissen: die Zeit mit Ulli, Norman, Stephan und Philipp in immer neuen locations, beim Bier in Kneipen und am Rhein und und und...

Mein besonderer Dank gilt meiner Familie für ihre immerstetige Hilfe, meinen Eltern, die mir eine Ausbildung ermöglicht haben und mein Interesse für Tiere und Pflanzen geweckt haben. Meinem Vater möchte ich herzlich danken, dass er mein Studium, welches nicht immer gradlinig verlief, bedingungslos unterstützt hat. Vielen, vielen Dank!

Table of contents

Abstract

Publications

Figure/table index

Abbreviations and gene names

A. Introduction	1
A 1. The secretory system.....	1
A 2. The ESCRT pathway.....	2
A 3. The vacuolar ATPase.....	4
A 4. Cytokinesis in plants.....	6
A 5. The <i>Arabidopsis elch</i> mutant.....	9
Aim.....	11
B. Results	12
B 1. The <i>elch</i> cluster consists of a single cell with multiple stems.....	13
B 2. The <i>elch</i> mutant develops nuclear abnormalities in epidermal tissue.....	15
B 2.1. Multinucleated trichomes form clusters.....	15
B 2.2. Multinucleated pavement cells display cytokinesis defects at low frequency.....	15
B 2.3. Stomata in <i>elch</i> develop cluster and cytokinesis defects at low frequency.....	15
B 2.4. DNA content is not altered in multinucleated trichomes.....	19
B 3. Molecular analysis of the <i>ELCH</i> gene.....	20
B 3.1. <i>ELCH</i> encodes an UEV domain containing protein.....	21
B 3.2. The <i>elch</i> mutant is rescued by a <i>CaMV 35S::ELCH-HA</i> construct.....	23
B 4. Biochemical analysis of ELCH.....	25
B 4.1. ELCH-HA protein binds to Ubiquitin <i>in vitro</i>	25
B 4.2. ELCH-HA protein binds ubiquitinated proteins <i>in vivo</i>	25
B 4.3. ELCH-HA protein is part of a high molecular weight complex.....	27
B 5. ESCRT-I interacting proteins in <i>Arabidopsis</i>	29
B 5.1. <i>Arabidopsis</i> ESCRT-I complex is associated with a UBA domain protein.....	29
B 5.2. Subunits of V-ATPase coimmunoprecipitate with ESCRT-I complex.....	30
B 5.3. VHA-a3-GFP of the V0 subcomplex is ubiquitinated.....	33
B 6. The <i>ELCH</i> pathway and microtubule dependent processes are closely linked.....	34
B 6.1. Genetic interaction of <i>ELCH</i> and <i>Tubulin-Folding Cofactor A</i>	35

B 6.2. The <i>elch</i> mutant is hypersensitive to taxol.....	37
B6.3. Microtubule organization of <i>elch</i> trichomes and dividing cells is not visibly altered.....	38
C. Discussion.....	41
C 1. A defect in the <i>ELCH</i> gene disrupts cytokinesis.....	41
C 2. The ELCH pathway and microtubule dependent processes are linked.....	44
C 3. The ESCRT-I complex in <i>Arabidopsis</i>	45
C 4. The ESCRT pathway in plants.....	47
C 5. Relevance of the putative targets and ELCH/ESCRT-I interacting proteins.....	48
C 6. Vacuolar ATPase- and ESCRT functions overlap to considerable extent.....	49
C 7. Putative requirement for ESCRT function during cytokinesis.....	53
C 8. Putative requirement for V-ATPase function during cytokinesis.....	53
Outlook.....	55
D. Material and Methods.....	56
D 1. Chemicals.....	56
D 2. Material.....	56
D 2.1. Enzymes for DNA manipulation.....	56
D 2.2. Primers.....	56
D 2.3. Vectors.....	56
D 2.4. Antibiotics.....	56
D 2.5. Bacterial strains.....	57
D 2.6. Plant lines.....	57
D 2.7. Biochemicals.....	58
D 2.8. Antibodies.....	58
D 2.9. Accession numbers.....	58
D 3. Methods.....	59
D 3.1. Maintenance and cultivation of <i>Arabidopsis thaliana</i>	59
D 3.2. Crossing of <i>Arabidopsis thaliana</i>	59
D 3.3. Microscopy and cell biology.....	60
D 3.4. Nuclear DNA measurements.....	60
D 3.5. Basic DNA manipulation techniques.....	60

D 3.6. Polymerase chain reaction conditions.....	61
D 3.7. Constructs.....	62
D 3.8. Blunt-end ligation.....	62
D 3.9. Transformation of <i>Agrobacterium tumefaciens</i>	63
D 3.10.Plant transformation.....	63
D 3.11.Isolation of genomic DNA from <i>Arabidopsis</i>	63
D 3.12.Isolation of RNA from plants.....	64
D 3.13.Reverse transcription.....	64
D 3.14.Semiquantitative RT-PCR.....	64
D 3.15.Basic protein techniques (SDS-PAGE, Western blotting).....	65
D 3.16.Denaturing protein extraction.....	65
D 3.17.Native protein extraction.....	65
D 3.18.Ubiquitin binding assay.....	66
D 3.19.Size exclusion chromatography (gel filtration).....	66
D 3.20.Immunoprecipitation.....	66
D 3.21.Antibody detection.....	66
D 3.22.Silverstaining.....	67
D 3.23.Two colour western analysis.....	67
D 3.24.Image processing.....	68
D 3.25.Sequence analysis.....	68
E. Appendix.....	69
E 1. TSG101 has a size of 49 kDa on PAGE.....	69
E 2. SC8017 anti-Ubiquitin is specific for ubiquitin.....	71
E 3. Mass spectrometry data of ESCRT components.....	72
E 4. Mass spectrometry data of ELCH/ESCRT-I interacting proteins.....	81
E 5. Mass spectrometry data of VHA-a3-GFP interacting proteins.....	91
E 6. Number of <i>T-DNA</i> insertions in the used <i>elch</i> mutant line.....	92
F. Literature.....	93
Zusammenfassung.....	
Erklärung.....	
Lebenslauf.....	

Abstract

The Endosomal Sorting Complex Required for Transport (ESCRT) regulates important functions in the secretory system of yeast and animals. The main responsibilities that have been described so far are sorting of biosynthetic cargo and receptor-downregulation. The scope of my PhD thesis was the analysis of the *Arabidopsis* ELCH protein that is similar to Vps23p and TSG101. These proteins represent the core components of ESCRT I complex in yeast and animals. I could show that ubiquitin binding and complex formation is conserved between *Arabidopsis*, yeast and animals, supporting the idea that ESCRT mediated protein sorting is a general strategy in eukaryotic organisms. New ELCH/ESCRT-I interacting proteins were isolated by immunoprecipitation and subsequent mass spectrometry. By this approach a plant specific protein containing a Ubiquitin Associated (UBA) domain and several subunits of the vacuolar (H⁺)-ATPase were identified. The VHA-a3 subunit of the vacuolar (H⁺)-ATPase was analysed in more detail for ubiquitin modifications because mono-ubiquitination constitutes the sorting signal for the ESCRT pathway. Two colour western analysis showed that VHA-a3 is mono-ubiquitinated indicating that VHA-a3 might be a target of ELCH/ESCRT-I. Similar to the ESCRT pathway the V-ATPase is involved in the sorting of biosynthetic cargo and receptor-downregulation in yeast. No interaction between the ESCRT pathway and the V-ATPase has been reported so far.

A T-DNA mutation in the *ELCH* gene of *Arabidopsis* results in multiple nuclei in a minority of epidermal cells. As multinucleated cells can be an indication for a cell division defect, trichomes, pavement cells and stomata were examined in respect to incomplete cell walls. Cell wall stubs were observed in pavement cells and stomata but not in trichomes. Similar defects have not been observed in yeast *vps23* but the multinucleated phenotype of *elch* resembles the phenotype observed in *TSG101* mutant cell lines. Furthermore cytokinesis defects are reported in *Arabidopsis* mutants lacking the VHA-E subunit of the V-ATPase. Plants mutant for *VHA-E* are embryonic lethal and display incomplete cell walls, multiple nuclei and aberrant vacuoles (Strompen et al., 2005). Although mutations in *ELCH*, *TSG101* and *VHA-E* cause a similar phenotype only vague ideas exist why compromising the ESCRT pathway or the V-ATPase lead to cell division defects. A cue was provided by genetic analysis, which suggests that ELCH influences cell division by regulating microtubules. This is apparent because a double mutant with *tubulin-folding cofactor a* (*tfc-a*) shows a strong synergistic phenotype. Cell wall development during plant cell division depends heavily on a plant specific structure, the phragmoplast. The secretory system and microtubules are the

main components of the phragmoplast. Therefore it seems reasonable to assume that subtle protein sorting defects, mislocalization of membranes or misregulation of microtubules can lead to the observed cell division defect.

Publications:

The *Arabidopsis elch* mutant reveals functions of an ESCRT component in cytokinesis

Christoph Spitzer, Swen Schellmann, Aneta Sabovljevic, Mojgan Shahriari, Channa Keshavaiah, Nicole Bechtold, Michel Herzog, Stefan Müller, Franz-Georg Hanisch, and Martin Hülskamp
Development 2006 **133**: 4679-4689.

First authorship: In this study I did the rescue experiments, the genetic analysis and the protein work including design and cloning of the corresponding constructs. For the phenotypic characterisation of *elch* and the double mutants I performed the statistics, DNA measurements, DAPI stainings and the corresponding microscopy, except the cell culture experiments. I also did part of the RT-PCRs and created the figures of the specified experiments.

Figure/table index

Figure A 1: Overview of the cellular endomembrane system.

Figure A 2: Overview of ESCRT dependent protein sorting.

Figure A 3: Structure and functions of the vacuolar ATPase.

Figure A 4: Cell division in plants.

Figure A 5: Modell of plant cytokinesis.

Figure A 6: Trichome cluster phenotype of the *Arabidopsis elch* mutant.

Figure A 7: Cloning of the *ELCH* gene.

Figure B 1: Trichome clusters consist of a single cell with multiple stems emerging from a single cell.

Figure B 2: Nuclear phenotype of *elch* in comparison to *wild type* in different epidermal cell types.

Figure B 3 A: Class I/II/III stomata cluster constitute a phenotypic series.

Figure B 3 B: *elch* stomata clusters are similar to *tmm2* clusters.

Figure B 4: DNA content of single nuclei in *wild type*, *elch* trichomes and multinucleated *elch* clusters is not changed.

Figure B 5: Sequence alignment of UEV domain containing proteins that are similar to ELCH.

Figure B 6: Expression analysis of *ELCH*.

Figure B 7: ELCH-HA binds Ubiquitin *in vitro*.

Figure B 8: ELCH-HA binds ubiquitinated proteins *in vivo*.

Figure B 9: ELCH is part of a high molecular weight complex.

Figure B 10: UBA domain protein At5g53330 coimmunoprecipitates with ELCH-HA.

Figure B 11: Subunits of the V-ATPase coimmunoprecipitate with ELCH-HA.

Figure B 12: VHA-a3 is modified with Ubiquitin.

Figure B 14: The *elch* mutant is hypersensitive to paclitaxel (Taxol).

Figure B 15: Microtubule arrangement appears normal in the *elch* mutant.

Figure C 1: Cell division defect model for trichome and stomata cluster development in the *elch* mutant

Figure C 2: A model for ESCRT mediated degradation of V-ATPase complexes.

Table 1: Cluster frequency, stems per cluster, branchpoints and nuclei per cluster in *wild type* plants, *elch* and *stichel 146*.

Table 2: Multinucleated cells are predominantly found in trichomes and pavement cells.

Table 3: *elch* stomata show a phenotypic series of cytokinesis defects.

Table 4: Core components of ESCRT-I, -II, -III complexes are found in *Arabidopsis*, *yeast* and *mammals*.

Table 5: ESCRT I components identified with MALDI-TOF mass spectrometry.

Table 6: Putative targets/associated proteins of ELCH/ESCRT-I identified with MALDI-TOF mass spectrometry.

Table 7: VHA-H coimmunoprecipitates with VHA-a3-GFP.

Table 8: Mass spectrometry analysis indicates that VHA-a3 is ubiquitinated.

Table 9: The cluster frequency is raised in the *tfc-a/elc* double mutant.

Abbreviations and gene names

::	fused to (in the context of promoter-gene fusion constructs)
<i>AN</i>	<i>ANGUSTIFOLIA</i>
<i>ARP2/3</i>	<i>ACTIN RELATED PROTEIN 2 and 3</i>
<i>AtELP</i>	<i>Arabidopsis thaliana EGFR-LIKE PROTEIN</i>
<i>A. thaliana</i>	<i>Arabidopsis thaliana</i>
ATP	adenosine triphosphate
bp	base pairs
<i>BP80</i>	<i>BINDING PROTEIN 80 kDa</i>
C	DNA-content of a haploid genome
<i>CaMV</i>	<i>Cauliflower mosaic virus</i>
CCV	clathrin coated vesicles
cDNA	complementary DNA
CLSM	confocal laser scanning microscopy
°C	degree Celsius
Da	dalton
DAPI	4',6-Diamidino-2-phenylindol
<i>DET3</i>	<i>DEETIOLATED3</i>
<i>DIS2</i>	<i>DISTORTED2</i>
DNA	Deoxyribonucleic acid
DTT	dithiothreitol
EGFR	epidermal growth factor receptor
<i>ELC</i>	<i>ELCH</i>
ESCRT	endosomal sorting complex required for targeting
FLAG	flagellin
g	gram (s)
x g	Gravitation constant (981 cm/s)
GFP	green fluorescent protein
HA	hemagglutinin of <i>influenza virus</i>
HIV	human immunodeficiency virus
IP	immunoprecipitation
k	kilo
kb	kilobase (s)
K	lysine
kDa	kilodalton (s)
<i>KIS</i>	<i>KIESEL</i>
LAP	lysosomal acid phosphatase
<i>Ler</i>	<i>Landsberg erecta</i>
μ	mikro
Maldi	matrix assisted laser desorption ionisation
mM	millimolar
MPR	manose-6-phosphate receptor
mRNA	messenger ribonucleic acid
MS	mass spectrometry
MVB	multi-vesicular body
n	number
ORF	open reading frame
PAGE	polyacrylamide gel electrophoresis
pCPS	precursor of CarboxypeptidaseS

PFS	planar fenestrated sheet
pH	negative decimal logarithm of H ⁺ concentration
PPB	pre-prophase band
RNA	ribonucleic acid
Rpm	rounds per minute
RT	room temperature
<i>STI</i>	<i>STICHEL</i>
T-DNA	transfer DNA
SDS	sodium dodecyl sulfate
T1	seeds that grow on a transformed plant
T2	seeds that grow on a T1 plant
<i>TFC-A</i>	<i>Tubulin-Cofactor A</i>
TOF	time of flight
Tris	Tris-(hydroxymethyl)-aminomethane
<i>TSG101</i>	<i>TUMOR SUSCEPTIBILITY GENE 101</i>
TN	tubular network
TVN	tubulo-vesicular network
UBA	Ubiquitin Associated domain
<i>UBAP1</i>	<i>UBIQUITIN ASSOCIATED PROTEIN1</i>
UEV	Ubiquitin Enzyme Variant domain
V-ATPase	vacuolar-ATPase
Vps23p	yeast nomenclature for protein
<i>VPS</i>	<i>VACUOLAR PROTEIN SORTING</i>
VHA-A,B,E,H	cytosolic subunits of the vacuolar (H ⁺) ATPase
VHA-a3	transmembrane subunits of the vacuolar (H ⁺) ATPase
<i>WRM</i>	<i>WURM</i>
<i>Ws2</i>	<i>Wassilewskija 2</i>
<i>Wt</i>	<i>wild type</i>
YFP	yellow fluorescent protein

Gene names are written in italics, in capital letters when referred to wild type and in small letters for the mutant. Protein names are written in capital letters.

A. Introduction

A 1. The secretory system

Eukaryotic cells share several elements like the plasma membrane, the endoplasmic reticulum, various endosomes, the golgi system and a vacuole/lysosome equivalent that are collectively referred to as the “secretory system”. The term secretory system was derived from the observation in yeast that many mutants defective in protein sorting secrete proteins (Johnson et al., 1987; Klionsky and Emr, 1990; Valls et al., 1987). The endosome is a vesicular compartment that is involved in the transport of internalised ligands from the plasma membrane to lysosomes. Moreover it has been implicated in intracellular transport from the golgi system to lysosomes. A lysosome is an acidic compartment that contains digestive enzymes that are responsible for the degradation of various macromolecules. All cells depend on membrane structures that establish compartments for various cellular functions. Furthermore, membrane vesicles are part of the transportation system that connects different organelles.

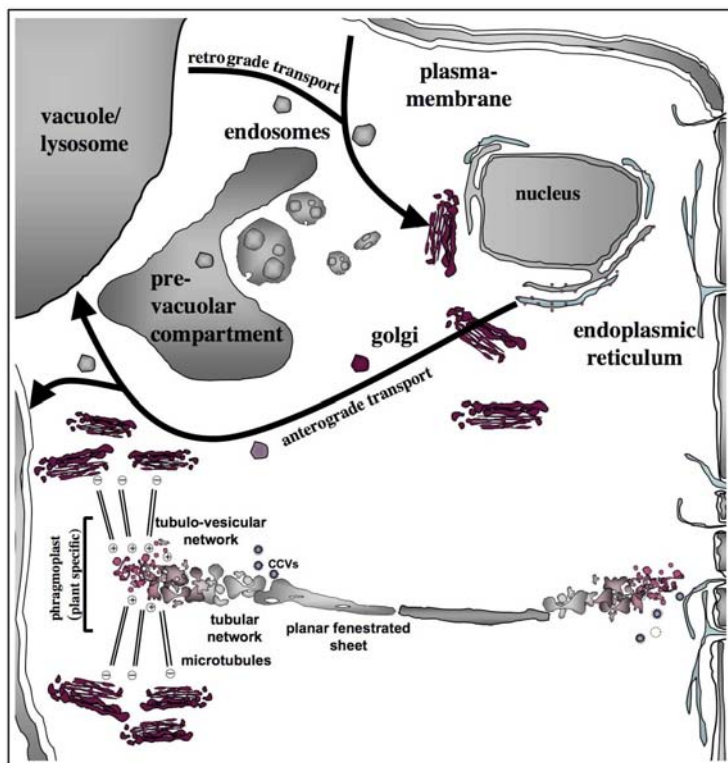


Figure A1: Overview of the cellular endomembrane system. Most membrane compartments are conserved in eukaryotic organisms or have equivalent structures. The yeast vacuole for example fulfils similar functions than the lysosomes in animals. The phragmoplast is a plant specific organelle required during plant cell division. There is no obvious equivalent for the phragmoplast in animals as different strategies of cell division have evolved. Vesicle movement from the endoplasmic reticulum (ER) via the golgi system towards vacuole or plasma membrane is called anterograde transport (i.e. biosynthetic cargo). The opposite direction is termed retrograde transport (i.e. maintaining membrane equilibrium). Recently more evidence became available that golgi derived vesicle are important for scission during late stages of animal cytokinesis. This indicates that the secretory system is more important for animal cytokinesis than thought previously.

Intracellular transport is accomplished mainly by small transport vesicles that bud from donor compartments and travel along the cytoskeleton to an acceptor vesicle or organelle. Membrane fusion then leads to the delivery or exchange of cargo between the fusing vesicles or compartments. Two main directions are defined for vesicle transport: Anterograde and retrograde transport. Anterograde transport originates at the endoplasmic reticulum, travels through the golgi system and flows towards plasma membrane and vacuole/lysosome. While anterograde transport is mainly of biosynthetic nature, retrograde transport redirects vesicles and ensures that membrane equilibrium is maintained. Retrograde transport therefore has opposite directionality with vesicle flow from the plasma membrane or vacuole to the golgi system and the endoplasmic reticulum. Important regulatory functions such as receptor down-regulation from the plasma membrane are mediated by retrograde transport (for reference see Sanderfoot and Raikhel, 2003).

A 2. The ESCRT pathway

The secretory system of the unicellular organism *Saccharomyces cerevisiae* is a model system for protein sorting. Large collections of yeast mutants were screened for aberrant endomembrane structures (Bankaitis et al., 1986; Banta et al., 1988) and classified into subclasses A to F (Raymond et al., 1992). The analysis of class E mutants revealed a pathway that specifically sorts proteins destined for the vacuolar lumen, a process that has been termed ESCRT pathway (Endosomal Sorting Complex Required for Transport) (Babst et al., 2002a; Babst et al., 2002b; Katzmann et al., 2001). The ESCRT pathway is responsible for sorting proteins labeled with a single ubiquitin moiety and delivering them to the vacuole in yeast (Babst, 2005; Odorizzi et al., 1998). In the vacuolar lumen the proteins are accessible to proteases and become subsequently degraded. Three fundamental steps are required for this process. The initial step in this sorting pathway is the recognition of mono-ubiquitinated proteins by Vps27p and Vps23p (Bilodeau et al., 2002; Bilodeau et al., 2003). *VPS23*, the ortholog of the *Arabidopsis* *ELCH* gene, is a component of the ESCRT-I complex that is located at the late endosome, also referred to as multivesicular body (MVB) (Katzmann et al., 2001). In a second step, vesicles invaginate from the outer membrane of the late endosome into the lumen. Proteins that are targeted to the MVB membrane by Vps27p and Vps23p become internalized with the help of ESCRT-II and ESCRT-III complexes (Babst et al., 2002a; Babst et al., 2002b; Katzmann et al., 2001). In step three the MVBs fuse with the vacuole where the cargo becomes degraded (Odorizzi et al., 1998). This sorting pathway specifically recognizes proteins marked with a single ubiquitin. This model is supported by

the observation that the precursor of carboxypeptidase S (pCPS) is misguided to the vacuolar membrane after mutating the N-terminal lysine to which ubiquitin is normally bound (Katzmann et al., 2001). Conversely, proteins that are normally not targeted into the vacuole are transported to the lumen when linked to a single ubiquitin moiety (Urbanowski and Piper, 2001). The ESCRT pathway is not fungi specific but is also found in animals. Homologs of all components of yeast ESCRT-complexes have been identified in animals (Katzmann et al., 2002). The human orthologue of *VPS23* was shown to be *TSG101* (Babst et al., 2000) and the equivalent compartment to the yeast vacuole is the lysosome in animals. The ESCRT pathway in yeast and animals sorts mainly two classes of proteins. As discussed above one targeted protein class is biosynthetic cargo like pCPS in yeast and lysosomal acid phosphatase (LAP) in animals.

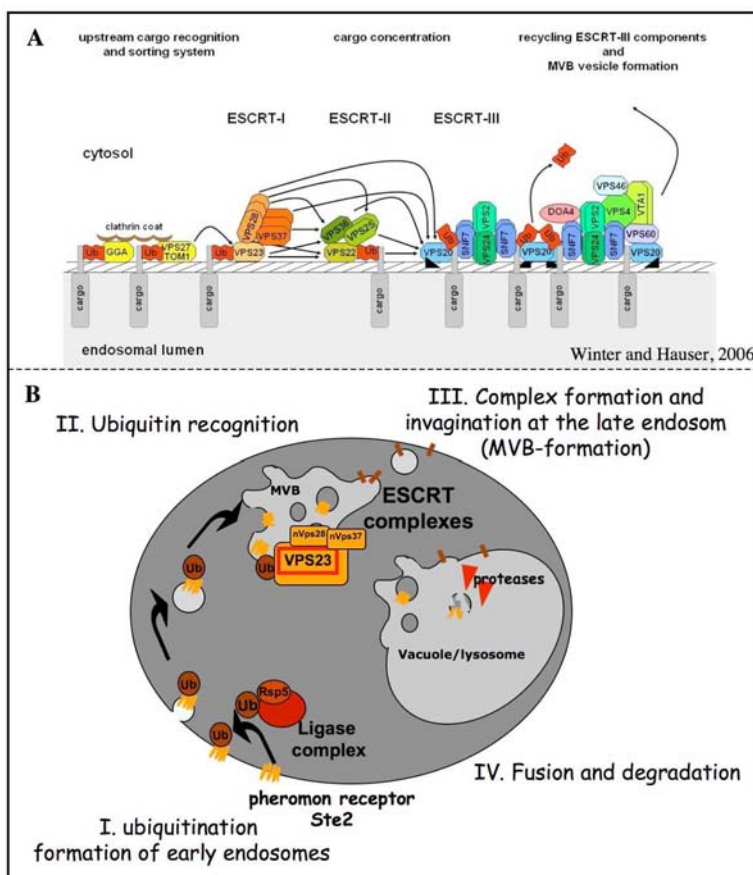


Figure A2: Overview of ESCRT dependent protein sorting. (A) Overview of the ESCRT machinery in eukaryotes as reviewed by Winter and Hauser, 2006. Proteins upstream of ESCRT-I presumably recruit targets together with VPS23/ELCH to the ESCRT complexes. The mechanism of cargo concentration, deubiquitination, budding and complex breakup is still under investigation. (B) Main stages of receptor mediated endocytosis and degradation in the yeast vacuole. Activated Ste2p receptor initiates a signal cascade. To inactivate the receptor he is monoubiquitinated, endocytosed and sorted by the ESCRT pathway into the vacuole for degradation. Not shown is transport of biosynthetic cargo but the principle of MVB sorting is the same. pCPS originates at the endoplasmic reticulum and travels through the golgi system to the late endosome (MVB). Fusion of MVBs with the vacuole results in the processing of pCPS by other proteases to its active form.

Both proteins are transported to the lumen of the vacuole/lysosome where they are processed to their active form (Babst et al., 2000). The other class of proteins sorted by the MVB pathway are plasma membrane proteins. The α -factor receptor Ste2p is transported via endosomes through the prevacuolar compartment into the yeast vacuole (Mulholland et al., 1999). Class E VPS genes are essential for this process (Katzmann et al., 2002; Odorizzi et

al., 1998). In animals, the plasma membrane receptor Notch and the receptor-tyrosine-kinase Epidermal Growth Factor Receptor (EGFR) are sorted by the ESCRT pathway. Receptor-mediated endocytosis removes Notch and EGFR from the plasma membrane by internalising them into late endosomes. The acidic environment in these compartments causes dissociation of receptor ligand complexes (Geuze et al., 1983). Receptor and ligand are sorted apart and either subject to lysosomal degradation or receptor recycling to the plasma membrane (Bache et al., 2004; Futter et al., 1996; Giebel and Wodarz, 2006; Herz et al., 2006; Thompson et al., 2005; Vaccari and Bilder, 2005). The ESCRT machinery not only sorts cellular proteins but is also exploited by enveloped viruses to exit their host cell. Human Immunodeficiency Virus (HIV) or Ebola produce enveloped particles through ESCRT mediated membrane budding, a reaction that is topologically equivalent to endosomal membrane invagination (Patnaik et al., 2000). Cells depleted of TSG101 or mutant for VPS4, another class E protein, prohibit efficient viral particle budding (Garrus et al., 2001). For review of ESCRT mediated viral budding see (Pornillos et al., 2002). A general overview of the ESCRT pathway and its cargo for yeast and animals is reviewed in (Katzmann et al., 2002).

The plant vacuole is considered to be equivalent to animal lysosomes (Vitale and Galili, 2001; Vitale and Raikhel, 1999). Furthermore, the class E genes found in yeast and animals are also present in *Arabidopsis* (Winter and Hauser, 2006), suggesting that the ESCRT machinery is functional in plants as well. However, no role has been assigned to *ELCH* so far and it is unclear whether ESCRT-like machinery in plants executes similar functions to those found in yeast and animals.

A 3. The vacuolar ATPase

Vacuolar (H^+)-ATPases (V-ATPases) reside not only in the vacuolar membrane as the name suggests, but are found throughout the secretory system. They acidify intracellular compartments in eukaryotic cells translocating protons from the cytosol into the lumen of various organelles. The V-ATPase is a multi subunit complex consisting of a membrane based V_0 complex and a cytosolic V_1 complex. Together, V_0 and V_1 form a stalk and ball like structure (Figure A3 A). In plants the V_1 complex consists of eight subunits that are sequentially named VHA-(A to H). The V_0 complex is composed of five subunits that are termed VHA-a, VHA-c, VHA-c', VHA-c'' and VHA-d. The V_0 subunits form the proton translocation channel and parts of the stalk to which the cytosolic V_1 unit is attached (Sze et al., 2002). The mechanism of proton translocation was elucidated in yeast and is driven by rotational movement of subunits of the cytosolic V_1 sub complex dependent on ATP

hydrolysis (Hirata et al., 2003). Vacuolar (H^+)-ATPase is reported to localize to the plasma membrane and a variety of intracellular compartments, including endosomes, lysosomes and secretory vesicles (Figure A3 B). The respective localisation and density of V-ATPases is highly cell type specific and varies enormously between different organisms. V-ATPases function in a variety of processes such as receptor-mediated endocytosis and intracellular sorting of lysosomal enzymes (Bowman and Bowman, 2000; Forgac, 1999; Geuze et al., 1983; Klionsky et al., 1992a; Klionsky et al., 1992b; Nishi and Forgac, 2002; Stevens and Forgac, 1997). Receptor-mediated endocytosis provides a mechanism by which eukaryotic cells selectively internalize macromolecules (Mellman, 1996a; Mellman, 1996b; Trowbridge et al., 1993). The most well understood endocytotic mechanism is clathrin-mediated endocytosis. Clathrin-mediated endocytosis mediates the internalization of plasma membrane proteins such as receptors. In this process, ligand-receptor complexes become clustered in specialised regions of the plasma membrane where they form clathrin-coated pits. Receptors that are to be internalised associate with clathrin via interaction with a family of adaptor proteins that bridge the cytoplasmic tails of receptors with the heavy chain of clathrin (Pearse and Robinson, 1990).

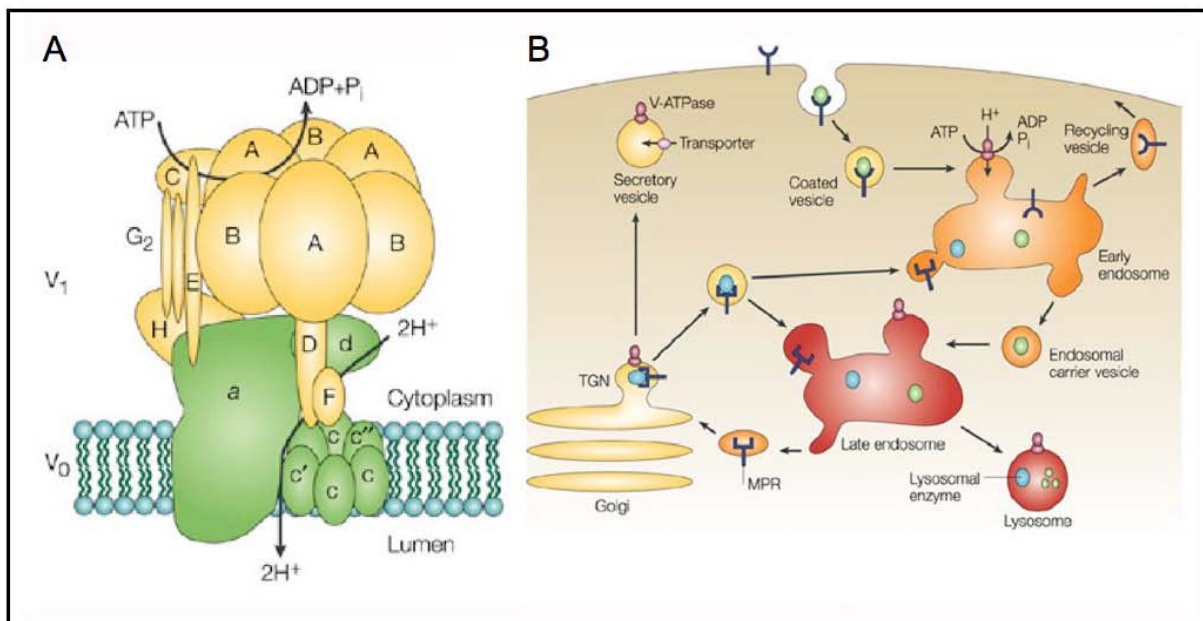


Figure A3: Structure and functions of the vacuolar ATPase. (A) The vacuolar ATPase is a multimeric protein complex that forms a stalk and ball like structure. The membrane integral V₀ subcomplex forms the proton channel whereas the ball is cytosolic and provides the ATP dependent rotational force that pumps protons across the membrane. (B) The V-ATPase is important for endocytosis and intracellular targeting. Acidification of early endosomes is required for dissociation of internalized ligand–receptor complexes and recycling of receptors to the plasmamembrane. Acidification of late endosomes is required for release of lysosomal enzymes from mannose 6-phosphate receptors (MPR) and recycling of these receptors to the trans-Golgi network (TGN). Yellow indicates neutral pH and red indicates acidic pH (adopted from Nishi and Forgac, 2002).

The budding of coated pits from the plasma membrane is a complex process that requires several steps (van der Bliek et al., 1993) and gives rise to clathrin-coated vesicles. These vesicles rapidly lose their clathrin coat to form uncoated endosomes (Rothman and Schmid, 1986). Fusion of endosomes with each other results in the delivery of ligand receptor complexes to an acidic endosomal compartment, where the low pH activates release of ligands from their receptors (Geuze et al., 1983). This process allows recycling of unoccupied receptors to the cell surface and targeting of the released ligands to lysosomes (Figure A3 B). Another well-studied process that depends on the V-ATPase is intracellular sorting of proteins from the biosynthetic pathway. Lysosomal enzymes like protease precursors use anterograde transport within the secretory system to reach the vacuolar lumen. Disruption of V-ATPase subunits in yeast led to the missorting of these proteins (Klionsky et al., 1992a; Klionsky et al., 1992b; Matsuoka et al., 1997). Yeast strains mutant for V-ATPase subunits were unable to acidify their vacuolar lumen and accumulated and secreted precursor forms of carboxypeptidase Y (CPY) and proteinase A (Klionsky et al., 1992a).

Like the ESCRT machinery, certain functions of the V-ATPase seem to be exploited by enveloped viruses. Lentiviruses like HIV or SIV (Simian immunodeficiency) depend on the vacuolar ATPase. This is indicated by physical interaction between the VHA-H subunit and the HIV accessory protein Nef. Nef is required for efficient viral infectivity and pathogenicity (Geyer et al., 2002; Lu et al., 1998).

A 4. Cytokinesis in plants

Like all cellular organisms plants grow and reproduce by dividing existing cells. The main stages of the cell cycle are S-phase (synthesis phase) where the DNA is replicated and M-phase (mitotic phase) when the DNA is divided between the two nuclei. Cytokinesis takes place during the second part of M-phase after DNA segregation where the two daughter nuclei are separated by a new cell wall. Cell division is a process that is common to all eukaryotes, however the way it is achieved differs, especially between animals and plants. Animal cells divide by pinching off daughter cells with the help of a contractile ring (Glotzer, 2001). This ring is attached to the plasma membrane in the plane of division leading either to equal or unequal divisions. Plant cells have evolved different mechanisms of cytokinesis, probably due to the limitations posed by the rigid cell wall. Conventional cytokinesis in plants is characterized by nuclear division followed by immediate cell wall formation between the sister nuclei. In contrast, during non-conventional cytokinesis nuclear division and cytokinesis are uncoupled leading to multinucleated cells. The cell wall is then established at later stages

(Otegui and Staehelin, 2000). Although there are differences in detail, both division modes utilize a common structure called phragmoplast to create the new cell wall (Figure A4). Microtubules, microfilaments and membranous elements are the predominant structural elements of the phragmoplast that is established in the plane where the new cell wall will form. The plane of division is marked by two elements that become apparent during cytokinesis. The preprophase band (PPB) is a ring like structure, consisting of microtubules and actin filaments, where a large proportion of the otherwise distributed microtubules is concentrated (Samuels et al., 1995). The other element is the golgi belt, an accumulation of golgi stacks that forms after nuclear division and also serves as a marker for the position of the emerging cell wall (Nebenfuhr et al., 2000).

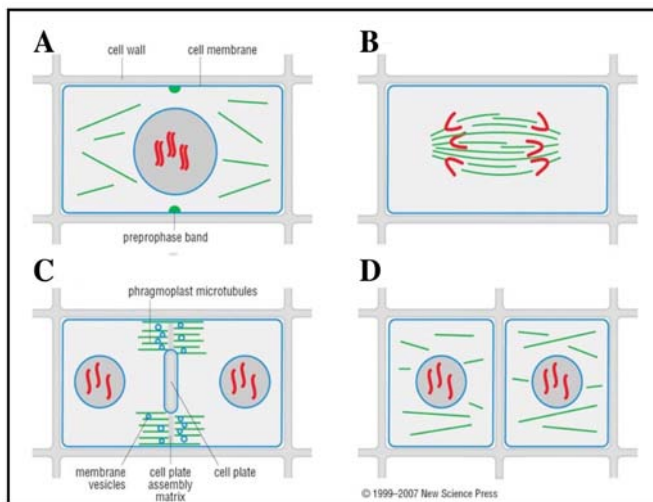


Figure A4: Cell division in plants. (A) Rearrangement of microtubules and formation of the preprophase band that will mark the site of future cytokinesis. (B) Rearrangement of microtubules and spindle formation. The chromosomes are segregated in late anaphase. (C) In late telophase mitosis is completed and cytokinesis starts by cell plate formation. Spindle microtubules are rearranged and form the phragmoplast that guides vesicle transport to the forming cell plate in the cell plate assembly matrix. (D) The cell plate contacts and fuses with the old cell wall thereby separating the two daughter cells. Microtubules rearrange to their normal state again (from “The cell cycle: Principles of control” by David O. Morgan).

The golgi stacks provide the materials needed to build the new cell wall while phragmoplast microtubules provide the infrastructure that transports the golgi derived vesicles to the forming cell plate (Figures A4 and A5). As a general principle, plant cells assemble a new cell wall by accumulating transport vesicles with cell wall material in the plane of division (Staehelin and Hepler, 1996). Recent evidence suggests that the aspect of vesicle trafficking, which dominates plant cytokinesis, also plays a critical role in animal cytokinesis (Albertson et al., 2005). Vesicle trafficking during plant cytokinesis could therefore serve as a model for similar processes in animal cytokinesis. Vesicle fusion forms the tubulo-vesicular-network (TVN) that is subsequently reduced through the tubular network (TN) to a planar fenestrated sheet (PFS). The PFS matures to the cell plate that will give rise to the new cell wall (Staehelin and Hepler, 1996). The acquisition of cell wall material is coupled to an accumulation of membranes but it is estimated that about 75 % of the golgi derived membranes involved in cell plate formation are recycled (Otegui et al., 2001). Although the mechanisms are only roughly defined, the reduction seems to be mediated by budding of

clathrin coated vesicles (CCV) from the TVN that are speculated to feed the endosomal/MVB pathway (Jurgens, 2005; Samuels et al., 1995; Segui-Simarro et al., 2004). The MVB is then thought to distribute membranes back to the different compartments of the endo-membrane system similar to the way it does during endocytosis (Figure A5). This is apparent as the number of MVBs is increased during cytokinesis compared to non-dividing cells (Segui-Simarro and Staehelin, 2005). The phragmoplast disassembles once the forming cell wall has completed making contact to the old cell walls.

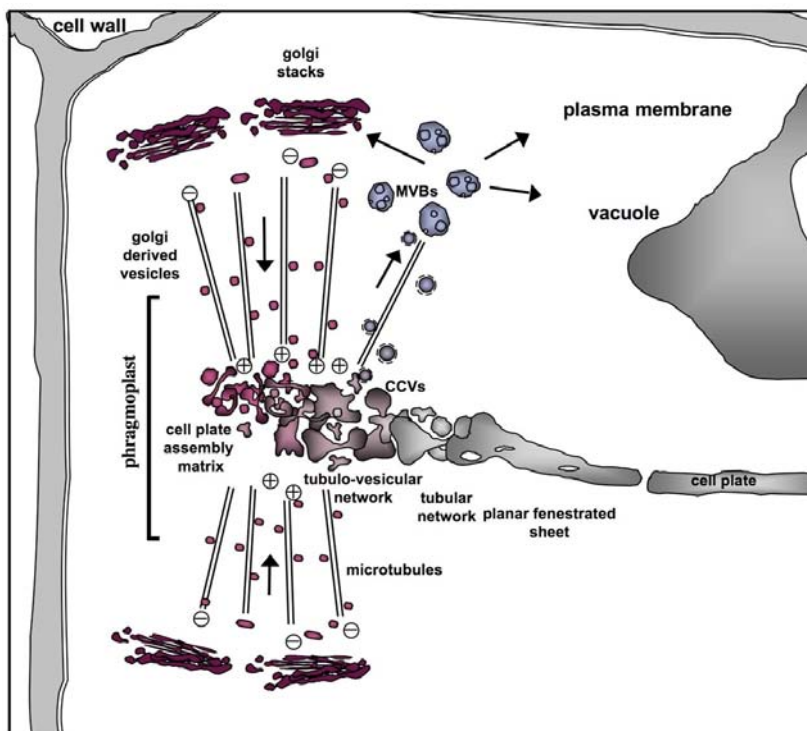


Figure A5: Model of plant cytokinesis. The phragmoplast guides golgi-derived vesicles towards the cell plate assembly matrix (CPAM). These vesicles fuse and form the tubulo-vesicular network. Fusion and maturation gradually forms the cell plate via the tubular network and the planar fenestrated sheet. The accumulation of membranes at the CPAM is balanced by budding of clathrin coated vesicles and presumably redistribution of membranes to the plasma membrane, golgi and other compartments of the secretory system. The accumulation of CCVs and MVBs during cytokinesis suggests that these vesicles are involved in membrane redistribution.

In contrast to the mitotic cell cycle, mitosis and cell division are bypassed during endoreduplication. Endoreduplicating cells undergo multiple rounds of DNA replication without intervening mitosis thereby amplifying the DNA content of individual cells. Mitotic- and endoreduplication cycle utilize the same cellular machinery and probably evolved from each other (Edgar and Orr-Weaver, 2001). This is apparent because a mutation in the *siamese* gene in *Arabidopsis* is sufficient to change cells that normally endoreduplicate to undergo cell division (Schnittger et al., 2002; Walker et al., 2000). Similar, ectopic expression of CYCLIN-B in unicellular trichomes is sufficient to induce cell divisions (Schnittger et al., 2002). Cells whose function requires high biosynthetic activity or fast growth frequently have endoreduplicated DNA. Therefore the biological sense of endoreduplication seems to be the generation of cells with more copies per gene that are larger and more productive than diploid cells.

A 5. The *Arabidopsis elch* mutant

The *elch* mutant was initially identified in a T-DNA collection from Versailles by Hilmar Ilgenfritz on the basis of a subtle leaf hair phenotype. Leaf hairs or trichomes of *Arabidopsis* are large epidermal cells that protrude from the leaf surface and are most likely a protection of the meristem against small herbivores (Figure A6 A). *Wild type* trichomes consist of one stem with several branches (Figure A6 B). By contrast *elch* mutants (*elc*) possess a small number of trichomes that show two or more stems originating from a single cell and are called trichome cluster. The splitting of stems close to the leaf surface gives these clusters a moose or elk horn like appearance (Figure A6 C). The mutant was therefore coined *elch* (Hulskamp et al., 2000). Previous work indicated that the phenotype is caused by a single T-DNA insertion (Dr S. Schellmann, personal communication; appendix E6)

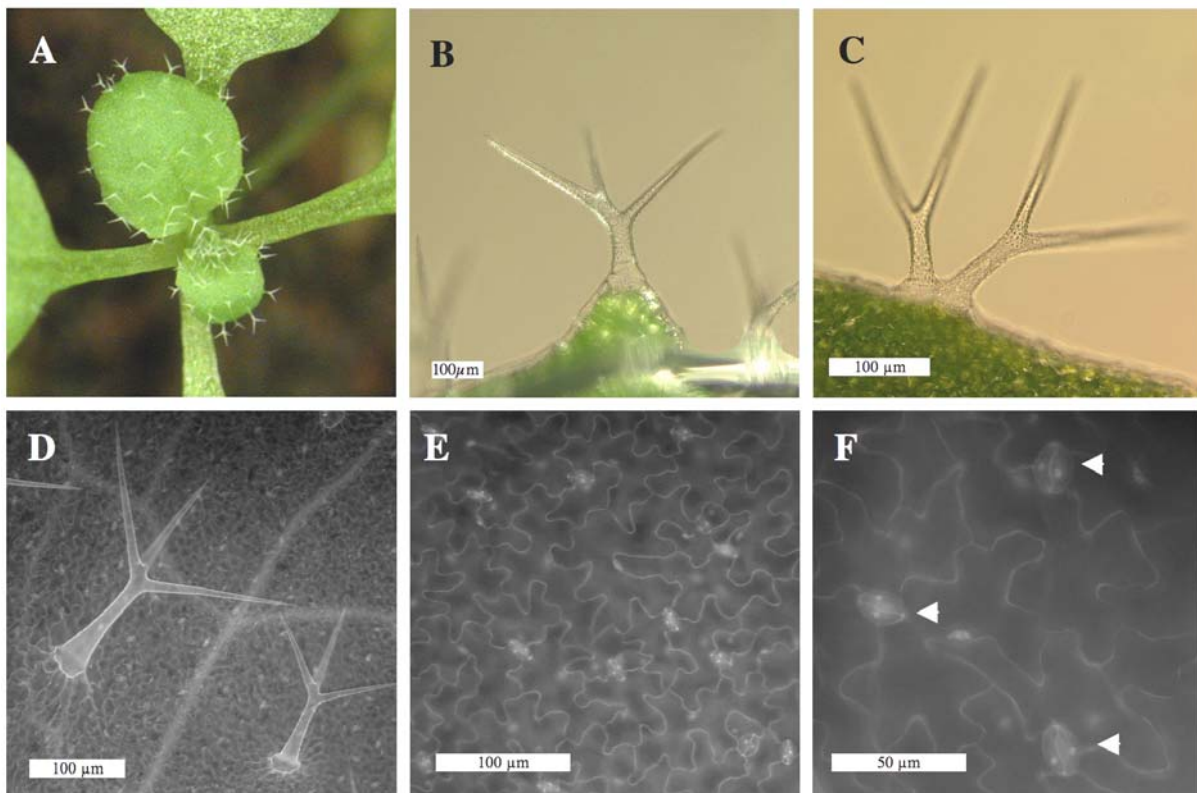


Figure A6: Trichome cluster phenotype of the *Arabidopsis elch* mutant. (A) Rosette with third and fourth leaf covered with trichomes (picture A is a courtesy of Katja Wester). The arrow marks the position of the shoot apical meristem from where new leaves develop. This area is densely covered with trichomes. (B) A single wild type trichome. (C) Trichome cluster of the *elch* mutant. Two stem like structures emerging from the base of the cell give the cluster a moose or elk like appearance. (D) Leaf section with the epidermal cell types used in this study (trichomes, pavement cells and stomata). (E) Typical pavement cells displaying their lobed shaped outline. (F) Section of a leaf with three stomata. These cells mediate gas exchange between atmosphere and the inner tissues of the leaf. (A) Picture was taken with a stereo microscope. (B-C) Leaves were DAPI-stained, whole mounted and observed by epi-fluorescence microscopy.

These trichome clusters are frequently multinucleated. Trichomes are used as a model to study developmental processes such as cell morphogenesis, patterning and cell cycle regulation in plants (Hulskamp, 2004). The current model of trichome development defines several distinct steps like trichome selection, switch from mitosis to endoreduplication, trichome differentiation, branching and expansion growth. Trichome development is most likely not affected in the *elch* mutant demonstrated by genetic analysis with mutants from different developmental processes (Spitzer, 2002; diploma thesis). A detailed dissection of trichome development is reviewed in Hulskamp, 2004. The cloning of the *ELCH* gene revealed that *ELCH* is similar to the *VPS23* gene in yeast (Spitzer et al., 2006). None of the so far cloned genes implicated in trichome development has similarity to *VPS* genes although some might have functions in the secretory system. *ANGUSTIFOLIA* (*AN*) has been implicated in golgi-related functions, however the molecular function of *AN* is still under investigation (Folkers et al., 2002; Kim et al., 2002). *Arabidopsis* lines that are mutant for *WURM* (*WRM*) and *DISTORTED1* (*DIS1*) show aberrant vacuolar fusions and cell shape alterations (Mathur et al., 2003). Both genes encode subunits of the Arabidopsis ARP2/3 complex that has central functions in actin regulation. The double mutant *elc/dis1* showed an additive phenotype indicating that there is no direct interaction between *ELCH* and actin related processes.

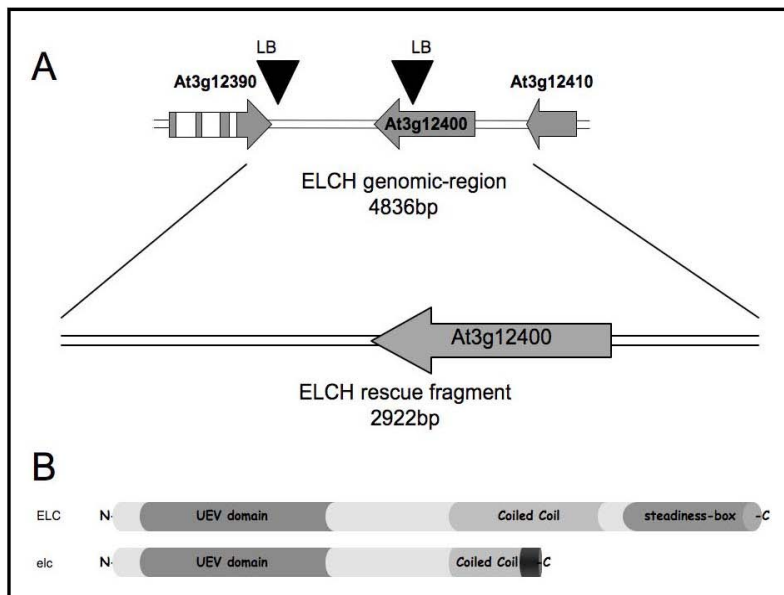


Figure A7: Cloning of the *ELCH* gene. (A) Rescue of the *elch* mutant by a genomic fragment of At3g12400 that includes 600 bp upstream of the ATG and 1100 bp downstream of the stop codon showed that *ELCH* encodes a *VPS23* homolog. Left border sequence was found downstream of At3g12390 and in the open reading frame of At3g12400 indicating multiple head to head insertions of the T-DNA. (B) Because of the T-DNA insertion in the *ELCH* gene the transcript is truncated in the *elch* mutant. Translation of this transcript would result in a partial *ELCH* protein that is truncated in the coiled coil domain.

The phenotype of *elch* and the molecular nature of the mutation (Figure A7) indicate that *elch* is not a complete knockout but rather a hypomorphic allele. This is apparent because only a small number of trichomes form clusters while the majority of *elch* trichomes is

indistinguishable from wild type. The *elch* mutant allele used in this study is a T-DNA line where vector sequence was found to be inserted 786 base pairs after the start codon. The mutation leads to a truncated transcript and a protein lacking the carboxy-terminal 166 amino acids (Spitzer et al., 2006). Approximately 2% of all leaf hair trichomes display the cluster phenotype while the remainder are indistinguishable from *wild type*. Next to trichomes other epidermal cell types are affected by the cytokinesis defect as well. In this study pavement cells (Figure A6 E) and stomata (Figure A6 F) are examined. Pavement cells establish the outer layer of arial plant organs. They strengthen the plant structure and protect the plant against desiccation. Stomata mediate gas exchange between atmosphere and inner plant tissue.

Aim

During my diploma thesis I cloned the *ELCH* gene and analysed the morphology of trichome clusters in the *elch* mutant. The presence of multinucleated cells in the *elch* mutant suggested that the phenotype is related to cytokinesis. Nevertheless it was not possible to provide experimental evidence at that time. Therefore one object of this PhD thesis was to determine whether cell division defects contribute to the multinucleated phenotype. To address this question further epidermal cell types were analysed in respect to incomplete cell walls that are characteristic for cytokinesis mutants. In a simple model the development of clusters will be explained. The main focus was laid on the biochemical characterization of the ELCH protein. The aim of these experiments was to establish whether an ESCRT-like pathway exists in *Arabidopsis*. Therefore an HA-tagged ELCH was investigated for interacting proteins that are part of the ESCRT machinery. The analysis of a putative ESCRT pathway was deliberately restricted to ESCRT-I as ELCH is assumed to be a component of this complex. Based on these studies was the approach to identify interacting proteins or targets of ELCH. A potential target, the vacuolar ATPase, is integrated into a plant specific variation of the ESCRT pathway.

B. Results

The existence of an ESCRT-like pathway in *Arabidopsis* is just emerging. In this pathway the *ELCH* gene is likely an important component and was therefore characterized in more detail. The biochemical properties of ELCH were tested with regard to ubiquitin-binding and complex formation. One of the ELCH/ESCRT-I interacting proteins that were found in this study is VHA-a3, which is a putative target of the ESCRT pathway. VHA-a3 was therefore analysed in more detail in regard to its modification with ubiquitin.

Previous studies provided evidence that compromising ELCH function leads to cytokinesis defects. This was confirmed by the finding of incomplete cell walls in different epidermal cell types. To substantiate the cytokinesis defect *elch* was crossed to the *tubulin-folding cofactor A* mutant (*tfc-a*) that has cell division defects (Kirik et al., 2002). The double mutant *elch tfc-a* shows a strong synergistic phenotype supporting the idea that *ELCH* is important during cytokinesis. Furthermore this result implies that *ELCH* regulates microtubules or microtubule dependent processes during cytokinesis.

The understanding of cluster morphology was advanced by showing experimentally, that clusters are single celled structures and consist of two or more stems emerging from one cell. It was shown that endoreduplication is not affected in multinucleated clusters demonstrating that *elch* induced defects occur during an early stage of trichome development.

B 1. The *elch* cluster consists of a single cell with multiple stems.

The *elch* mutant has an inconspicuous phenotype. General growth behaviour of *wild type* plants and *elch* mutant plants is indistinguishable and no penetrant phenotype is observed in epidermal tissues. The most obvious phenotype was found in trichome clusters that appear with a frequency of 1,93% on true leaves three and four (Tab. 1). In addition, these clusters were found to be multinucleated with up to four nuclei per cell (Figure 2 B-F). Trichome clusters are characteristic for the *elch* mutant and not found in *Wassilewskija 2 wild type* background (*Ws2*).

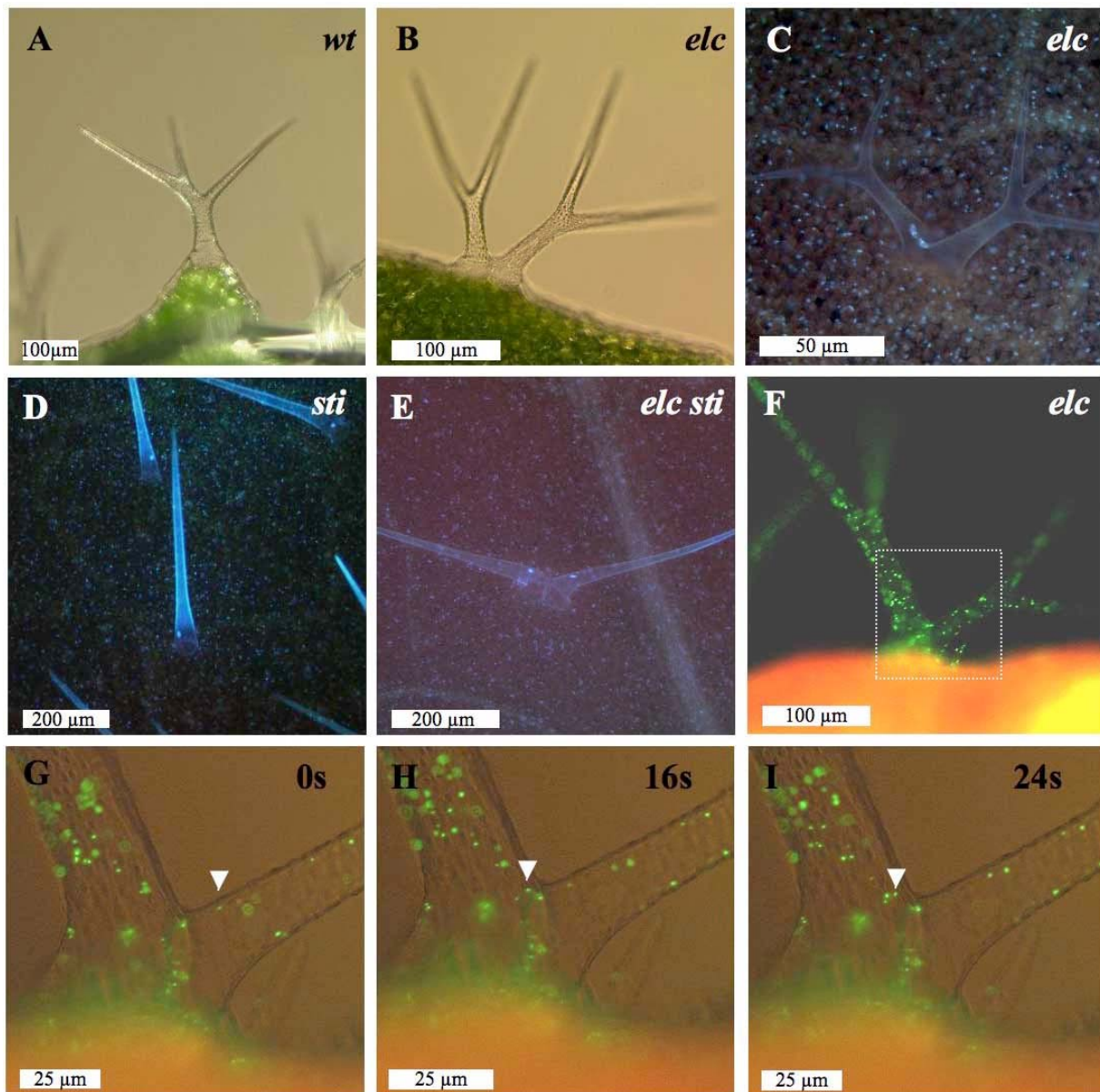


Figure B1: Trichome clusters consist of a single cell with multiple stems emerging from a single cell. A small number of *elch* trichomes has two stems that emerge from a single cell. (A) Wild type trichome compared to *elch* trichome in B and C. (D) Unbranched stichel trichome compared to *elch/stichel* trichome in E. The double mutant between unbranched *sti* and *elch* retains the basal splitting. This indicates that branching is not involved in cluster formation. (F) Overview of an *elch* trichome cluster expressing the EYFP-peroxy construct. (G-I) Time lapse observation of peroxisomes indicate that a cluster consists of a single cell. All pictures are from whole mounted leaves. (A-B) light-microscopy. (C-I) epi-fluorescence microscopy. (C-E) DAPI-staining.

The *Landsberg erecta* (*Ler*) ecotype is known to form occasional trichome nests that resemble clusters. However these are more likely patterning defects as no multinucleated trichomes have been observed (Table 1). The appearance of trichome clusters raised the question of whether the basal splitting constitutes an early branching event or whether two stems protrude from one cell. To address this question genetic and cell biology approaches were chosen. The *elch* mutant was crossed with *stichel*, a mutant that is epistatic to most trichome mutants (Folkers et al., 1997). Furthermore, genetic and morphologic analysis of the *elc/sti146* double mutant indicated that *ELCH* acts independently from *STICHEL* (Spitzer C., 2002; diploma thesis). Several *stichel* alleles exist that are less branched than *wild type*. Trichomes of *sti146* are unbranched, indicating that it is a strong allele (Table 1) and therefore appropriate to this analysis. The multinucleated clusters found in the double mutant retained the basal splitting that is characteristic for *elch* clusters. This strongly argues against the branching model (Figure B1 E). To rule out the possibility that a patterning defect leads to two trichomes directly adjacent to each other, cytoplasmic streaming within *elch* clusters was monitored. To visualize cytoplasmic streaming between two stems in a cluster *elch* was crossed with a line expressing a marker that labels peroxisomes with YFP (Mathur et al., 2002). Peroxisomes were observed by epi-fluorescence microscopy and were shown to pass from one stem of a cluster into the other. As the peroxisomal size is beyond the exclusion limit for passing through plasmodesmata this observation confirmed that a trichome cluster consists of a single cell.

Table 1: Cluster frequency, stems per cluster, branchpoints and nuclei per cluster in *wild type* plants, *elch* and *stichel 146*.

	<i>cluster frequency</i>	<i>stems/cluster</i>	<i>branchpoints</i>	<i>Nuclei/cluster</i>	<i>n</i>
<i>Ws2</i>	0% ¹	--	1,62+-0,50 ²	--	2971
<i>Ler</i>	0% ¹	--	1,99+-0,21 ²	--	2253
<i>elch</i> (<i>Ws2</i>)	1,93%	2,03+-0,17	1,04+-0,69 ³	1,97+-0,34	3529
<i>elch</i> (<i>Ler</i>) ⁴	1,66%	2,13+-0,34	1,92+-0,29 ³	1,87+-0,52	963
<i>stichel146</i>	0%		0+-0	--	463
<i>stichel146/elch</i>	1,07%	2+-0	0,04+-0,30 ³	1,85+-0,6	2060

¹ trichomes without multinucleated stems were not considered as clusters

² branchpoint number of wild type trichomes; ³ branchpoint number of clustered trichomes

⁴ F2 cross *elch* to *Ler*

B 2. The *elch* mutant develops nuclear abnormalities in epidermal tissue

The trichome cluster is the only morphological difference that is obvious at low magnification. The nuclear phenotype found in trichome clusters was dissected in more detail; other epidermal cell types were also included in this study. The multiple nuclei phenotype is not trichome specific but was observed in different epidermal cell types. Multiple nuclei in subepidermal cells were observed but are not accessible by whole mount observation.

B 2.1. Multinucleated trichomes form clusters

To visualise leaf trichomes and DNA simultaneously the dye 4',6-Diamidino-2-phenylindol (DAPI) was applied. DAPI is a nucleic acid specific dye but stained cell walls as well under the applied conditions. True leaves three and four (The leaves that appear after the seed leaves, or cotyledons) were stained and trichomes visualised by epi-fluorescence microscopy. 2.3% of all trichomes had more than one nucleus (n=3529) compared to 0% in the wild type (n=2971). The multinucleated phenotype coincides with the cluster like trichome structure (Figure B2 B-E). Only 0,4% of all multinucleated trichomes display the wild type morphology (Figure B2 F; Tab. 2). Incomplete cell walls were not observed in *wild type* and *elch* trichomes.

B 2.2. Multinucleated pavement cells display cytokinesis defects at low frequency

True leaves three and four were stained with DAPI and the DNA was visualized by epi-fluorescence microscopy. Pavement cells were scored for multiple nuclei and incomplete cell walls. In *elch* 0,67% of all pavement cells are multinucleated (n=3448). Cell shape seems unaffected but 17% of all multinucleated pavement cells show incomplete cell walls (Figure B2 H-I), that are characteristic for mutants defective in cytokinesis or cell plate formation (Nacry et al., 2000). In *wild type* plants the number of multinucleated cells is lower with a frequency of 0,22%. Incomplete cell walls have not been observed in *Ws2*.

B 2.3. Stomata in *elch* develop cluster and cytokinesis defects at low frequency

Arabidopsis stomata consist of two guard cells that flank the pore and lack any distinct accessory cells. Patterning mechanisms ensure that stomata are not in contact with each other but are equally distributed among the leaf surface (Geisler et al., 1998). True leaves three and four were stained with DAPI and nuclei visualized by epi-fluorescence microscopy. Stomata

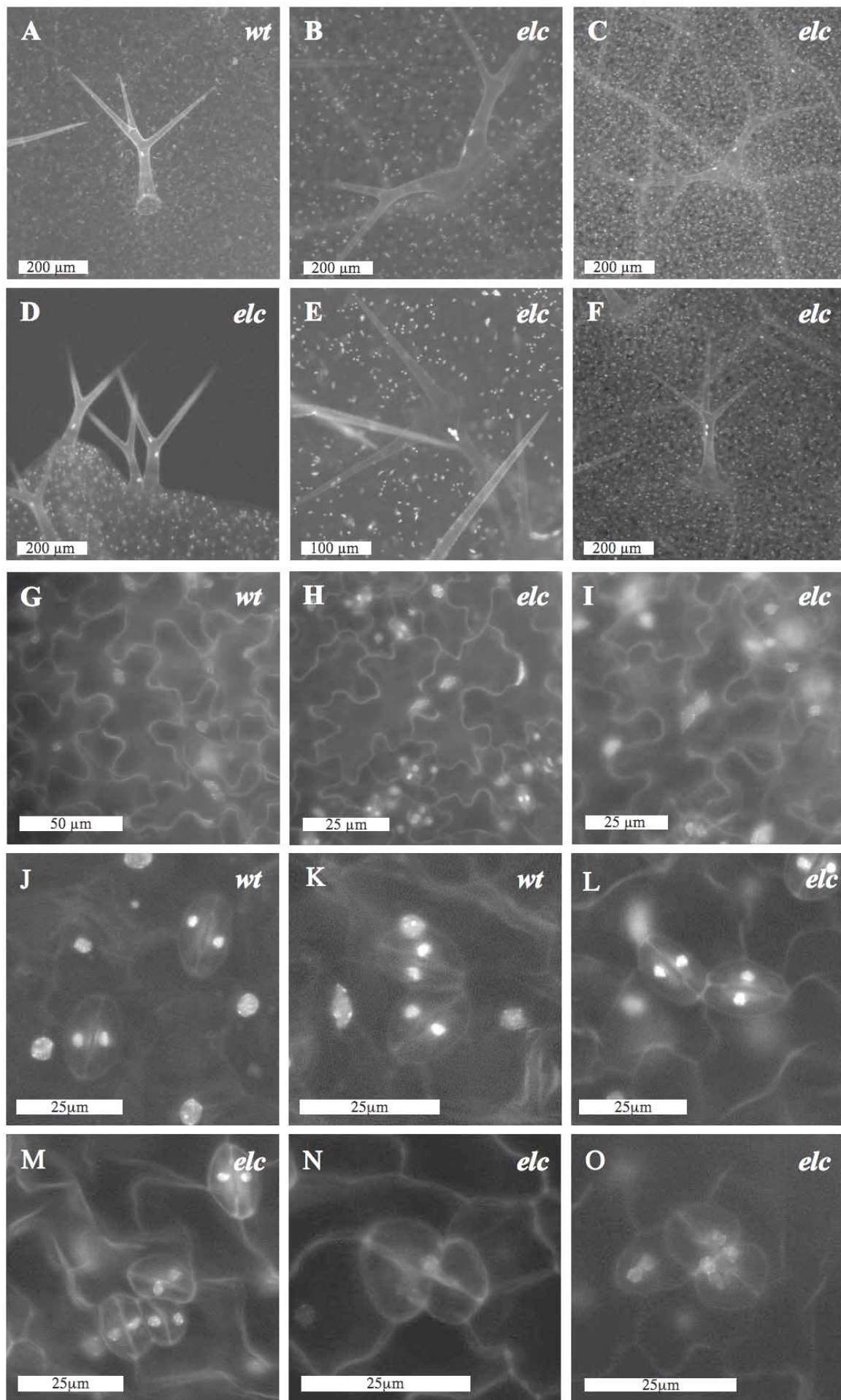






Figure B2: Nuclear phenotype of *elch* in comparison to *wild type* in different epidermal cell types. (A) *Wild type* trichome with single stem and one nucleus. (B-E) Trichomes mutant for *ELCH* with two or more stems and multiple nuclei or with a single stem but two nuclei (F). (G) Nuclear phenotype of leaf pavement cells in *wild type* showing characteristic *lobbing* of the cell wall. (H-I) Multinucleated pavement cell with cell wall stubs in *elch*. Cell wall stubs are characteristic for cell division mutants. (J-K) Phenotype of stomata in *wild type*. Next to normal stomata that are separated by at least one cell (J) stomata cluster are found with up to two stomata touching each other (K). (L-O) In *elch* the number of stomata cluster is raised compared to *wild type*. Three different classes of trichome cluster were defined. Class I cluster in L, class II cluster in M and class III cluster in N and O. Leafs were DAPI-stained, whole mounted and observed by epi-fluorescence microscopy.

were scored for multiple nuclei and cytokinesis defects. More than 21000 stomata were analysed and the occurrence of only one multinucleated guard cell was observed in *elch*. In *wild type* plants no multinucleated guard cells were observed (n = 25000). In this study a low number of stomata clusters (0,03%) was observed in *wild type* (Figure B2 K). The stomata clusters in *wild type* are restricted to two stomata adjacent to each other. These clusters were termed class I cluster while in *elch* two more classes were observed. These are three stomata adjacent to each other without cytokinesis defects (class II cluster) and stomata cluster with

Table 2: Multinucleated cells are predominantly found in trichomes and pavement cells.

	<i>trichome cells</i>	<i>pavement cells</i>	<i>Stomata</i>
multinucleated cells in <i>Ws2</i>	0% (0)	0,221% (4)	0% (0)
n	2971	1807	25691
multinucleated cells in <i>elch</i>	2,30% (81)	0,667% (23)	0,0047% (1)
n	3529	3448	21052

Table 3: *elch* stomata show a phenotypic series of cytokinesis defects. Frequency of different stomata cluster in *wild type* and *elch*.

	 class I*	 class II	 class III	 total**	N
<i>Ws2</i>	0,03%	0 %	0%	0,03%	(100%)
n	(8)	(0)	(0)	(8)	25691
<i>elch</i>	0,27%	0,05%	0,04%	0,36%	(100%)
n	(58)	(10)	(9)	(77)	21052

*The mutant shows significantly higher frequencies than *wild type* (99%, odds ratio test).

**The mutant shows significantly higher frequencies than *wild type* (99%, odds ratio test).

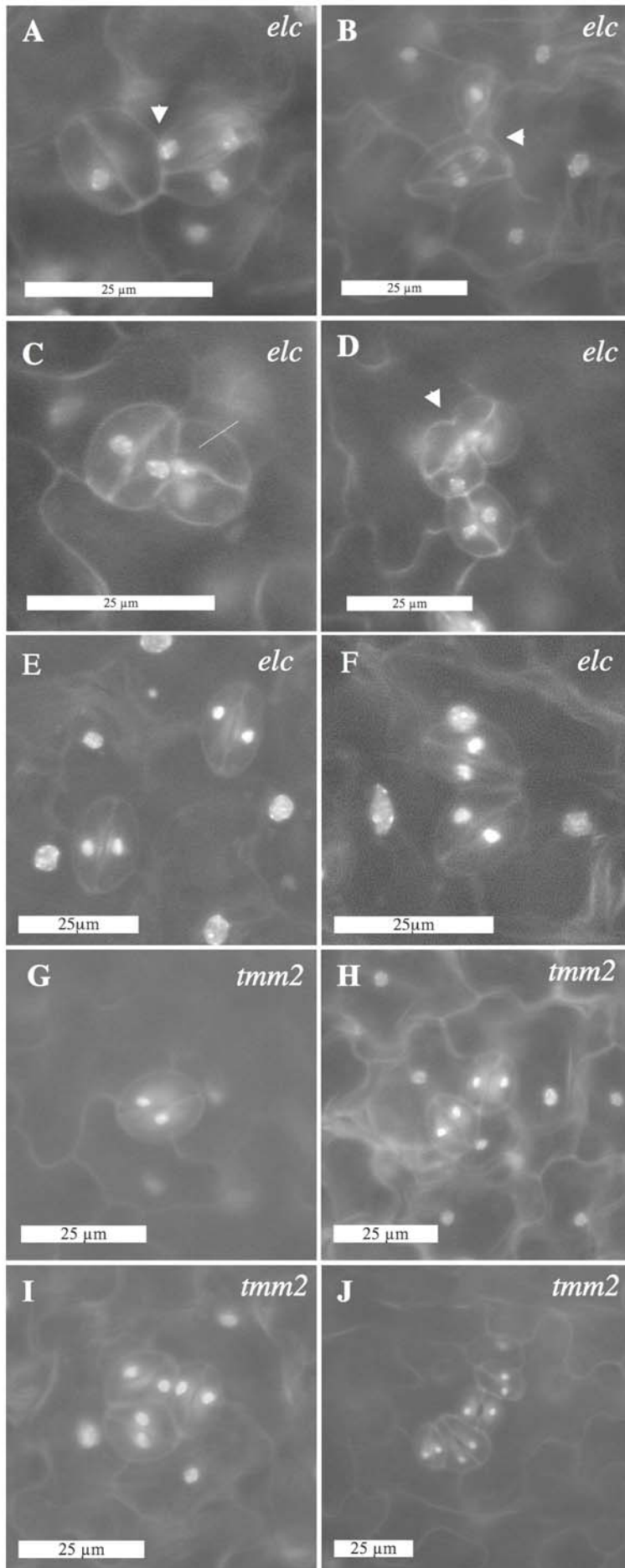


Figure B3 I: Class I/II/III stomata cluster constitute a phenotypic series. (A-D) Incomplete cell walls are found in class I and class II like stomata cluster. (A-C) Unusual arrangement of nuclei in class II like cluster. (B-C) Missing cell wall between two guard cells. (D) Class III like cluster with two guard cells missing a dividing cell wall. The third stomata of this cluster appears to be separated by a complete cell wall. All clusters shown in A-D were considered class III clusters due to obvious cytokinesis defects (Table 3). Leafs were DAPI-stained, whole mounted and observed by epi-fluorescence microscopy. These pictures suggest that stomata clusters in general are an aftereffect of cell division defects. In class I and II clusters these defects are not visible.

Figure B3 II: *elch* stomata clusters are similar to *tmm2* clusters.

(E-J) Comparison *elch* stomata (E) with *elch* stomata cluster (F) and stomata clusters in the *two many mouth mutant2* mutant (*tmm2*). (G) wild type *tmm2* stomata. (H-J) Stomata cluster in *tmm2*. *tmm2* is defective for a leucine-rich repeat receptor-like protein that is implicated in the regulation of orientated cell division. Clusters that consist of two or three stomata are indistinguishable from *elch* stomata cluster. Class III like clusters that have incomplete cell walls and abnormal distributions of nuclei have not been observed in the *tmm2* mutant. Cluster that consist of more than three stomata are observed frequently in this mutant but are absent in *elch*. Leafs were DAPI-stained, whole mounted and observed by epi-fluorescence microscopy.

cytokinesis defects (class III). In the *elch* mutant the number of all classes is increased to 0,36%. Class II and III have not been found in *wild type* (Tab.3). Comparison of different class III clusters suggests that they constitute a phenotypic series (Figure B3). Class III stomata with cytokinesis defects sometimes resemble class I or class II cluster due to the number of stomata involved. These clusters display unusual arrangement of nuclei like two nuclei per guard cell or no nucleus at all (A-D). The left stomata in figure B3A seems to have a complete cell wall but lacks a nucleus. The neighbouring stomata has two nuclei and one of them appears to belong to the left stomata. This indicates that the cell wall in this regions has a hole that is not visible when looking from above. The majority of trichome clusters has no visible cytokinesis defects. In some cases parts of the cell wall are clearly missing (Figure B3 B-D).

B 2.4. DNA content is not altered in multinucleated trichomes

Trichome clusters frequently have two or more nuclei. An obvious question is whether DNA content is altered in multinucleated clusters. During wild type development, trichome cells proceed through four endoreduplication cycles resulting in a final DNA content of 32 C (Hulskamp et al., 1994). If *ELCH* acts at the switch from mitosis to endoreduplication, either of two scenarios could occur in *elch* mutants. Either an incomplete cell division could take place instead of the first endoreduplication cycle. In this case the DNA content of each of the two nuclei should be 16C and the total cellular DNA content would amount to 32C. Alternatively, the first incomplete cell division is followed by the normal trichome differentiation program. In this case each of the two nuclei is 32C and the total DNA content is doubled. When measuring the DNA content of nuclei in *elch* mutants individual nuclei in bi-nucleated *elch* trichomes had a DNA content of approximately 32C (Figure B4) suggesting that the second scenario is true. This result also indicates that the defect occurs at a very early stage during trichome development as the switch from mitosis to endoreduplication itself is considered to take place after trichome selection (Hulskamp, 2004).

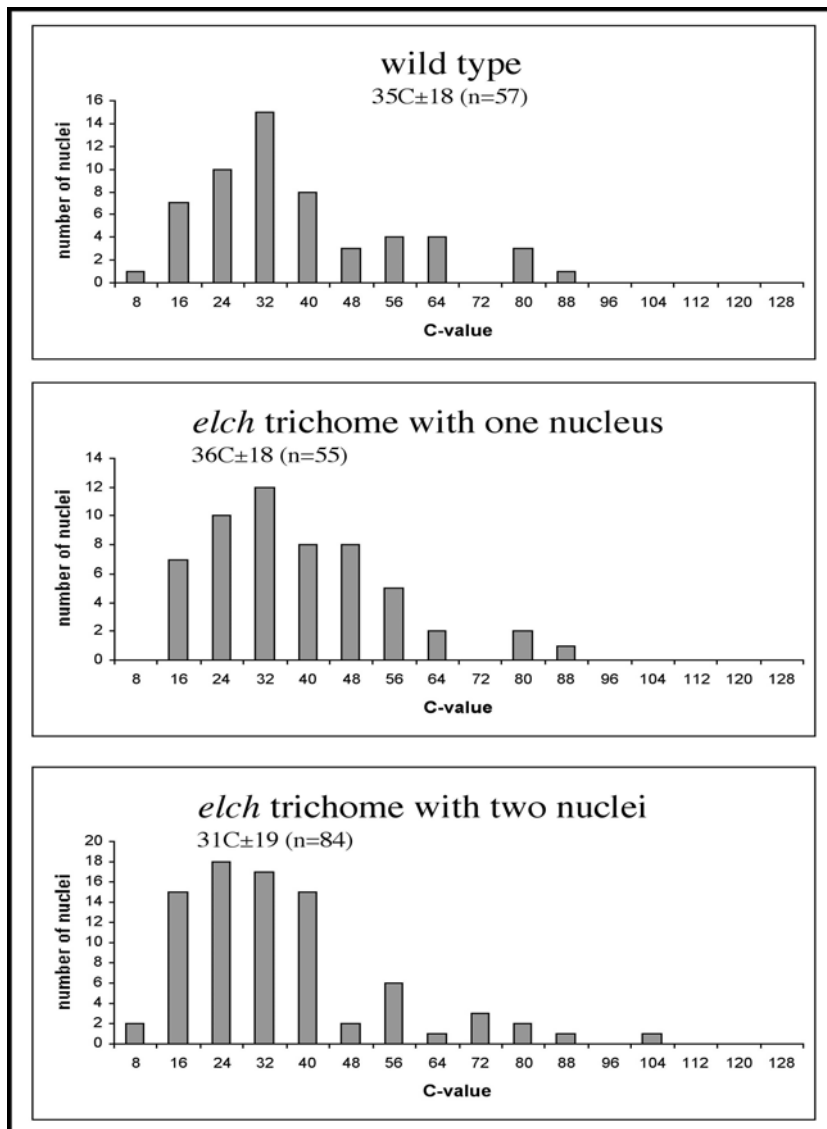


Figure B4: DNA content of single nuclei in *wild type*, *elch* trichomes and multinucleated *elch* clusters is not changed. Comparison of DNA content between *wild type* trichomes (top), *elch* trichomes (one stem, one nucleus) (middle) and *elch* clusters with multiple nuclei (bottom). Whole leaves were DAPI-stained, observed by epifluorescence microscopy and photographed. The pictures were analysed by marking single nuclei and recording the pixel intensity (fluorescence intensity is considered to be linear to DNA-content). The intensity of single nuclei was compared to fluorescence of stomata nuclei. Stomata do not endoreduplicate and therefore have a DNA content of 2C.

B 3. Molecular analysis of the *ELCH* gene

The ELCH protein is similar to yeast Vps23p. VPS23-like genes are found in different animals and plants indicating a conserved function of this gene. *ELCH* expression level was determined in *elch* mutant plants and compared with *wild type* and lines overexpressing *ELCH*. An HA-tagged ELCH protein was expressed in *elch* mutant background and used for the biochemical analysis of ELCH. The construct is functional as it can rescue the cluster phenotype of *elch*.

B 3.1. *ELCH* encodes an UEV domain containing protein

Sequence analysis of *At3g12400* revealed moderate similarity to the *VPS23* gene in yeast (*VACUOLAR PROTEIN SORTING GENE 23*) and *TSG101* gene from mammals (*TUMOR SUSCEPTIBILITY GENE 101*). On protein level *ELCH*, *Vps23p* and *TSG101* share 60% positives and 11% identical amino acids. In contrast to human *TSG101* the *ELCH* gene has no introns. (Figure B5 A). Although overall similarity is not high, the proteins of the three

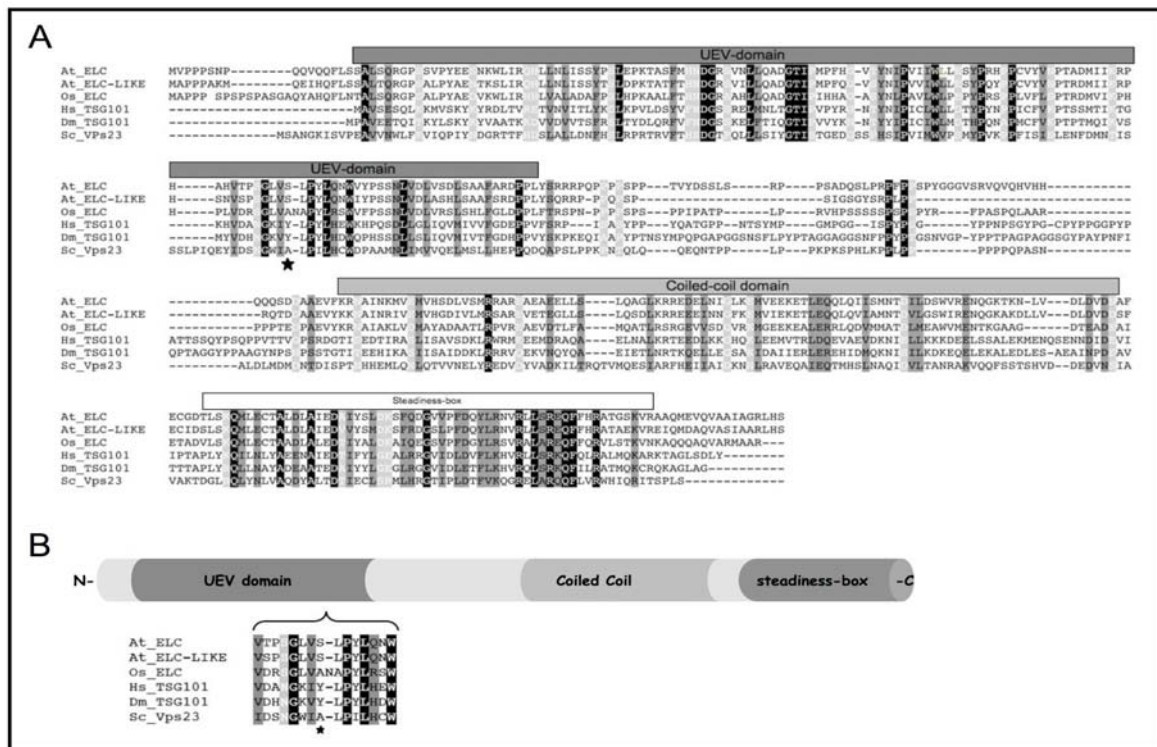


Figure B5: Sequence alignment of UEV domain containing proteins that are similar to *ELCH*.

(A) Alignment of six UEV domain containing proteins from different species show moderate overall similarity but the same domain arrangement. *ELCH* (*At3g12400*) and *ELCH*-like (*At5g13860*) from *Arabidopsis thaliana*, *ELCH* from *Oriza sativum* (*BAD28453*), yeast *Vps23* (*Af004731*), human *TSG101* (*U82130*) and drosophila *TSG101* (*NM_079396*). Letters in a black background indicate identity, dark grey backgrounds indicate strong similarity and a light grey background indicates weak similarity. (B) Schematic presentation of the protein domain arrangement of *ELCH*, *TSG101* and *Vps23*. The characteristic absence of a cysteine that is conserved in UBC domains is depicted below. Multiple sequence analysis was performed with CLUSTALW at the NPS server (Combet et al., 2000).

genes share the same size and conserved domain arrangement (Figure B5 A). At the N-terminus *Vps23p*, *TSG101* and *ELCH* have an ubiquitin conjugating enzyme variant (UEV) domain that is missing a cysteine conserved in all ubiquitin conjugating enzyme (UBC) domains. The UEV domain shows high similarity to UBC domains that are a common feature to all E2. E2 enzymes are known from the proteasom pathway and are required for the covalent attachment of ubiquitin to substrate proteins (Pickart and Rose, 1985).

Table 4: Core components of ESCRT-I,-II, -III complexes are found in *Arabidopsis*, yeast and mammals. The amino acid sequence of ESCRT components from yeast was searched in mammalian and *Arabidopsis* databases. The ten core proteins are conserved to an equal extent between yeast, mammals and *Arabidopsis*. For a detailed analysis of all known ESCRT components see (Winter and Hauser, 2006)

Saccharomyces	ident./simil. to Arabidopsis (%)	Mammals	ident./simil. to Arabidopsis (%)	Arabidopsis	Arabidopsis locus
ESCRT-I					
Vps23p/Stp22p	19 / 33	TSG101	25 / 39	ELCH	At3g12400
	19 / 34		24 / 37	ELCH-like	At5g13860
Vps28p	32 / 47	Vps28	35 / 51	VPS28-1	At4g21560
	31 / 46		35 / 52	VPS28-2	At4g05000
Vps37p	18 / 29	Vps37	9 / 16	VPS37-1	At3g53120
	18 / 29		9 / 16	VPS37-2	At2g36680
ESCRT-II					
Vps22p	24 / 34	EAP30	35 / 43	VPS22	At4g27040
	9 / 15		14 / 19	VPS22	At3g31960
Vps25p	25 / 40	EAP25	33 / 48	VPS25	At4g19003
Vps36p	13 / 24	EAP45	6 / 13	VPS36	At5g04920
ESCRT-III					
Vps2p	26 / 38	Chmp2	55 / 74	VPS2	At2g06530
	18 / 31		34 / 56	VPS2	At1g03950
	19 / 32		35 / 55	VPS2	At5g44560
Vps20p	28 / 41	Champ6	33 / 49	VPS20	At5g63880
	29 / 41		33 / 50	VPS20	At5g09260
Vps24p	30 / 50	Champ3	39 / 57	VPS24	At5g22950
	22 / 40		33 / 47	VPS24	At3g45000
Vps32p	29 / 40	Champ4	33 / 44	VPS32	At2g19830
	30 / 44		36 / 47	VPS32	At4g29160

The covalent attachment depends on a conserved cysteine in the UBA domain of E2 proteins (Sancho et al., 1998). In the central region of the protein a coiled-coil domain is found according to homology comparison and the COILS program (Lupas et al., 1991). At the carboxy terminus a conserved domain is found that has been named steadiness box because it is involved in the control of the stability of TSG101 (Feng et al., 2000) and the interaction

with Vps28p and Vps37 in yeast (Kostelansky et al., 2006). Figure B 5 B shows the domain arrangement of UEV domain containing proteins and the position of the conserved cysteine in UBC domains. A similar degree of conservation is found in other plant and animal species. TSG101 from the invertebrate *Drosophila* and ELCH from the monocotyledon *Oryza (rize)* share the same domain organisation (Figure B5 A). The *Arabidopsis* genome contains a close homolog of *ELCH* (72% identity) sharing the same domain structure and also lacking the critical cysteine in the UEV domain. The main differences are two small deletions in the first half of the protein that do not affect the UEV- or the coiled-coil domain.

Vps23p and TSG101 do not act independently but have been shown to form a complex together with Vps28p and Vps37p. ESCRT-I interacts with components of ESCRT-II and ESCRT-III. Like ELCH, TSG101 and Vps23p the other ESCRT components do not share high similarity but are approximately equally conserved. The percentage of identical amino acids ranges from approximately 10 - 30% (Table 4).

B 3.2. The *elch* mutant is rescued by a *CaMV 35S::ELCH-HA* construct

As a tool for biochemical analysis of ELCH a tagged version of ELCH was overexpressed in plants. Expression *in planta* was chosen because no information was available about posttranslational modifications of the ELCH protein. In an attempt to determine whether overexpression of ELCH results in additional phenotypes the open reading frame of *ELCH* was cloned under the control of the *Cauliflower mosaic virus 35S* promoter (*CaMV35S* or *35S*) that is constitutive active in most plant tissues. This construct was transformed into the *elch* mutant background. From three independent transformation events five transgenic plants were obtained that all showed rescue of the cluster phenotype in the T1 generation. Two of these lines (T2-12 and T2-14) were followed up in the T2 generation and segregated into mutant phenotype and wild type. Line T2-12 yielded two plants with mutant phenotype and 16 plants that were *wild type*. Line T2-14 segregated into seven mutant and 23 *wild type* plants. No additional phenotypes were observed. The expected segregation ratios for a single T-DNA insertion are three *wild type* and one mutant plant in the T2 generation (see Discussion). Line T2-14 was used to test expression levels of *35S::ELCH* in comparison to *elch* and *wild type* by semi-quantitative RT-PCR. Primers for cDNA synthesis and RT-PCR were designed to discriminate *ELCH* and *ELCH-LIKE* and at the same time to detect a putative truncated *elch* transcript (Figure B6A). The RT-PCR showed that higher levels of *ELCH* are detected in the overexpression lines compared to *wild type*.

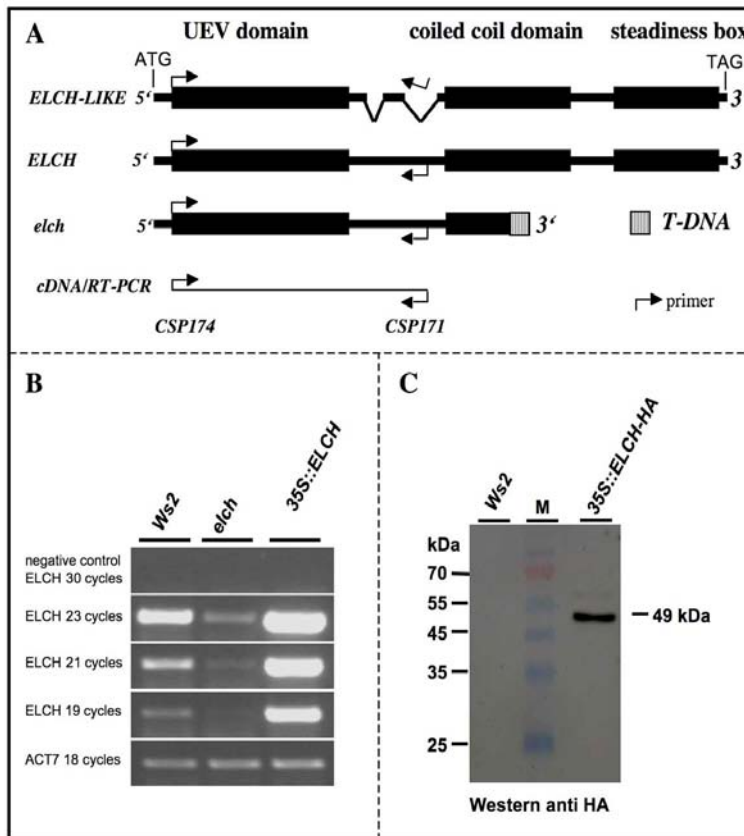


Figure B6: Expression analysis of *ELCH*. (A) DNA structure of *ELCH-LIKE*, *ELCH* and *elch*. *ELCH-LIKE* has two deletions between UEV and coiled coil domain. Primer *CSP171* used for cDNA synthesis and RT-PCR anneals in *ELCH* and *elch* but not in *ELCH-LIKE*. *CSP171* was designed for the region upstream of the T-DNA insertion thereby allowing amplification of *elch* transcript (563 bp). (B) Expression analysis of *ELCH* in comparison with *wild type elch* and *CaMV35S::ELCH* by semi-quantitative RT-PCR. As negative control isolated RNA was used for cDNA synthesis without reverse transcriptase. Transcript of *At3g12400* is abundant in the *elch* mutant though at lower levels compared to *wild type*. (C) *ELCH-HA* protein is expressed in *elch* mutant background and detected by anti-HA antibody. In contrast to the calculated size of 46 kDa the *ELCH-HA* protein runs on denaturing SDS gels at approximately 49 kDa. This observation is consistent with experiments done with TSG101 in mammals.

Furthermore it was possible to show that a certain level of *elch* RNA is abundant in the *elch* mutant (Figure B6B). To determine whether overexpression in addition to *wild type* levels of *ELCH* yields overexpression effects *wild type Ws2* plants were transformed with the same construct. Two independent transformation events yielded ten transgenic plants. All of them were indistinguishable from the *wild type* in the T1 generation. Five of the ten T1 plants were followed up into the T2 generation. No difference from *wild type* was observed. For biochemical analysis of *ELCH* a similar construct was cloned with the hemagglutinin sequence of *influenza virus* (HA-tag) fused to the C-terminus of *ELCH* for detection and purification. Therefore the open reading frame of *ELCH* was fused to the HA-tag and expressed ectopically under the *CaMV::35S* promoter. The HA-tag was selected because its short sequence likely does not interfere with protein function of *ELCH*. Furthermore small fusion proteins tend to express better than large ones. The use of the *CaMV 35S* promoter promised high protein expression *in planta* that is desirable for protein work. The functionality of the construct was tested by transformation into the *elch* mutant. The *35S::ELCH-HA* construct rescues the cluster phenotype in T1 plants. Expression of HA-tagged *ELCH* was determined by western blotting with anti-HA antibody resulting in a clear signal that is absent in lanes loaded with *wild type* protein (Figure 6 C). The *ELCH-HA* protein runs at 49 kDa slightly higher than its calculated size of 46 kDa. This is consistent

with observations with the TSG101 antibody in animals (Bishop and Woodman, 2001) and human cell lines (see appendix E1). The line that was transformed with the *CaMV 35S::ELCH-HA* construct will be referred to as ELCH-HA line or ELCH-HA plants.

B 4. Biochemical analysis of ELCH

In order to determine whether an ESCRT-like pathway is conserved in *Arabidopsis* known properties of yeast Vps23p and ESCRT-I were analysed. The HA tagged ELCH was used in several experiments to determine binding capacity, complex formation and ELCH/ESCRT-I interacting proteins. Ubiquitin-binding capacity was shown *in vitro* and *in vivo*. Complex formation was indicated by gelfiltration and verified by immunoprecipitation of ELCH-HA proteins. Putative targets or interacting proteins of ELCH/ESCRT-I were isolated by coimmunoprecipitation and identified by mass spectrometry.

B 4.1. ELCH-HA protein binds to Ubiquitin *in vitro*

The central role of VPS23/TSG101 in the ESCRT-I complex appears to be the binding of ubiquitinated target proteins from other upstream-acting VPS proteins. To test whether ELCH has the ability to bind to ubiquitin, pull-down experiments were performed with ubiquitin agarose (Figure B7). Protein extracts from ELCH-HA plants were incubated with ubiquitin agarose and protein G agarose as a negative control. ELCH-HA binds to ubiquitin but not protein G agarose. To exclude unspecific binding of random protein to the ubiquitin agarose protein extract from *elch* mutant plants was incubated with ubiquitin and protein G agarose. In both cases no signal was obtained.

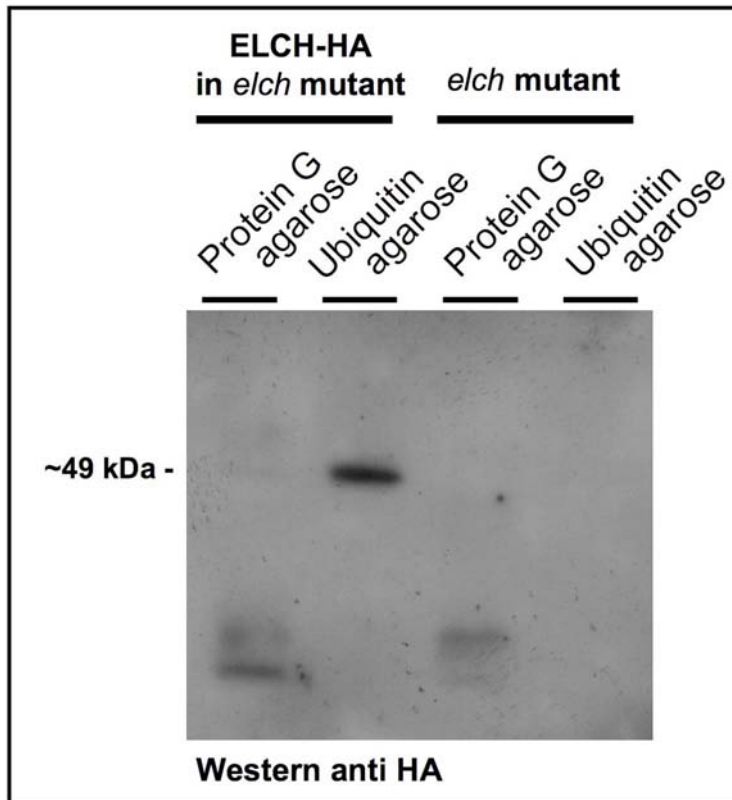


Figure B7: ELCH-HA binds Ubiquitin *in vitro*. ELCH-HA pulldown assay with ubiquitin agarose and protein G agarose as negative control. Ubiquitin and protein G beads were incubated with protein extracts from plants expressing the ELCH-HA constructs and *elch* plants. The faint lower bands are HA antibody cross-reacting with protein G. The HA antibody recognizes specifically ELCH-HA as can be seen in the control experiment with protein extract from *elch* plants not carrying an HA construct.

B 4.2 ELCH-HA protein binds ubiquitinated proteins *in vivo*

The ELCH-HA construct was used to test whether ELCH binds ubiquitinated proteins *in vivo*. ELCH-HA was isolated by immunoprecipitation from plant extracts and the eluate was probed for ubiquitinated proteins. Extracts from ELCH-HA were incubated with basic beads (no antibody) or HA antibody beads. Western blotting shows the cross reaction band of the light antibody chain at 26kDa and signals from ubiquitinated proteins in particular around 100 kDa. No signal was detected with the control basic beads (Figure B8 A). Basic beads and HA beads were loaded with 3 mg of protein. The signal is specific for ubiquitin as control FLAG-tagged ubiquitin produces a specific band around 10 kDa (see appendix E2). To exclude unspecific binding to the antibody itself *wild type* (3,4 mg) and ELCH-HA extracts (4,9 mg) were incubated with HA beads only. Next to the cross reacting band from the light antibody chain a signal was either detected in the input or the eluate containing ELCH-HA. No signal was detected in the *wild type* control (Figure B8 B).

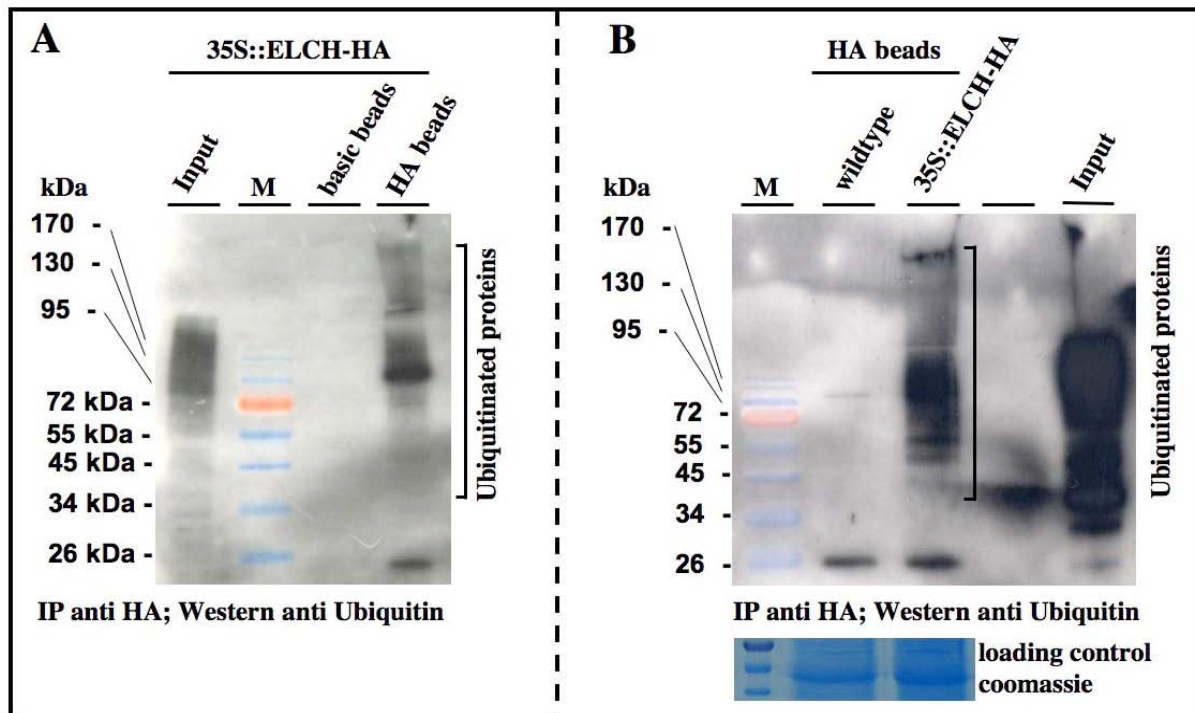


Figure B8: ELCH-HA binds ubiquitinated proteins in vivo. (A) Protein extract from ELCH-HA expressing plants was incubated with basic beads and HA beads. (B) To exclude unspecific binding of ubiquitinated proteins to the antibody itself HA beads were incubated with protein extract from wild type and ELCH-HA expressing plants. Equal amounts of protein from wild type and 35S::ELCH-HA separated by PAGE and stained with coomassie. Ubiquitinated proteins were detected by western blotting anti ubiquitin.

B 4.3 ELCH-HA protein is part of a high molecular weight complex

The ESCRT pathway in yeast and mammals was shown to consist of a protein network with distinct sub-complexes. To determine whether ELCH is part of a complex ELCH-HA extract was examined by gelfiltration. ELCH eluted in early fractions between 200 and 600 kDa indicating that ELCH is part of a high molecular weight complex (Figure B9 A). To verify this observation ELCH-HA was immunoprecipitated from plant extracts, separated by PAGE and visualised by silver staining. Bands from proteins that coprecipitated were cut out and analysed by MALDI-TOF mass spectrometry. Under stringent washing conditions a 49 kDa band was identified as ELCH (At3g12400) while two bands of approximately 24-26 kDa turned out to be VPS28 and VPS37 (Figure B9 B). Peptides of two isoforms of VPS28 were found [VPS28-1 (At4g21580) / VPS28-2 At4g05000] as well as two isoforms of VPS37 [VPS37-1 (At3g53120) / VPS37-2 (At2g36680)]. The result of the mass spectrometry data is summarised in Table 5. The isoforms of VPS28 and VPS37 respectively are highly similar and differ in only few amino acid residues. The amino acid sequences of At4g05000 and At4g21580 are 91% identical while At3g53120 and At2g36680 share 84% identical amino acid residues.

Table 5: ESCRT-I components identified with MALDI-TOF mass spectrometry. Shown is the locus number, the internal identification number of the mass spectrometry data and the score for each hit. A score greater than 60 is considered significant. Some proteins were identified more than once in independent immunoprecipitation experiments. For identified peptides and further details see Appendix E3.

#	Protein	MS-ID	Score
1	ELCH At3g12400	4487	183
2	ELCH At3g12400	4493	213
3	ELCH At3g12400	4692	192
4	VPS28/1 At4g21560	4557	127
5	VPS28/1 At4g21560	4485	79
6	VPS28/2 At4g05000	4557H a	82
7	VPS37/1 At3g53120	4556H1	119
8	VPS37/2 AT2g36680	4556H 2	102
9	Ig kappa chain constant region	4486a_seq	86

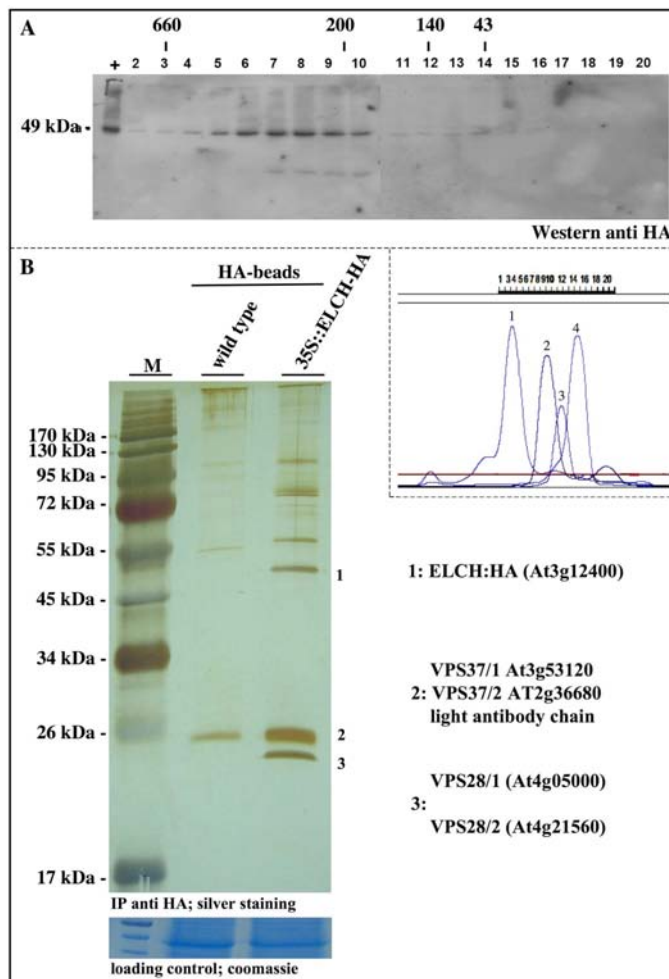


Figure B9: ELCH is part of a high molecular weight complex. (A) Gelfiltration assay using protein extract from transgenic CaMV 35S::ELCH-HA plants. Protein size markers are indicated in the top in kilodaltons. The expected size of ELCH-HA is approximately 49 kD judged from SDS PAGE. The column was calibrated with 1. thyroglobulin (660 kDa), 2. β -amylase (200 kDa), 3. alcohol-dehydrogenase (140 kDa), 4. ovalbumin (43 kDa). (B) Immunoprecipitation assay of ELCH-HA. HA antibody beads were incubated with protein extract from *wild type* and transgenic CaMV 35S::ELCH-HA plants. Marked bands were identified by mass spectrometry as components of ESCRT-I. VPS37 co-migrates with the light chain of the HA antibody. Mass spectrometry analysis identified peptides of the antibody and both isoforms of VPS28 as well as both isoforms of VPS37. Equal amounts of extract from *wild type* and 35S::ELCH-HA was stained with coomassie as loading control.

B 5. ESCRT-I interacting proteins in *Arabidopsis*

In order to determine unknown interactors or putative targets of ELCH/ESCRT-I immunoprecipitation of ELCH-HA was performed. Besides the bands that were identified as ESCRT-I components a number of bands were observed that seem to interact with ELCH/ESCRT-I (Table 6). Mass spectrometry revealed a 26 kDa protein with unknown function that contains an UBA domain while the others are subunits of the vacuolar ATPase.

Table 6: Putative targets/associated proteins of ELCH/ESCRT-I identified with MALDI-TOF mass spectrometry. Shown is the locus number, the internal identification of the mass spectrometry data and the score for each hit. A score greater than 60 is considered significant. For DET3 (10610) a score greater than 78 is significant. Some proteins were identified more than once in independent immunoprecipitation assays. For identified peptides and further details see Appendix E4.

#	Protein	MS-ID	Score
10	UBA domain protein AT5g53330	4486	85
11	UBA domain protein AT5g53330	4497H	162
12	VHA-a3 AT4G39080	4491Re	64
13	VHA-a3 AT4G39080	4491UBQ*	54
14	VHA-A AT1G78900	4492	254
15	VHA-B AT1G76030	4457	127
16	DET3 AT1G12840	10610	101

* mass spectrometry data was reanalysed with regard to ubiquitin modification. Mascot analysis of VHA-a3 with regard to ubiquitin modification was performed by Stephan Müller (Center for Molecular Medicine Cologne)

B 5.1. *Arabidopsis* ESCRT-I complex is associated with a UBA domain protein

A band slightly larger than 26 kDa was identified as At5g53330 (Figure B10 A). At5g53330 is listed as unknown protein in NCBI and is predicted to have a pI of 6,37 and a molecular weight of 24,3 kDa. It consists of 221 amino acids and is prolin rich (11.8%). In contrast to all ESCRT proteins it has no coiled coil domain (Lupas et al., 1991). A search for potential trans membrane domains of At5g53330 adduced negative results. Besides its high prolin content the only other known feature is a UBiquitin-Associated (UBA) domain at its carboxy terminus (aa 180-216). The UBA domain was predicted by InterPro (EMBL-EBI). At5g53330 is a single copy gene in *Arabidopsis* and no orthologs in other organisms have been identified by sequence analysis. Blast search in the mouse proteom found very weak similarity to UBAP1 (UBiquitin-Associated Protein1) mostly due to the UBA domain. The function of UBAP1 is unknown but it has been implicated in tumor suppression (Qian et al., 2001). A

known protein containing a functional UBA domain is RAD23. Its UBA domain has been shown to bind ubiquitin (Chen et al., 2001). The sequence alignment of the UBA domain of UBAP1, At5g53330 and Rad23 shows 11% identical, 31% strongly similar and 4,4% weakly similar amino acids (Figure B10 B).

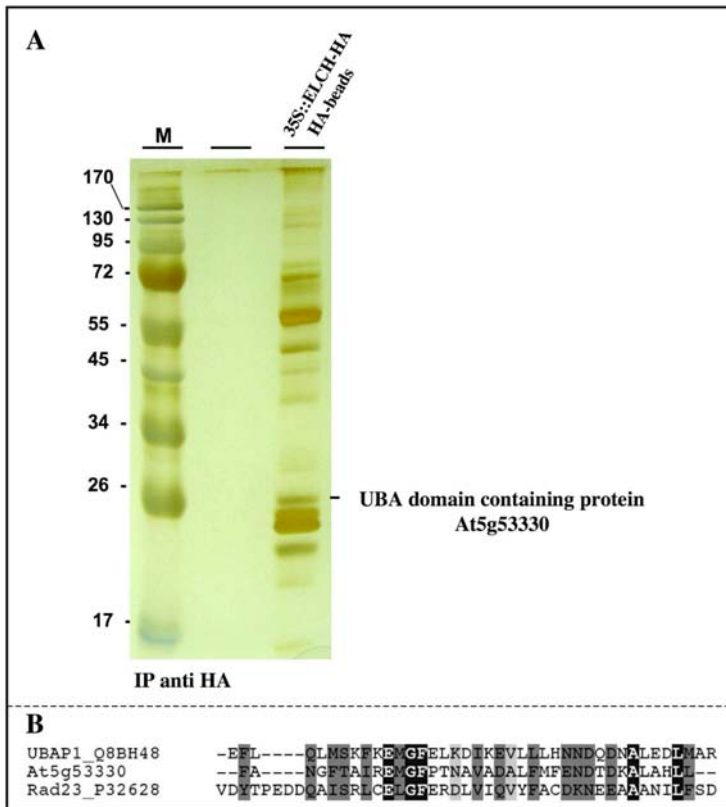


Figure B10: UBA domain protein At5g53330 coimmunoprecipitates with ELCH-HA. A) Immunoprecipitation assay of ELCH-HA. HA antibody beads were incubated with protein extract from ELCH-HA plants. The marked band was identified by mass spectrometry as UBA domain protein At5g53330. B) Alignment of the UBA domain of At5g53330 (aa 180-216), UBAP1 (aa 459-498) and Rad23 (aa 351-395). Identical: black (11%); strongly similar: dark grey (31%); weakly similar: light grey (4,4%). Multiple sequence alignment was done with CLUSTALW at the NPS server (Combet et al., 2000).

B 5.2. Subunits of V-ATPase coimmunoprecipitate with ESCRT-I complex

Two additional bands were identified in the complex purification experiment next to ELCH, VPS28 and VPS37. Mass spectrometry analysis showed that these bands correspond to two subunits of the vacuolar ATPase (Figure B10 A). The vacuolar ATPase in *Arabidopsis* consist of 14 subunits ranging from seven to 110 kDa in size. The smaller subunits have been observed but have not been identified by mass spectrometry. The 110-120 kDa band was identified as VHA-a3, the largest subunit of the vacuolar ATPase. VHA-a3 is one of three isoforms in the *Arabidopsis* genome and was shown to localize to the tonoplast (Dettmer et al., 2006). The 69 kDa band yielded VHA-A, one of three identical subunits that are part of each V1 subcomplex. VHA-A has ATP binding capacity and forms together with VHA-B a large proportion of the cytosolic ball-like structure.

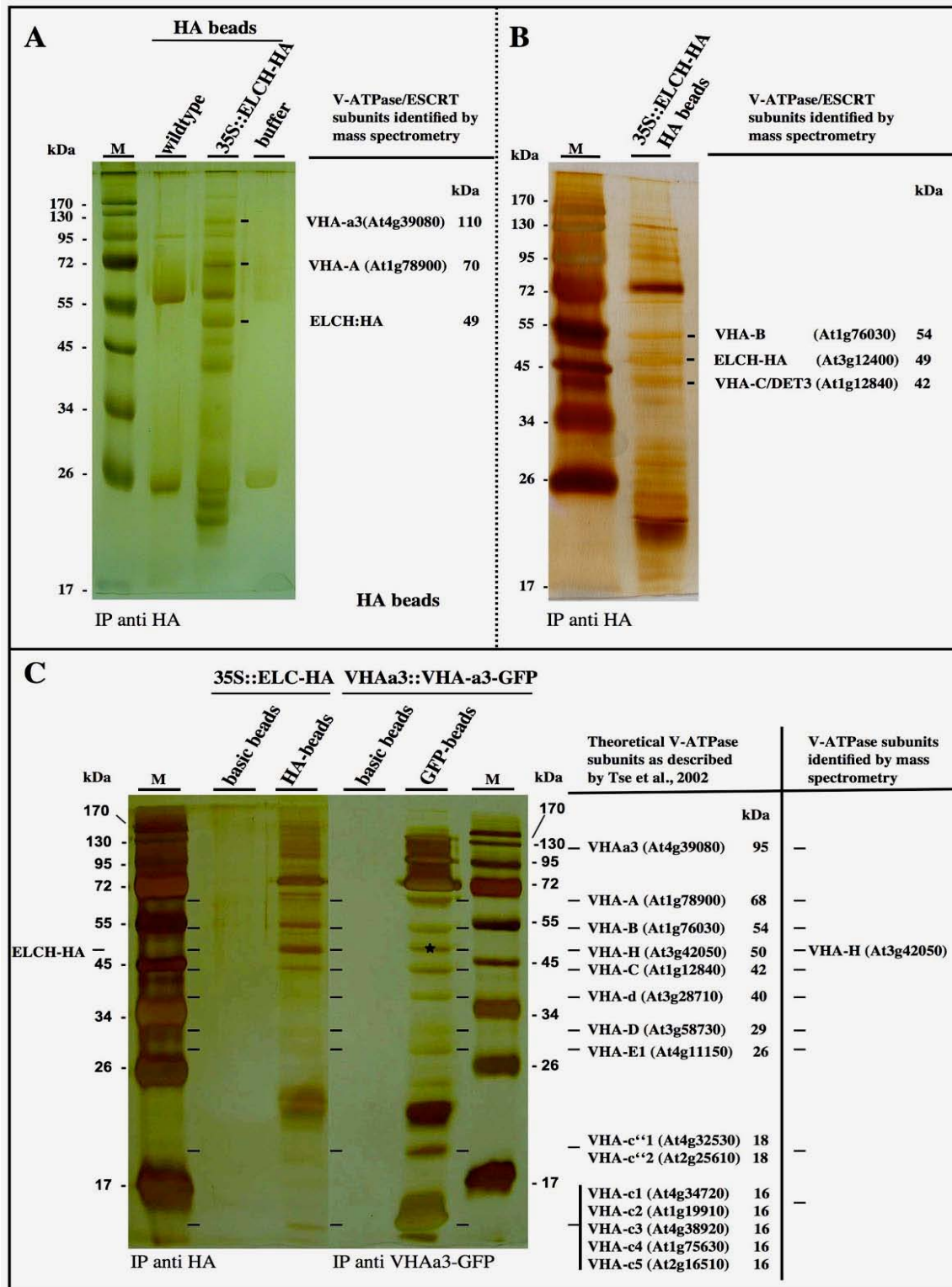


Figure B11: Subunits of the V-ATPase coimmunoprecipitate with ELCH-HA. Immunoprecipitation assay of ELCH-HA and VHA-a3-GFP. (A) Protein from wild type plants (8 mg), 35S::ELCH-HA plants (15 mg) or buffer alone were incubated with HA antibody coated beads. VHA-a3 and VHA-A coimmunoprecipitated with ELCH-HA. (B) VHA-B and DET3 were identified in this assay. The column was loaded with 15,4 mg protein. (C) Extracts from 35S::ELCH-HA and VHA-a3::VHA-a3-GFP were incubated with HA/GFP antibody coated beads or with basic beads as control in parallel and run on the same gel. In both cases protein was extracted from 0,9 g plant material. The eluates were subjected to PAGE and silver stained. A similar band pattern suggests that bands of the ELCH-HA coimmunoprecipitation that were not identified by mass spectrometry are subunits of the V-ATPase as well. Horizontal orientation bars indicate same size. On the right side known V-ATPase subunits are listed together with the VHA-H subunit that was identified by mass spectrometry (asterisk)

Further immunoprecipitations using higher input levels and adjusted washing conditions revealed a band pattern that is characteristic for the vacuolar ATPase (Arai et al., 1988). Two of these bands were identified as subunits VHA-B and VHA-C/DET3 (Figure B11 B) that are both part of the cytosolic V1 complex. VHA-A, VHA-B and DET3 were identified with moderate to high scores well above significance value (Table 5). The score of VHA-a3 (4491Re) is low and just above significance level probably due to its amino acid composition and topology. VHA-a3 is an integral membrane protein whose amino acids 1 – 405 make up the main cytosolic domain while amino acids 406 – 821 hold nine transmembrane domains that contain fewer Trypsin cutting sites (Trypsin cuts after lysine and arginine unless the next amino acid is a proline). There are 53 Trypsin sites in the first 405 amino acids (seven recovered peptides) with only 22 in the remaining 438 amino acids of the protein (2 recovered peptides). Although most theoretical subunits of the V-ATPase were observed, only four were identified by mass spectrometry due to low protein levels. To support the idea that these are indeed subunits of the V-ATPase, immunoprecipitation with VHA-a3-GFP (Dettmer et al., 2006) was performed in parallel together with ELCH-HA and separated on the same gel. The band pattern of proteins that coprecipitate with VHA-a3-GFP resembles the one obtained from the ELCH-HA precipitation assay (Figure 11 C) and the pattern described in literature (Arai et al., 1988). Exemplary the 49 kDa band was isolated and analysed by mass spectrometry. Peptides from VHA-H were identified indicating that other VHA subunits coprecipitate with VHA-a3-GFP (Figure 11C, Table 7).

Table 7: VHA-H coimmunoprecipitates with VHA-a3:GFP. For identified peptides and further details see Appendix E5.

#	Protein	MS-ID	Score
17	VHA-H	10632	149

B 5.3. VHA-a3-GFP of the V0 subcomplex is ubiquitinated

The VHA-a3 subunit of the V-ATPase coprecipitates with the ESCRT-I complex. As VHA-a3 is a trans-membrane protein with cytosolic domains it represents a putative target of the MVB pathway. VHA-a3 was therefore investigated for ubiquitin modification. Analysis by mass spectrometry revealed two amino terminal peptides whose masses differ in a way characteristic for ubiquitin modification. Trypsin digestion prior to MALDI-TOF mass spectrometry of ubiquitinated proteins leaves two glycins of the Ubiquitin carboxy-terminus bound to the target protein. This leads to a characteristic mass difference of 114 between the observed and theoretical mass value which is used to identify ubiquitinated peptides. The mass spectrometry data indicates that lysin 56 (K56) and lysin 68 (K68) of VHA-a3 are putative acceptor sites for ubiquitination (Tab. 8). Both lysins are located in the cytosolic amino terminal region of VHA-a3 (Kluge et al., 2004; Nishi and Forgac, 2002).

Table 8: Mass spectrometry analysis indicates that VHA-a3 is ubiquitinated. Theoretical peptide masses and observed masses of trypsin digested VHA-a3 after MALDI-TOF mass spectrometry. The mass difference of 114 suggest that K56 and K68 are ubiquitinated.

Position	Sequence	calculated mass* MH+	observed mass m/z	mass difference	source**
51 – 61	DLNSEKSPFQR	1320.6542	1320.57	0.08	4491UBQ
51 – 61	DLNSEKSPFQR	1320.6542	1434.72	114.0658	4491UBQ
57 – 68	SPFQRTYAAQIK	1409.7535	1523.87	114.1165	4491UBQ
62 – 69	TYAAQIKR	950.5418	1064.56	114.0182	4491UBQ

* mass calculated with ExPASy tool PeptideMass (Wilkins et al., 1997)

** see appendix E3

To confirm that VHA-a3 is ubiquitinated, a GFP tagged version of VHA-a3 (Dettmer et al., 2006) was immunoprecipitated with GFP antibody beads and probed with ubiquitin and GFP antibodies. To monitor Ubiquitin- and GFP signals simultaneously two-color western analysis was performed using near infrared imaging (Odyssey®). The secondary antibodies were coupled to dyes that emit light at 700 nm and 800 nm respectively thereby allowing the discrimination of two signals on the same blot. Proteins marked with Ubiquitin antibodies and coomassie stained proteins were detected in the 700 nm channel giving a red signal (Figure

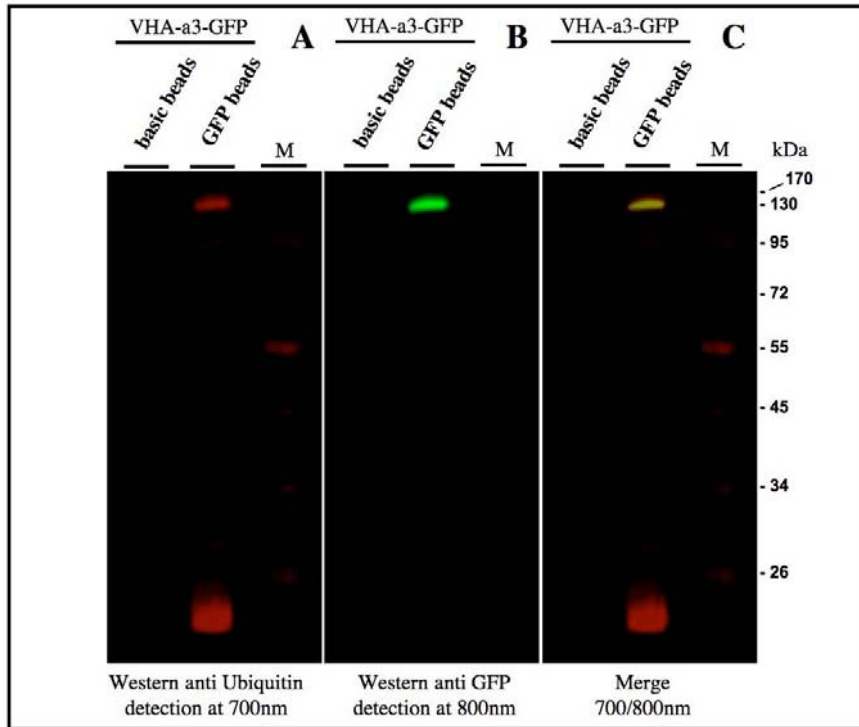


Figure B12: VHA-a3 is modified with Ubiquitin. VHA-a3-GFP was immunoprecipitated and probed with antibodies against Ubiquitin and GFP. Two-colour Western analysis of VHA-a3-GFP detected ubiquitin at 700 nm (red, A) and GFP at 800 nm (green, B). The merged image shows VHA-a3-GFP at 130 kDa in yellow (C) indicating that VHA-a3 is ubiquitinated. The size and the fact that only one distinct band is visible indicates that VHA-a3 is monoubiquitinated. In this assay basic beads and GFP beads were incubated with 8,2 mg protein each.

B12 A) while GFP marked protein was detected at 800 nm giving a green signal (Figure B12 B). Merging of both pictures revealed a yellow band at 130 kDa showing that VHA-a3GFP is ubiquitinated (Figure B12 C). The calculated mass of VHA-a3-GFP is approximately 120kDa. Modification with a single Ubiquitin would lead to an approximate weight of 130 kDa which is observed in silver stained gels (Figure B11 C) and on Western blots (Figure B12 B - C). Next to the 130 kDa band a strong signal is detected below 26 kDa which represents the cross-reaction with the light chain of the antibody used for immunoprecipitation.

B 6. The *ELCH* pathway and microtubule dependent processes are closely linked. The cytokinesis phenotype of *elch* is reminiscent to the phenotype of the *tfc-a* mutant that has cell division defects (Kirik et al., 2002). *tfc-a* mutants have smaller under-branched trichomes that form multinucleated clusters (Table 8). Other cell types are multinucleated as well (Kirik et al., 2002; Steinborn et al., 2002b). To examine whether *elch* is involved in microtubule dependent processes the double mutant *elc/tfc-a* was made and the cellular morphology compared to the single mutants. Growth behavior of *wild type* and *elch* was compared under

different concentrations of microtubule modulating drugs Furthermore the microtubule arrangement of trichomes and dividing pavement cells was analysed for obvious changes.

B 6.1. Genetic interaction of *ELCH* and *Tubulin-Folding Cofactor A*

Tubulin Folding Cofactor A (TFC-A) or *KIESEL* (*KIS*) belongs to the *PILZ* group genes (Steinborn et al., 2002b). Like the other members of this group *KIS/TFC-A* encodes a chaperone important for supporting the correct formation of assembly competent α/β tubulin heterodimers (Dobrzynski et al., 1996; Lewis et al., 1996; Martin et al., 2000; Tian et al., 1996). Strong *kis* mutants have multiple nuclei and are embryo lethal (Steinborn et al., 2002a). For the genetic analysis the weak *kis*-T1 mutant was used that displays a mild growth defect, slightly reduced cell division frequency, reduced trichome branching and cells with multiple nuclei (Kirik et al., 2002). The double mutant shows a synergistic phenotype: Plants are smaller than the single mutants, leaf edges are bend downwards and the leaf surface is disturbed (Figure B13 A-C). The frequency of trichomes with more stems is drastically increased (16,29%; n=743) as compared to *elch* (1,93%; n=3529) and *tfc-a* (0,81%; n=1356) (Table 9). For observation on the cellular level whole leafs were stained with propidium iodide (PI) embedded in agarose, sectioned and visualized by confocal laser scanning microscopy (CLSM). Epidermal pavement cells are reduced in size (Figure B13 G-H), the leaf architecture is grossly disturbed (Figure B13 J-L) and a large number of cells contain multiple nuclei. Some cells display abnormal nuclear morphology such as nuclear bridges that connect two or more nuclei. (Figure B13 M-O).

Table 9: The cluster frequency is raised in the *tfc-a/elc* double mutant.

	<i>cluster frequency</i>	<i>stems/cluster</i>	<i>Branchpoints</i>	<i>Nuclei/cluster</i>	<i>N</i>
<i>Ws2</i>	0% ¹	--	1,62+-0,50 ²	--	2971
<i>elch (Ws2)</i>	1,93%	2,03+-0,17	1,04+-0,69 ³	1,97+-0,34	3529
<i>tfc-a (Ws2)</i>	0,81%	2,09+-0,3	0+-0	2,27+-0,65	1356
<i>tfc-a/elch</i>	16,29%	2,13+-0,43	0,32+-0,52 ³	2,43+-0,59	743

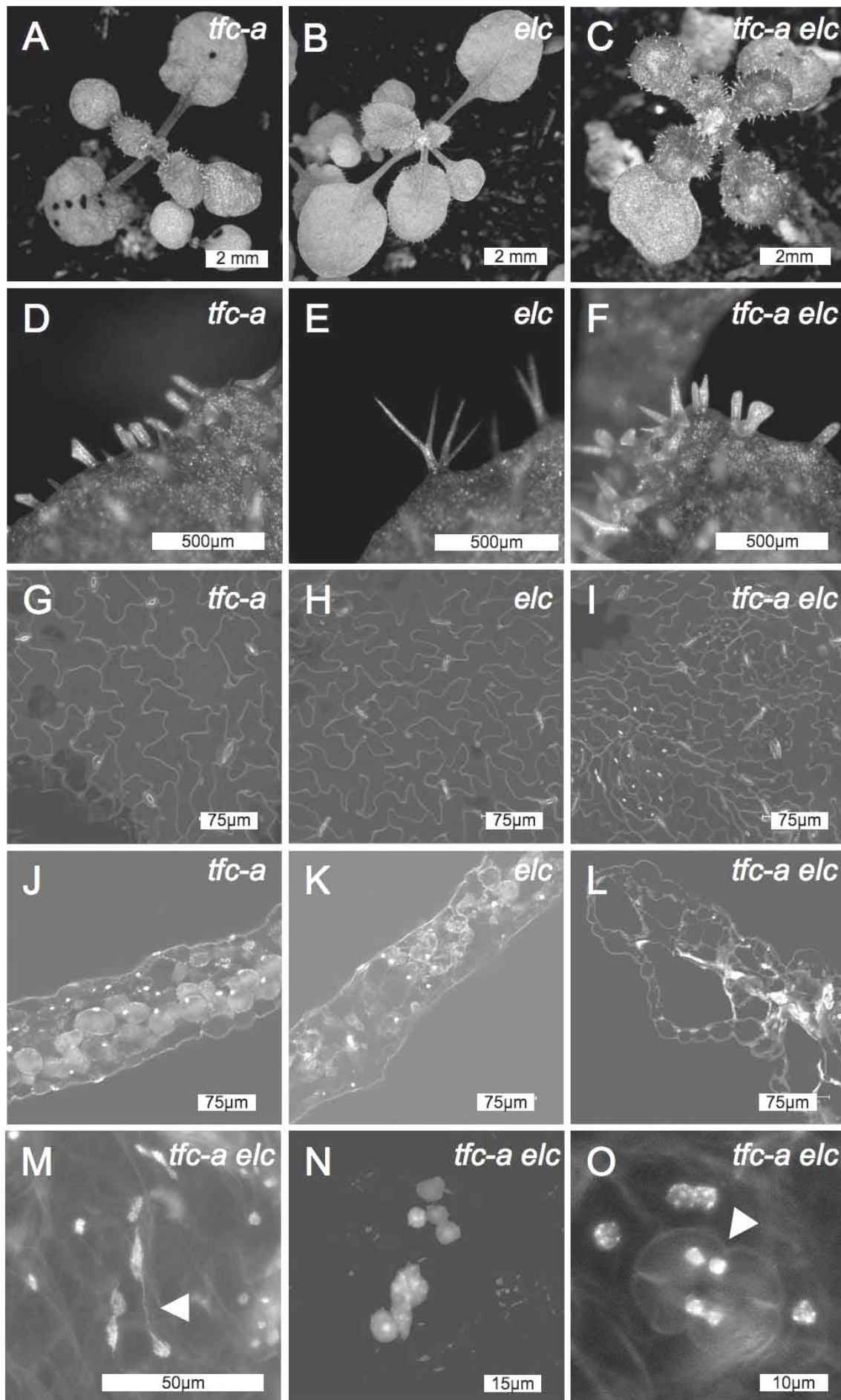


Figure B13: Genetic analysis of *elch* and *tfc-a* mutant. Comparison of *tfc-a* (A), *elc* (B) and *tfc-a/elc* (C) mutant rosette leaves. Comparison of *tfc-a* (D), *elc* (E) and *tfc-a/elc* (F) mutant trichomes. Note that the cluster frequency is strongly enhanced in the double mutant. Comparison of *tfc-a* (G), *elc* (H) and *tfc-a/elc* (I) mutant epidermal pavement cells. Cell size is reduced in the double mutant. Comparison of *tfc-a* (J), *elc* (K) and *tfc-a/elc* (L) sections of rosette leaves. The integrity of the leaf is strongly disturbed in the double mutant. Higher magnification of propidium iodide stained leaf sections of *tfc-a/elc* double mutant (M-O). Multinucleated cells are frequently observed in the *tfc-a/elc* double mutants. Nuclear anomalies like nuclear bridges (M) and high numbers of nuclei per cell (N) are found frequently. In very rare cases multinucleated stomata with incomplete cell walls were observed (O). (A-F) young plants were observed under a stereomicroscope. (G-O) Whole leaves were stained with propidium iodide embedded in agarose, sectioned and visualized by CLSM.

B 6.2. The *elch* mutant is hypersensitive to taxol

To support the genetic evidence that microtubules influence the ESCRT pathway drug studies were undertaken using agents that influence microtubules in various ways: Paclitaxel (Taxol) stabilizes microtubules leading to grave disturbance especially in dividing cells (Jordan et al., 1998; Schiff et al., 1979). While *wild type* plants are still able to grow on 3 μ M paclitaxel growth of the *elch* mutant is completely abolished (Figure B14). This experiment was repeated three times with the first two showing this effect while the third experiment had no effect at all. It is assumed that the paclitaxel used had decayed and this experiment has to be

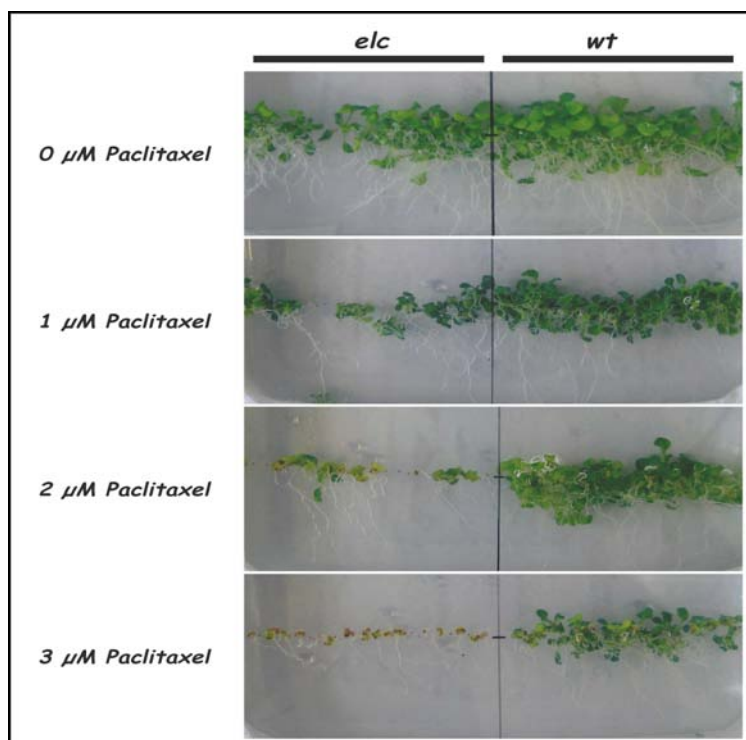


Figure B14: The *elch* mutant is hypersensitive to paclitaxel (Taxol). *elch* and *wild type* plants were grown together on MS plates containing 0, 1, 2 and 3 μ M paclitaxel. Growth differences are observed at 2 and 3 μ M paclitaxel. The *elch* mutant does not survive 3 μ M of this drug.

confirmed. The second drug used is Oryzalin that in contrast to Paclitaxel destabilizes microtubules by slowing down microtubule assembly (Hugdahl and Morejohn, 1993). Growth

on 0,2-0,5 μM oryzalin had no different effect on *elch* and *wild type*. At 0,5 μM growth of *elch* and *wild type* was strongly retarded and both died after three weeks (data not shown). The third drug that was used has a similar effect like Oryzalin. Nocodazole is known as antimitotic agent that disrupts microtubules by binding to β -tubulin and preventing formation of some of the disulfide linkages (Luduena and Roach, 1991). *Wild type* and *elch* was grown on 0, 10, 100 and 1000 μM nocodazole. No difference was observed between *wild type* and *elch* mutant but both lines showed slight growth retardations at 1000 μM of the drug (data not shown).

B 6.3. Microtubule organization of *elch* trichomes and dividing cells is not visibly altered

The genetic studies and the drug experiment suggest that microtubules are more directly involved in a putative ESCRT-like pathway in *Arabidopsis*. To examine microtubule organization a *MAP4-GFP* construct that decorates microtubules was introduced into *elch* mutant background using a previously established transgenic line (Mathur and Chua, 2000). The *elch/MAP4-GFP* line was compared to *wild type* plants transformed with *Map4-GFP* by confocal laser scanning microscopy (CLSM). As defects are most prominent in trichomes, cluster and morphological normal *elch* trichomes were compared with *wild type* trichomes. Multinucleated cluster (Figure B15 B-D) and *elch* trichomes with normal morphology (E-F) show a similar microtubule organization like *wild type* (A). Both, fine and thick microtubule strands were observed in *wild type* and *elch*. The phenotype of pavement cells (Figure B15 H-I) and stomata (Figure B15 L-O) shows that *elch* is a cytokinesis mutant. Trichomes on the other hand do not divide anymore and very early stages that might still undergo mitotic divisions are difficult to identify. Therefore pavement cells were examined during early leaf development when cell division is frequently observed (Figure B15 G-O). It was possible to see new cell walls and cells in various division stages. Newly formed cell walls are decorated more heavily by microtubules compared to established cell walls (J). Dividing cells with two nuclei and spindle were observed in *wild type* (G-I) and *elch* mutant (K). Leafs were counterstained with DAPI and mitotic figures like condensed chromosomes were observed (L-O). Neither in trichomes nor in dividing pavement cells an obvious difference could be determined.

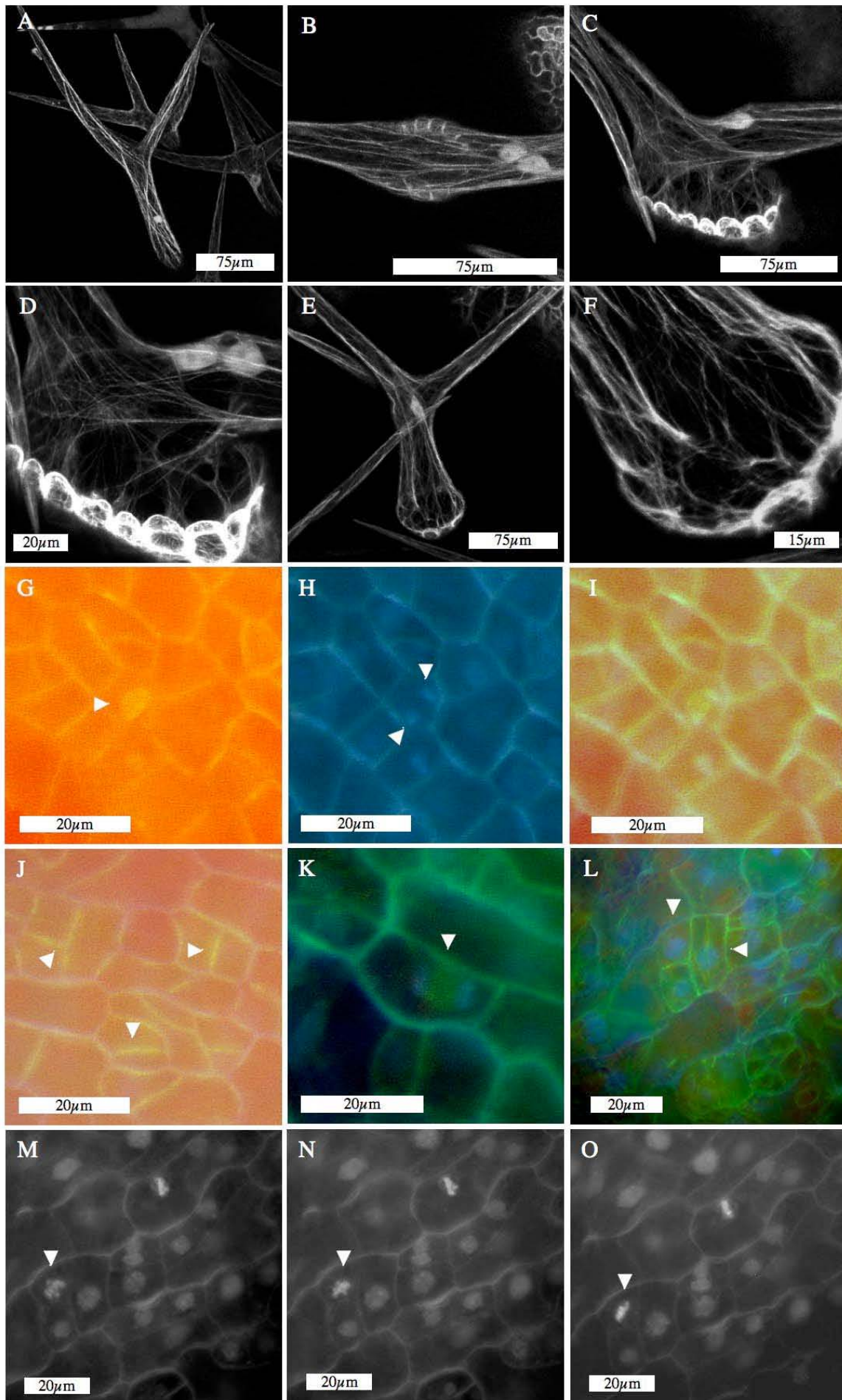


Figure B15: Microtubule arrangement appears normal in the *elch* mutant. Microtubules were visualized by crossing a *Map4-GFP* line to *elch* and observed in mature trichomes and early leaf epidermal cells. Compared to *wild type* (A & G-J) no obvious effects was found in *elch* trichomes (B-F) and young pavement cells of *elch* (K-O). B-D) Base of an *elch* cluster with nuclear pockets. E-F) Base of an *elch* trichome with *wild type* morphology. G-L) *Wild type* and *elch* plants expressing *MAP4-GFP* were counterstained with DAPI. G-I) Mitotic *wild type* cell with two nuclei and spindle. Young cell walls are recognized because they are more heavily associated with microtubules compared to older cell walls (J, see arrows). K-L) Mitotic pavement cells of the *elch* mutant. K) Mitotic cell with two nuclei and spindle. L) Cell, presumably with forming spindle. M-O) Time lapse series of a mitotic cell (arrow). Chromosomes are condensed and arrange at the future plane of division. No abnormalities were observed in mitotic cells.

C. Discussion

Genetic analysis of the *elch* mutant has shown previously that *ELCH* acts independently from known trichome developmental processes. Furthermore the nuclear phenotype of *elch* trichomes was described in my diploma thesis though it was not possible to provide experimental evidence for a defect in cytokinesis. With the cloning of the *Arabidopsis ELCH* gene the exploration of the ESCRT pathway in plants is just in the early stages (Spitzer et al., 2006). In the available study experimental evidence is provided that characteristic features of yeast and animal ESCRT-I complex are conserved in *Arabidopsis*. In addition, a putative and so far unknown link between ESCRT-I and the vacuolar ATPase, another component of the secretory system is shown in this study.

C 1. A defect in the *ELCH* gene disrupts cytokinesis

The *Arabidopsis elch* mutant harbours a T-DNA insertion in the gene *At3g12400* that is similar to the *VACUOLAR PROTEIN SORTING 23* gene (*VPS23*). Although the insertion site was characterised on the molecular level it is not clear how severe the effect of the mutation is. Three lines of evidence indicate that *elch* is a hypomorphic allele. First, even the most obvious phenotype that is found in leaf hairs or trichomes are subtle clusters that appear at a frequency of 2%. The remaining trichomes are indistinguishable from *wild type* as is the overall growth of the mutant. Second, the analysis of the mutation revealed that the T-DNA is inserted 786 bp after the start codon of *ELCH* (Spitzer et al., 2006). As the total sequence of *ELCH* has a length of 1194 bp it is conceivable that two thirds of the *wild type* gene, including the promoter is intact in *elch* and might be transcribed. Third, comparative RT-PCR between *wild type* and mutant indicated that a partial *ELCH* transcript is expressed in *elch* although the amount is strongly reduced (figure B6 B). The strategy chosen allowed the discrimination between *ELCH* and *ELCH-LIKE* and simultaneously the detection of *elch* mutant transcript. It is important to notice that a truncated transcript is most likely unstable as is also indicated by the lower expression level. The phenotype and the abundance of a transcript that is missing only the last third of the coding sequence make it conceivable that a truncated protein is synthesised. This protein might retain partial functions. Alternatively it is possible that *ELCH* and *ELCH-LIKE* act redundantly and the truncated *elch* protein interferes with *ELCH-LIKE* function. A way to address this question could be the overexpression of a truncated version of *ELCH*. Ideally this construct should have exactly the same 3' sequence that was left by the T-DNA insertion in *elch*.

The *elch* mutant displays a subtle phenotype in trichomes. The cluster morphology and the nuclear phenotype of trichomes prompted the analysis of other epidermal cell types in the *elch* mutant. Whereas the morphological phenotype is most obvious in trichomes, the analysis of pavement cells and stomata revealed more information concerning a disruption of cytokinesis. Scoring of multinucleated pavement cells showed that a fraction of the examined cells has cell wall stubs that are characteristic for cytokinesis mutants (Nacry et al., 2000). Cell wall stubs are found in multinucleated cells only with a frequency of 17 %. If multinucleated cells are a consequence of incomplete cell divisions a higher frequency of cells with cell wall stubs would be expected. However incomplete cell walls are not necessarily visible. Defects during cell division lead to holes in the cell wall between two cells. The cell wall margins of an opening could obscure observation of the cell wall stubs. This holds especially true if cell division is aborted at a very late stage, which would cause only a small hole. This would result in two cytoplasmic connected pavement cells with overall *wild type* morphology. Another cell type analysed for cytokinesis defects were stomata. Their analysis resulted in an additional phenotype that has not been observed before. It was found that 0,36 % of all stomata in the *elch* mutant are not separated from each other by pavement cells (Figure B 2; table 3). These stomata clusters resemble a phenotype that has been observed in the *too many mouth (tmm)* mutant (Geisler et al., 2000; Geisler et al., 1998; Nadeau and Sack, 2002). In contrast to the *tmm* mutant a phenotypic series was observed in *elch* stomata (Figure B 3). This series ranges from two and three stomata adjacent to each other (class I and class II clusters) to stomata with incomplete cell walls (class III cluster). Class I and class II clusters are indistinguishable between both mutants (Figure B 2 L-M and B 3 H-I). Cytokinesis defects like those found in class III clusters have not been reported for *tmm*. On the other hand *tmm* tends to form clusters with more than three stomata involved (Figure B3 J), which is not the case in the *elch* mutant. The crucial event that causes cluster phenotypes in *elch* seems to be the failure to close the cell wall gap between dividing cells during early stomata development. This is apparent by the phenotypic series in the *elch* mutant that highlights a relationship between stomata clusters and cell division defects in stomata. This cell division defect model for cluster formation in trichomes and stomata is summarised in Figure C 1. A cell that has adopted a certain fate produces determinants that initiate cell specific morphogenesis. These determinants can spread through the cytoplasmic connection between two cells and will cause both cells to adopt the same fate. This model has one weak point. So far it was not possible to proof the existence of incomplete cell walls in trichomes. It is assumed that the applied observation method actually prohibits the view to the base of the

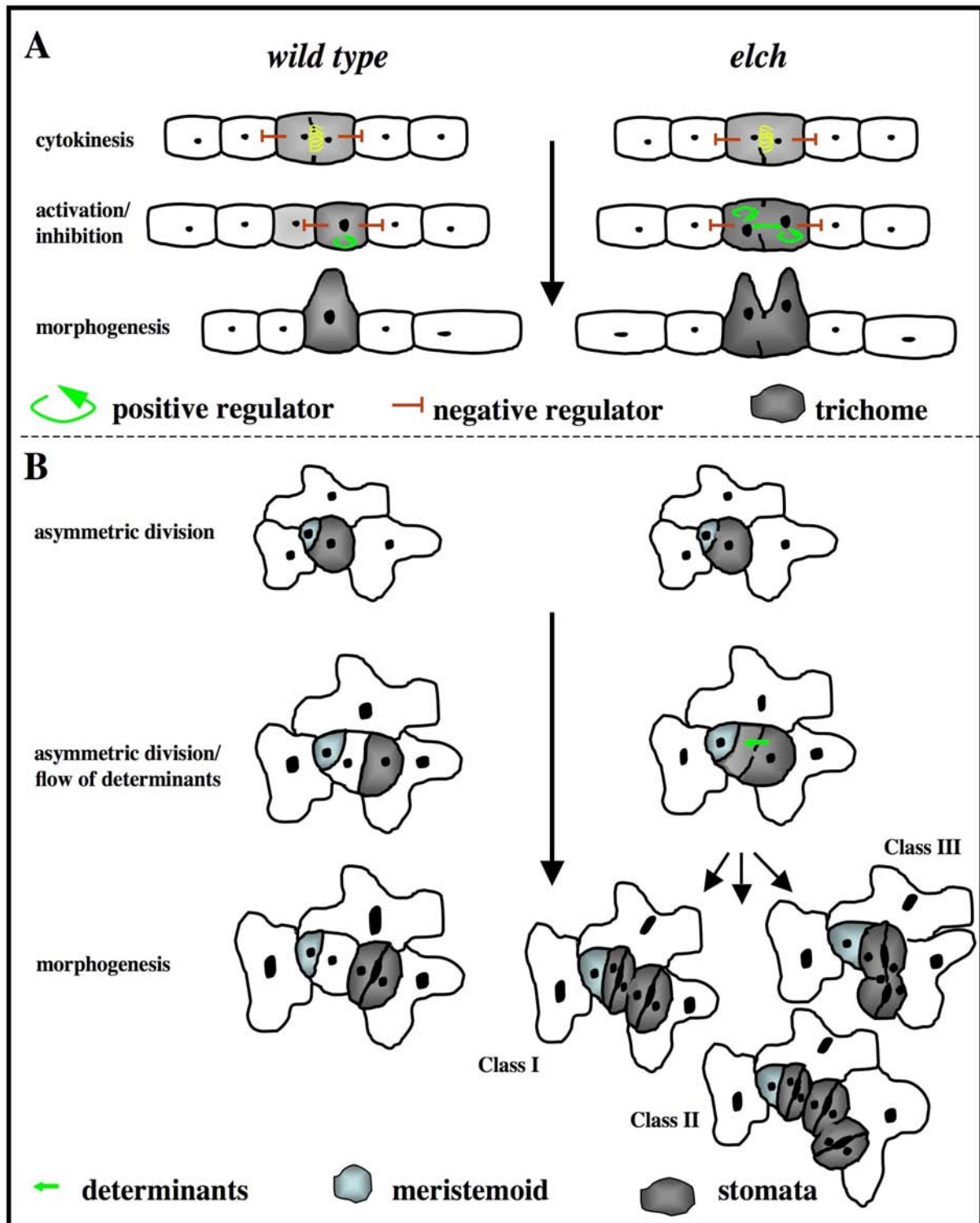


Figure C1: Cell division defect model for trichome and stomata cluster development in the *elch* mutant. (A) According to the mutual inhibition model a trichome precursor cell promotes its own trichome fate and inhibits that of the neighbour cells (Hulskamp, 2004). If the cytoplasm of two cells is connected by cell wall gaps the positive regulators are able to promote the fate of both cells while neighbouring cells are inhibited. It has to be noted that incomplete cell walls have not been observed in clusters so far. (B) Stomata are separated from each other by cell lineage and orientated cell division. Stomata cluster develop after incomplete cell division allows the flow of determinants from the stomata cell to its sister cell.

trichome cell where incomplete cell walls most likely are situated. When observing trichomes the stems are bend onto the leaf surface by the coverslip. In this position the trichome base is

obscured by the accessory cells that support the trichome stem. A different technique like sectioning of embedded clusters or optical sections by CLSM could be used to make the trichome base accessible. Also the presented model explains the different phenotypes observed in trichomes and especially in stomata another possibility exists. In this model TMM is a target of the ESCRT pathway. The *TOO MANY MOUTH* gene encodes a leucine-rich repeat receptor-like protein that localises to the plasma membrane. TMM has been implicated in stomata development where it regulates stomata patterning. The underlying mechanism depends on orientated cell division that places the developing stomata away from the meristemoid mother cell (MMC). The MMC is able to produce further stomata by unequal cell division (Geisler et al., 2000). The potential function of TMM as a receptor and the similar phenotype found in *elch* mutant plants makes TMM a potential target for an ESCRT-like pathway. In this case, the stomata cluster phenotype observed in *elch* could be a consequence of mislocalisation or impaired downregulation of the TMM receptor. To support this model the cluster phenotype of *tmm* should be studied in more detail in case cytokinesis defects have been missed. A genetic dissection by double mutant analysis is necessary to determine how both pathways are connected. As *tmm* mutants are induced mostly in backgrounds that are devoid of trichomes it will be interesting to study leaf hairs in the double mutant. Biochemical analysis of TMM in regard to ubiquitin modification could support the role of TMM as a target of the ESCRT pathway.

If there is a link between trichome clusters, stomata clusters and cell division defects there is still the problem why trichomes seem to be affected more often compared to other cell types. Both models do not address this question, especially because no data exists for trichomes in the *tmm* mutant background. The higher cluster frequency observed in trichomes could be a function of cell size and DNA content. Both decrease from trichomes over pavement cells to stomata. Higher DNA content is an indication for faster growth, which in turn might be the reason for more cytokinesis defects in endoreduplicated cells. However a prerequisite is that a still dividing trichome precursor cell already grows faster than pavement cells and stomata. Otherwise the same frequency of cluster formation would be expected. However it will be important to determine whether incomplete cell walls exist in *elch* trichome clusters at all. Furthermore the *tmm* mutation should be induced in lines that have trichomes and can be examined for cluster formation.

C 2. The ELCH pathway and microtubule dependent processes are linked

Two different lines of experiments indicate that ELCH or ESCRT dependent processes require an intact microtubule system: The cytokinesis defect of *elch* is strongly enhanced in *elc/tfc-a* double mutants and *elch* is hypersensitive to microtubule stabilization.

These results seem to oppose each other. The impairment of TUBULIN-FOLDING COFACTOR A (TFC-A) suggests that less assembly competent α/β tubulin heterodimers are abundant in the mutant (Dobrzynski et al., 1996; Lewis et al., 1996; Martin et al., 2000; Tian et al., 1996). Less α/β tubulin heterodimers should therefore lead to microtubule destabilisation or at least a slow down in microtubule dynamics. The observation that the double mutant is much more affected than the single mutants implicates that *elch* is sensitive to microtubule destabilization. This is difficult to understand as the effect of paclitaxel (taxol) demonstrates that *elch* is hypersensitive to microtubule stabilisation. A possible explanation is that the right balance of microtubule polymerisation/depolymerisation is crucial. Both experiments show that the *elch* mutant is sensitive to changes of the proper microtubule balance.

Observation of microtubules in trichomes and dividing pavement cells did not reveal any abnormalities of the microtubule cytoskeleton. Defects that occurred during cell division are probably not visible anymore in mature trichomes as the microtubule system changes considerably during trichome development (Mathur and Chua, 2000). Dividing cells in *wild type* and *elch* failed to show any difference as well. Possibly the defects are hardly visible at early stages but the effects become more obvious with progressing cell growth in affected cells.

The synergistic phenotype observed in the *elc/tfc* double mutant as well as the observation that *elch* is hypersensitive to microtubule stabilisation raises the question, which processes are involved that enhance the phenotype to this extent. Obviously the secretory system depends on the cytoskeleton to move vesicles throughout the cytosol to their destination. So far experimental data is very limited in literature and only recently more evidence has become available that endosomes travel bidirectional along microtubules (Lenz et al., 2006). However it is known that both, the secretory system as well as microtubules have a dominant role during plant cytokinesis. Close interaction between both, for instance by microtubule dependent vesicle transport could be an explanation for the synergistic phenotype of the *elch/tfc-a* double mutant or the hypersensitivity of *elch* towards taxol.

An obvious experiment will be the visualisation of microtubules in *elch*, *tfc-a* and the double mutant *elch/tfc-a*. The higher frequency of cluster formation and aberrant cell morphology compared to the single mutants should facilitate the determination of differences.

C 3. The ESCRT-I complex in *Arabidopsis*

A first indication that the ESCRT machinery exists in *Arabidopsis* was the discovery that the *VPS* genes that are known from yeast and animals are found in the *Arabidopsis* genome as well (Table B4). In a separate more detailed study it was shown that this is true for many eukaryotic organisms (Winter and Hauser, 2006). In independent experiments it was established that the *Arabidopsis* ELCH protein binds ubiquitin and is part of a high molecular weight complex (Spitzer et al., 2006).

The experiments are based on an HA-tagged ELCH that was overexpressed *in planta*. Preparatory experiments showed that overexpression of *ELCH* in *elch* mutant background is able to rescue the cluster phenotype in the T1 generation. One of the analysed lines (line T2-14) showed the expected three to one segregation ratio in the T2 generation. Out of 30 T2 plants 23 were rescued in respect to the cluster phenotype (expected were 22.5 plants) with seven showing clusters. Analysis of line T2-12 resulted in an odd segregation ratio of 14 rescued plants out of 16 in the T2 generation. These ratios were not analysed any further but a possible explanation could be that multiple T-DNA insertions occurred. In neither case any additional phenotypes were observed indicating that overexpression of *ELCH* in *elch* mutant background results in a functional substitution for native ELCH protein. Therefore an HA-tagged version of the *35S::ELCH* construct was introduced in *elch* mutant background and analysed for rescue and expression. The complementation in the T1 generation and western analysis showed that the fusion protein is functional and expressed. The line with the highest ELCH-HA expression was used for further biochemical assays.

Gel filtration indicated that ELCH-HA is incorporated into a complex with a molecular weight between 200 and 600 kDa. This data was supported by immunoprecipitation of the ELCH-HA fusion protein that revealed interactions with the *Arabidopsis* orthologs of Vps28p and Vps37p (Spitzer et al., 2006). The *Arabidopsis* genome contains at least two copies of VPS28 and VPS37. Peptides that are specific for both isoforms of VPS28 and VPS37 respectively have been identified by mass spectrometry showing that both are part of an *Arabidopsis* ESCRT-I-like complex (Table 5). Their high homology makes it difficult to judge whether they act redundantly or have divergent functions. It is also possible that the isoforms of VPS28 and VPS37 are expressed tissue specific as lysates from whole plants were

used for these experiments. Genetic analysis of *vps28* and *vps37* mutants should help to clarify this question. Gelfiltration suggests that plant ESCRT-I has a molecular weight of approximately 350 kDa. This result corresponds to observations in yeast (Katzmann et al., 2001). Nevertheless 350 kDa appear to be too much for a complex of ELCH, VPS28 and VPS37. Although this is a rough estimation, the sum of the molecular weights of ELCH, VPS28 and VPS37 amounts to less than 100 kDa. A solution could be that one or more subunits are represented more than once in ESCRT-I complex (Katzmann et al., 2001). In contrast to this model the recently resolved crystal structure of the core ESCRT-I in yeast suggests that Vps23p, Vps28p and Vps37p are abundant in a 1:1:1 stoichiometry (Kostelansky et al., 2006). Moreover, no signs were detected for di- or oligomerization of the single components. However, Hurley and co-workers discuss the possibility that Vps23p/Vps28p/Vps37p complexes might dimerize (Kostelansky et al., 2006). Conversely another group reported that the amino-terminal part of Vps28p (residues 1-113) contains a dimerization domain and is able to form Vps28p dimers. Their data is supported by gelfiltration of purified Vps28p and crosslinking experiments (Pineda-Molina et al., 2006). Extensive posttranslational modifications of ELCH or TSG101 does not contribute to the considerable size discrepancy as ELCH separated by SDS-PAGE runs at 49 kDa (see Figure B6 C; Appendix E1).

TSG101 has been reported to bind Ubiquitin directly (Bishop et al., 2002). Furthermore ubiquitination has been shown to serve as a signal for ESCRT dependent protein sorting in yeast (Katzmann et al., 2001). ELCH shares the ubiquitin enzyme variant domain with Vps23p and TSG101 and binds ubiquitin *in vitro* and *in vivo* (Figure B7-B8). In summary these data provide for the first time experimental evidence that the ESCRT-I machinery is conserved in *Arabidopsis*.

C 4. The ESCRT pathway in plants

Two main functions of the ESCRT pathway are known from yeast and animals: sorting of biosynthetic cargo to the vacuolar lumen and the downregulation of plasma membrane receptors. Based on the similarity of the involved components in yeast, animals and plants both pathways are most likely needed in *Arabidopsis* as well. The plant vacuole shares characteristics with the yeast vacuole and the lysosome in animals (Vitale and Galili, 2001; Vitale and Raikhel, 1999). In general the plant vacuole and the animal lysosome are considered to be their equivalent. Proteases are resident in the plant vacuole (Bethke et al., 1996) and a pathways depending on BP-80/AtELP has been described that sorts proteins into

the vacuolar lumen (Ahmed et al., 1997; Paris and Neuhaus, 2002). These studies however are by far less advanced than in yeast. In yeast and animals, plasma membrane receptors play an important role in cell communication and some of them such as EPIDERMAL GROWTH FAKTOR RECEPTOR (EGFR) or the α -factor receptor Ste2p are targets of the ESCRT pathway (Katzmann et al., 2001; Lu et al., 2003). Probably these are no exceptions but represent a large number of plasma membrane proteins that are sorted by the ESCRT pathway (Scott Emr, personal communication). Plasma membrane receptors are abundant in plants such as the leucin-rich repeat receptor-like kinase BRASSINOSTEROID INSENSITIVE1 (BRI1). BRI1 has been shown to undergo endocytosis (Rusinova et al., 2004) but the regulation of this process is still under investigation.

Both, the biosynthetic and receptor downregulation pathways converge at the multi-vesicular body. Here the decision is converted whether cargo is redirected to the plasma membrane, the vacuolar membrane or the vacuolar lumen (Hicke, 2001). All known genes of the ESCRT machinery reported in yeast are present in *Arabidopsis* but nevertheless it remains difficult to predict whether function is conserved as well. ESCRT-II and ESCRT-III-like complexes still have to be identified in *Arabidopsis*. More importantly, it was so far not possible to determine proteins that are sorted by an ESCRT-like pathway. The identification of ESCRT targets would allow to track sorting events or missorting in mutants. In the *elch* mutant the identification of targets is complicated by its phenotype that is difficult to access by conventional screens. A suppressor screen is impracticable as the mutant itself is hard to recognize. An enhancer screen is difficult assuming that ELCH is involved in MVB sorting and vacuolar degradation like Vps23p and TSG101. If a target protein is knocked out, for example a receptor that is not efficiently downregulated in the *elch* mutant, this knock out would probably not enhance the *elch* phenotype. Gain of function mutations that result in higher expression of the receptor are more likely to enhance the phenotype. Gain of function mutations on the other hand are seldom although not impossible to achieve. Another well established method for the identification of interacting proteins is the yeast two-hybrid screen. Yeast two-hybrid screening might produce candidates that interact with ELCH itself and are part of the sorting machinery. An ESCRT target on the other hand is recognized by its monoubiquitin modification. The correct recognition and ubiquitination of a plant target in yeast is rather unlikely. Therefore the yeast two-hybrid system is not ideal for this purpose. Another method to identify interacting proteins is the biochemical isolation of the protein of interest. Proteins that interact with the protein of interest can be copurified and identified by mass spectrometry. For this method stability and amount of the involved proteins is crucial.

Furthermore binding strength between an ELCH/ESCRT-I complex and its target needs to be sufficient for purification.

Although no target has been analysed so far the abundance of the ESCRT machinery, the ESCRT-I complex and the assumed requirement for multi-vesicular body sorting in *Arabidopsis* provides well founded evidence that an ESCRT-like pathway exists in plants.

C 5. Relevance of the putative targets and ELCH/ESCRT-I interacting proteins

The identification of ELCH/ESCRT-I targets was attempted using biochemical methods. The coimmunoprecipitation experiments resulted in the identification of expected ESCRT-I components (VPS28 and VPS37) as well as in a number of proteins that are new to the ESCRT pathway in yeast and animals. Two groups of new interactors were isolated: One is the V-ATPase with several components of this protein complex while the other consists of the UBiquitin Associated domain containing protein At5g53330. The UBA domain is the only feature that indicates putative functions of this otherwise unknown protein. The result that not only unexpected proteins but also ESCRT-I components were precipitated enhances the credibility of the V-ATPase components and At5g53330 as targets or ELCH/ESCRT-I interacting proteins. The UBA domain of At5g53330 indicates that this protein could be involved in a mono-ubiquitin dependent ESCRT pathway. It is a single copy gene in *Arabidopsis* and has no homologs in other organisms. The analysis of a plant specific protein could reveal new ESCRT functions or a plant specific component of the ESCRT machinery. The V-ATPase on the other hand has been studied in great detail, showing that it is involved in different functions within the secretory system in all eucaryotes (Kane, 1999; Nishi and Forgac, 2002; Schumacher, 2006). Although the V-ATPase has been implicated in a variety of pathways the ESCRT machinery is not among them. Extensive genetic studies that were done in yeast resulted in the isolation and identification of more than 30 complementation groups (Robinson et al., 1988) and most of these genes are by now identified and were themselves subject to genetic studies. The classE genes, that comprise the members of the ESCRT pathway total at least 13 genes (Raymond et al., 1992). The V-ATPase comprises 14 subunits but this number varies depending on the studied organism. It seems unlikely that there is an interaction between two pathways with nearly 30 genes altogether that has not been discovered. This holds especially true in an organism that is easily accessible to genetic manipulation such as yeast. An intriguing possibility is of course that the V-ATPase is only a target of the ESCRT pathway in plants and is regulated differently in yeast and animals. Although this is highly speculative it has to be remembered that ESCRT and V-ATPase are

involved in functions of an organelle that evolved additional functions in plants. The plant vacuole is considered equivalent to the yeast vacuole and the animal lysosome. Nevertheless obvious additional functions like turgor maintenance or waste disposal might have required the recruitment of established components of the secretory system.

Nevertheless besides the functional analysis of these proteins independent evidence should be provided to support the biochemical interaction. A genetic analysis of the ESCRT pathway on one side and the V-ATPase pathway and At5g53330 on the other is necessary to determine the biological relevance of the interaction.

C 6. Vacuolar ATPase and ESCRT functions overlap to considerable extent

The vacuolar ATPase has been implicated in a variety of functions including sorting of biosynthetic cargo and receptor mediated endocytosis (Nishi and Forgac, 2002). The ESCRT pathway is involved in both functions by internalizing cargo proteins from endosomes into luminal vesicles. Acidification of these vesicles is needed to release ligands or process biosynthetic cargo (Geuze et al., 1983; Morano and Klionsky, 1994). The V-ATPase acidifies various organelles by translocating protons from the cytosol into the lumen of these endosomes (Nishi and Forgac, 2002). Sorting of biosynthetic cargo has been shown to be compromised in V-ATPase mutants in yeast (Banta et al., 1988; Morano and Klionsky, 1994). Careful control of pH at various stages of protein transport seems to be necessary for successful protein sorting. Nevertheless the reason why pH is important for sorting is still illusive. V-ATPase- and ESCRT complexes are clearly involved in similar processes but so far no direct interaction has been shown.

The physical interaction of ELCH with subunits of the V-ATPase was shown in co-immunoprecipitation assays. Next to VPS28 and VPS37 further bands were observed and four were identified as subunits of the V-ATPase by mass spectrometry. As not all subunits were verified by mass spectrometry the V-ATPase was isolated by immunoprecipitation of VHAa3-GFP and the band pattern compared to immunoprecipitation of ELCH-HA. The similar band pattern suggests that several weak bands that were not accessible by mass spectrometry from the ELCH-HA immunoprecipitation are subunits of the V-ATPase. There are at least two possibilities for the V-ATPase to interact with ELCH/ESCRT-I. An intriguing possibility is that the V-ATPase is a target of the ESCRT pathway. Known targets from yeast and animals are either vacuolar proteins like proteolytic enzymes or plasma membrane receptors that are monoubiquitinated and endocytosed. Mass spectrometry data indicates that two amino terminal lysins (K56 and K68) are ubiquitinated. VHA-a3 is not necessarily

ubiquitinated on both lysins simultaneously. Corresponding peptides were found with and without ubiquitin modification (Table 8). Western analysis of VHA-a3 suggests that only one lysine is ubiquitinated as one discreet band is found at 130 kDa. VHA-a3 is a transmembrane protein but it does not localize to the plasma membrane like Ste2p or EGFR, two well-studied targets of the ESCRT pathway in yeast and animals respectively. *Arabidopsis* contains three isoforms of VHA-a that have been reported to localize to different endomembrane compartments. While VHA-a1 is found mainly at the trans-Golgi network, VHA-a2 and -a3 localize to the tonoplast (Dettmer et al., 2006). This observation is in concord with yeast studies demonstrating that VPH1 localizes to the vacuole whereas STV1 containing complexes are found at the late Golgi (Kawasaki-Nishi et al., 2001). VPH1 and STV1 are isoforms of the VHA-a subunit from the yeast V0 subcomplex. The observation that VHA-a3-GFP is exclusively found at the tonoplast contradicts the idea that this protein is a conventional ESCRT target. A model that includes the biochemical interaction from this study and localization data of VHA-a3-GFP is based on the assumption that the ESCRT pathway is not restricted to biosynthetic cargo and plasma membrane proteins. In addition tonoplast derived vesicles containing V-ATPase complexes in their membrane are processed by the ESCRT machinery as well. Multi-vesicular bodies (MVBs) that originate from tonoplast budding could then distribute membranes and proteins much like conventional MVB sorting does. This could be internalisation of proteins and subsequent vacuolar degradation (Figure C2 I), delivery back to the tonoplast (Figure C2 II) or membrane transfer to other secretory compartments (Figure C2 III). A model in which membranes are removed from the vacuole is conceivable because the tonoplast receives membranes by vesicle fusions and thereby has to reduce membranes again to keep the equilibrium. Multi-vesicular bodies are frequently found in close association with the vacuole but they are regarded as pre-vacuolar compartments that are about to fuse with the vacuole (Prescianotto-Baschong and Riezman, 2002). The close association of MVBs with the vacuole and their capability to direct membranes to different locations makes them suitable candidates for a membrane reduction process. Regulation of the V-ATPase by vacuolar degradation has not been described. A way to support this model could be ultrastructure analysis in combination with immunogold labelling against the V-ATPase. If the discussed model is correct it should be possible to find V-ATPase positive MVBs in close association with vacuoles. In contrast to the hypothesis that the V-ATPase is a target of the ESCRT pathway it is conceivable that ELCH/ESCRT-I interacts direct and not via monoubiquitination with the V-ATPase. A possibility is that the V-ATPase is involved in the ESCRT sorting machinery and the binding

is mediated by protein-protein interaction.

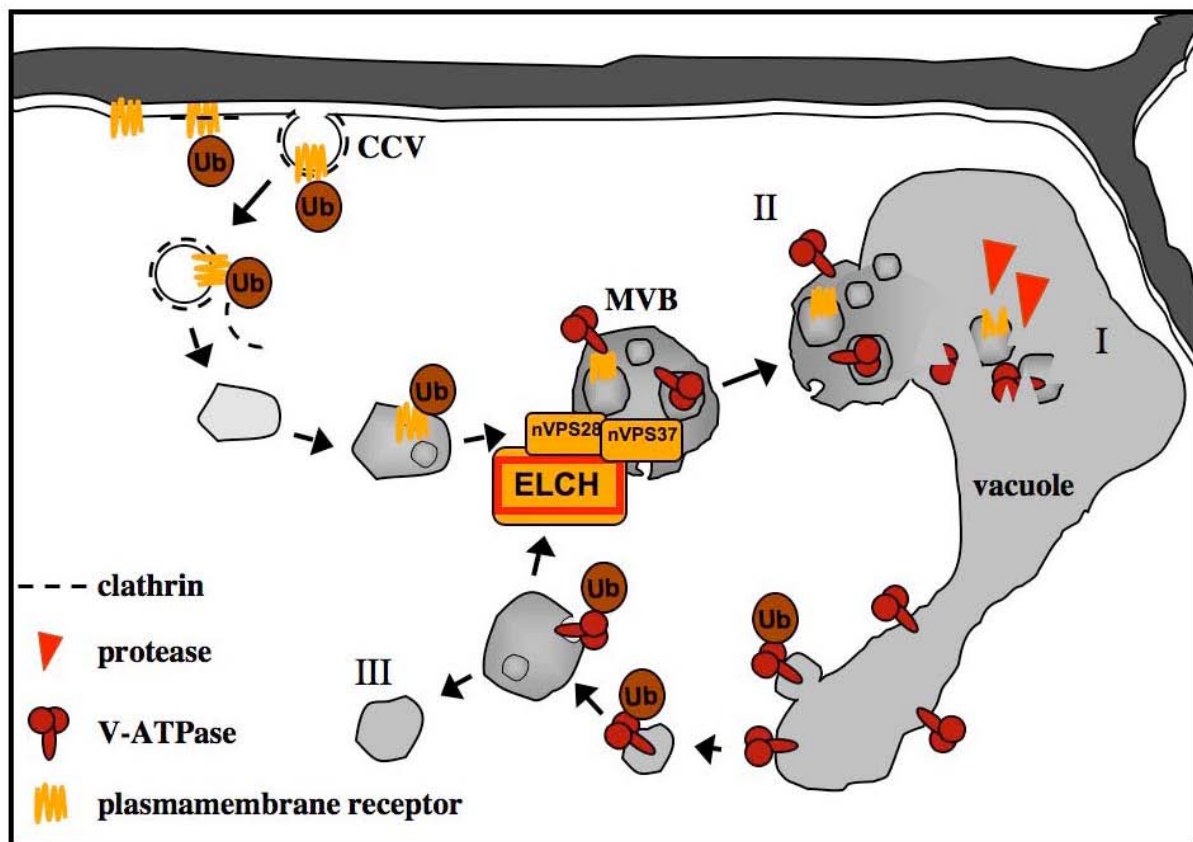


Figure C 2: A model for ESCRT mediated degradation of V-ATPase complexes. The ESCRT pathway not only downregulates plasmamembrane receptors but also tonoplast intrinsic proteins (I). Furthermore this model shows an option how proteins are recycled back to the tonoplast (II) or how membranes are removed from the tonoplast (III). The assumed mechanisms are the same that act at the plasmamembrane and are known from yeast. As clathrin mediated vesicle budding has not been observed at the vacuole other mechanisms might regulate this process.

Binding might be mediated via the coiled coil domains that are found in ELCH, VPS37, DET3 and VHA-a3 with the COILS program (Lupas et al., 1991) Weaker coiled coil scores were found for VHA-A and VHA-B. It has to be considered that the coiled coil domains found in VHA-a3 and DET3 are probably needed for complex formation of the V-ATPase itself and not necessarily for interaction with other proteins. ESCRT-I proteins are involved in late endosom/MVB formation (Razi and Futter, 2006). Furthermore it was shown that early- to late endosomes develop decreasing pH values (Clague et al., 1994). Therefore an interaction between the sorting machinery and the pH controlling system would make sense. On the other hand the observed localization at the vacuolar membrane of VHA-a3 contrasts sharply with the localization of ELCH or its yeast homolog Vps23p. Both are found at vesicular structures (Spitzer et al., 2006) and MVBs respectively. If a direct protein protein interaction of ESCRT and V-ATPase components is true colocalisation would be expected.

Therefore this model seems more unlikely.

The reported localisation of VHA-a3-GFP indicates that this protein is not a target in the sense of known ESCRT mediated sorting. The idea that ESCRT mediated sorting in plants includes tonoplast proteins requires more experimental data. One approach would be a detailed genetic dissection of ESCRT and V-ATPase components. Mutants from different V-ATPase proteins i.e. *det3* (Schumacher et al., 1999) are available or can be screened in various T-DNA collections. The cytokinesis phenotype observed in *vha-E* mutants could be an indication that the cell division defect observed in *elch* mutant plants is a result of V-ATPase misregulation. If VHA-a3 is interacting directly with ELCH/ESCRT-I the *elch* phenotype should be enhanced in mutants compromised in ELCH and VHA-a3. If the target hypothesis is true an enhancement of the *elch* phenotype is only expected if VHA-a3 is expressed at higher levels. Higher amounts of VHA-a3 would put more strain on the (presumably) already compromised ESCRT machinery in *elch* mutants. Co-localisation studies should be made using the CaMV 35S::CFP-ELCH construct (Spitzer et al., 2006) and the VHA-a3::VHA-a3-GFP construct (Dettmer et al., 2006). The possibility to use ultrastructure analysis in combination with immunogold techniques was already discussed. An obvious experiment would be to introduce point mutations at K56 and K68 in a VHA-a3-GFP construct and introduce it into *vha-a3* mutant background. These lines should be analysed for rescue and localization of VHA-a3-GFP^{K56,68R}. A similar experiment described in yeast lead to cargo mislocalisation (Katzmann et al., 2001). The ubiquitination pattern of VHA-a3-GFP^{K56,68R} would be interesting as well.

C 7. Putative requirement for ESCRT function during cytokinesis

The ESCRT pathway has so far not been implicated in cytokinesis. However multi-vesicular bodies seem to be important during the late stages of cytokinesis, especially during cell plate formation. This has been shown by quantifying numbers and volume of MVBs during different mitotic stages (Segui-Simarro and Staehelin, 2005). Number and volume of MVBs as well as clathrin coated vesicles (CCV) density were increased at the same time during cell plate formation. This supports the hypothesis that accumulation of membranes due to vesicle fusion during cell plate formation is balanced by clathrin mediated vesicle budding from the cell plate. MVB formation during this period might be needed to redistribute membranes again to different compartments, presumably especially to the golgi system. The process of membrane reduction from the cell plate is topological equivalent to receptor-mediated endocytosis where the function of the ESCRT pathway is established (Katzmann et al., 2001;

Katzmann et al., 2003). The primary purpose of this process seems to be the sorting of peptides and proteins however it equals the redistribution of membranes. For that reason the ESCRT pathway is a likely candidate for a player in membrane recycling and redistribution during cell plate formation.

C 8. Putative requirement for V-ATPase function during cytokinesis

The observation that *vha-A* and *vha-E* mutants show multinucleated cells and incomplete cell walls (Dettmer et al., 2005; Strompen et al., 2005) demonstrates that the V-ATPase is required during cytokinesis. It has been shown that impaired V-ATPase function leads to disorders in the secretory system. As the secretory system plays a key role during plant cytokinesis this observation makes sense. However it is not clear what precisely this role is. Is the V-ATPase important for maintaining the structure of the secretory system in general? Does the V-ATPase regulate protein sorting specifically (Banta et al., 1988; Matsuoka et al., 1997; Morano and Klionsky, 1994)? Does the V-ATPase only acidify certain compartments needed for protein processing or receptor ligand dissociation (Geuze et al., 1983)? Each of these steps can be imagined to lead to cell division defects as cytokinesis depends on many processes. Evidence for a general role of the V-ATPase in maintenance of the secretory system is found in *vha-E/tuff* mutants. Mutations in the *VHA-E* gene result in disturbed golgi organisation (Strompen et al., 2005). V-ATPase subunits localise to different membranes of the secretory system. These are for example the plasma membrane (Frattini et al., 2000), the trans-golgi network (Dettmer et al., 2006), MVBs, endosomes and other compartments (Stevens and Forgac, 1997). Localisation in the golgi has not been reported, indicating that the golgi system is influenced by V-ATPase defects in other compartments.

Interactions with cellular components that are needed for cell division might unravel more specific functions for the V-ATPase during cell division. The interaction with ELCH/ESCRT-I indicates that the V-ATPase is involved during multi-vesicular body formation (Razi and Futter, 2006). As multi-vesicular bodies are more numerous during cytokinesis (Segui-Simarro and Staehelin, 2005) the V-ATPase might be involved in cell division during multi-vesicular body formation.

Outlook

Although the analysis of the first plant component of ESCRT-I showed that this pathway likely operates in plants a number of basic questions still remain. It will be interesting to identify other ESCRT mutants and determine their phenotype. The creation of double mutants might result in more penetrant phenotypes that, unlike *elch*, are accessible to genetic screens. The analysis of the *ELCH-LIKE* gene in combination with *ELCH* itself could answer open questions: So far it is not clear whether both act redundantly, are expressed differentially or have different functions altogether. Promoter studies and genetic analysis of both could be used to address some of these questions.

With more and more evidence that the ESCRT machinery is functional in plants the main tasks for coming projects will be the determination of whether *Arabidopsis* ESCRTs fulfil similar functions like yeast or animal ESCRTs. In a next step it will be important to work out differences between plants and other systems.

In this study the central component of ESCRT-I was analysed biochemically and first evidence was provided for new interacting partners. These interactors have to be verified by genetic means. If these proteins are targets of the plant ESCRT pathway it might be possible to study ESCRT mediated sorting in plants. This is especially interesting as the identified proteins are either plant specific or have not been implicated in ESCRT mediated sorting.

D. Material and Methods

D 1. Chemicals

All chemicals were purchased from Sigma-Aldrich (Taufkirchen), Boehringer Mannheim (Mannheim), Serva (Heidelberg), Merck (Darmstadt), Qiagen (Hilden), Roth (Karlsruhe),

D 2. Material

D 2.1. Enzymes for DNA manipulation

All restriction enzymes were purchased from Fermentas

D 2.2. Primer

CS023	5' ggggacaagtttgtaaaaaagcaggct <u>caagcaggagtgtctagg</u>
CS038	5' ggggaccactttgtacaagaaagctgggt <u>gttgaggaatgtatgggc</u>
CS063	5' aagggcccgctgaccatggtcccccgcc
CS064	5' tagggcccgcgccgcTCAAGCGTAATCTGGAACATCATA TGGGT <u>Acctacctgcgatggctgc</u>
IMZ003	tgcgacaatggaactggaatg
IMZ004	ggatagcatgtggaagtgcatac
CSP171	ggtggtgaacatgctgcactgcacc
CSP174	ttcagtccttacgaagagtc

Gene specific sequence is underlined, the HA coding sequence is capitalized.

D 2.3. Vectors

pCAMBIA1300 (Genbank accession number AF234296)

pBinAR (Höffgens and Willmitzer, 1990).

into pGEMTEasy, Promega

D 2.4. Antibiotics

Ampicillin (Amp) 100 mg/ml in H₂O

Gentamycin (Gent) 15 mg/ml in H₂O

Kanamycin (Kan) 50 mg/ml in H₂O

Rifampicin (Rif) 100 mg/ml in DMSO

Those stock solutions (1000x) stored at -20°C . Aqueous solutions were sterile filtrated.

D 2.5. Bacterial strains

DH5a: *80lacZ* Δ M15, *recA1*, *endA1*, *gyrA96*, *thi-1*, *hsdR17* (r_B^- , m_B^+), *supE44*, *relA1*, Δ (*lacZYA-argF*)U169; Bachmann (1983,1990), Sambrook J. et al. (1989).

E. coli

GV3101: *A. tumefaciens*

D 2.6. Plant lines

Arabidopsis thaliana ecotype *Ws2*

Arabidopsis thaliana ecotype *Ler*

The *elch* allele was isolated from a T-DNA-transformed *Ws2* ecotype population generated at the INRA, Versailles (Spitzer et al., 2006).

sti146 (Ilgenfritz et al., 2003)

The *tfc-a* allele was isolated from a T-DNA-transformed *Ws2* ecotype population generated at the INRA, Versailles (Kirik et al., 2002).

GFP::MAP4 (Mathur and Chua, 2000)

ELCH::ELCH in *elch* background (Spitzer et al., 2006)

CaMV35S::ELCH in *elch* background (Spitzer et al., 2006)

CaMV35S::ELCH-HA in *elch* background (Spitzer et al., 2006)

VHAa3::VHA-a3-GFP (Dettmer et al., 2006)

CaMV35S::EGFP-peroxi (Mathur et al., 2002)

D 2.7. Biochemicals

Complete Protease Inhibitor	Roche (11873580001)
Protein G agarose	Roche (11719416001)
Ubiquitin agarose	Sigma (U5632)
Basic beads	Miltenyi (130-048-001)
Anti HA protein isolation kit	Miltenyi (130-091-122)
Anti GFP protein isolation kit	Miltenyi (130-091-125)
Superose™ 6 10/300 GL	Amersham (17-5172-01)
Flag::Ubiquitin	Alexis Biochemicals (BST-U-120-M001)
Protein marker (PAGE RULER)	Fermentas (SM0671; lot: 13809)
Blocking buffer for IRDyes	Rockland (MB-070)
Blocking buffer	Skimmed milk powder (Sucrofin)

D 2.8. Antibodies

rat anti HA antibody	Roche (1867423)
mouse anti Ub antibody	Santa Cruz (SC8017)
mouse anti GFP antibody	Roche (11814460001)
rabbit anti GFP antibody	Millipore (AB3080)
goat anti rat HRP	Jackson Immuno Research (112-035-003)
goat anti mouse HRP	Jackson Immuno Research (115-035-003)
goat anti mouse IRDye® 700DX	Rockland (610-130-007)
goat anti rabbit IRDye® 800CW	Licor (926-32211)

D 2.9. Accession numbers

Arabidopsis ELCH (NP_566423)
 Arabidopsis ELCH-LIKE (NP_196890)
 Rice ELCH BAD28453 ()

yeast VPS23 (Accession number AF004731)
human TSG101 (Accession number U82130).
Drosophila TSG101 (NP_524120)

D 3. Methods

D 3.1. Maintenance and cultivation of *Arabidopsis thaliana*

Soil grown conditions: *Arabidopsis* seeds were germinated by sowing directly onto moist soil. Seeds were cold treated by placing pots on a tray covered with a lid and incubated in the dark at 4°C for three to four days. Trays were subsequently transferred to a controlled environment growth chamber, covered with a propagator lid and maintained under long day conditions (16 h photoperiod and 24°C). Propagator lids were removed when seeds had germinated.

In vitro culture: Seeds were preincubated for five minutes in 95% Ethanol and then sterilized for 15 minutes in a 3% NaClO₃ solution containing 0.1% triton X-100. After removing the sterilization solution seeds were washed three times with sterile water and then plated. MS-agar-plates (1% Murashige-Skoog salts, 1% sucrose, 0.7% plant agar, pH 5.7) were either used without antibiotic or with kanamycin (50*µg/ml) or hygromycin (25*µg/ml). Plants were grown under long day conditions (16 h photoperiod and 22°C) for 20 days and then stored at 8°C for protein work.

Plants were protected from various herbivores by applying 10 mg/l Confidor® WG 70 (Bayer, Germany). The solution was applied by watering the plants.

D 3.2. Crossing of *Arabidopsis thaliana*

Flower buds were carefully opened with a pair of fine tweezers and immature stamens were removed. Carpels were immediately covered with ripe pollen from donor plant. Untreated buds were removed and plants placed back into the growth chamber for seed ripening. F1 and F2 plants were germinated under appropriate selection and analysed.

D 3.3. Microscopy and cell biology

DNA was stained with 4',6-Diamidino-2-phenylindol (DAPI). Solid DAPI was diluted to 10 mg/ml in H₂O (stock solution). For DAPI stainings leafs were incubated in DAPI solution (40µg/ml final concentration) for 15 minutes under vacuum (0,6 bar). Leafs were washed in 70% EtOH at 4°C to reduce background and visualized by epi-fluorescence microscopy [excitation filter (BP 340-380), emission filter (LP425)]. Microscopy was done with a LEICA DMRE equipped with a high-resolution KY-F70-3CCD JVC camera and a frame grabbing DISKUS software.

Confocal microscopy was done using a TCS SP2, Leica, Wetzlar, Germany. Leaf sections were stained with 500 µg/ml propidium iodide and infiltrated for 15 min at 0,9 bar. After staining, leaves were embedded in 5% low meltin agarose and sectioned with a razor blade. Images were processed using the Adobe Photoshop 6.0 software.

D 3.4. Nuclear DNA measurements

Whole leafs were DAPI-stained, mounted on a slide and observed by epi-fluorescence microscopy (see also D 3.3). The C value of trichome nuclei was determined using the DISCUS software package (Carl H. Hilgers-Technisches Büro, Königswinter, Germany). The fluorescence intensity of DAPI stained nuclei was determined and set into proportion to the intensity of stomata nuclei. Stomata nuclei have a DNA content of 2C (Galbraith et al., 1991).

D 3.5. Basic DNA manipulation techniques

(Plasmid preparation from bacteria, DNA digest, agarose gel electrophoresis, etc)

See “Molecular Cloning: A Laboratory Manual (Third Edition) By Joseph Sambrook, Peter MacCallum Cancer Institute, Melbourne, Australia; David Russell, University of Texas Southwestern Medical Center, Dallas”

D 3.6. Polymerase chain reaction conditions

To amplify the ELCHgenomic region for the *pCAMBIA1300-DM-CS023-038* construct the following PCR conditions were used:

Initial denaturation	96°C		
Denaturation	96°C		
Annealing	58°C	Annealing gradient:	58±5°C
Elongation	72°C	Number of cycles:	32
End-elongation	72°C		

The different DNA products from the gradient PCR were combined and gel purified.

To amplify the ELCHgenomic region for the *pGEMT::CS063-064* construct the following PCR conditions were used:

Initial denaturation	96°C		
Denaturation	96°C		
Annealing	58°C	Annealing gradient:	58±5°C
Elongation	72°C	Number of cycles:	32
End-elongation	72°C		

The different DNA products from the gradient PCR were combined and gel purified.

D 3.7. Constructs

pCAMBIA1300-DM-CS023-038 (this construct rescues the elch mutant)

the ELCH genomic region was amplified with Expand High Fidelity Polymerase (Roche) from the P1 clone MQC3 using primers CS023 and CS038. The 2.9kb PCR product was gel purified and ligated blunt into the Ecl136II restriction site of pCAMBIA1300 (Genbank accession number AF234296).

pBinAR::35S-ELCH (this construct rescues the elch mutant)

The ELCH gene was excised from *pCAMBIA1300-DM-CS023-038* using MluI and BspHI. The 1.3kb fragment was gel purified and ligated blunt into the SmaI site of pBinAR (Höffgens and Willmitzer, 1990).

pGEMT-CS063-064

The ELCH Gen was amplified using Tag polymerase from *pCAMBIA1300-DM-CS023-038* using primers CS063 and CS064. Primer CS064 contains the sequence of the HA tag. The 1.2kb fragment was gel purified and subcloned into pGEMTEasy (Promega) by AT cloning.

pBinAR::35S-ELC-HA (this construct rescues the elch mutant)

The ELC::HA sequence was excised from *pGEMT::CS063-CS064* using Sal I and NotI, blunt-ended and ligated into the SalI site of pBinAR (Höffgens and Willmitzer, 1990).

D 3.8. Blunt-end ligation

For blunt-end ligations the DNA was either cut with blunt-cutters or DNA overhangs were filled in with T4 Polymerase. The vector was cut with a blunt-cutter and gel-purified. After the fill-in reaction the fragment was ligated into the blunt site of the vector RT over night. Additionally 0,1 units of the enzyme, used to digest the vector, was added. The ligase was inactivated by heating the reaction to 65°C and 0.5 units of the enzyme, used to digest the vector, was added and incubated at optimal temperature. As negative control the same reaction with all conditions preserved was done in parallel but the insert was replaced by water.

D 3.9. Transformation of *Agrobacterium tumefaciens*

Agrobacteria were transformed via electroporation using a MicroPulser Electroporator from BioRad (165-2100) according to the manufactures instructions. Procedure was performed in 2 mm MicroPulser Cuvettes (165-2086).

D 3.10. Plant transformation

Transgenic plants were generated by *Agrobacterium* mediated T-DNA transformation (Koncz et al., 1989; Zambryski et al., 1983). The selection marker, the gene of interest and its regulatory elements are cloned into the T-DNA vector that harbours the essential elements needed by *Agrobacterium tumefaciens* for DNA transfer into the plant genome. Transformation of germ line cells results in transgenic seed that can be screened for the selection marker.

Stable transformations of *Arabidopsis* were generated by the “floral dip” method (Clough and Bent, 1998). Plants were grown at 16°C until inflorescences with buds of various stages had developed. The *Agrobacterium* strain GV3101 carrying the T-DNA vector was grown in YEB media containing the appropriate antibiotics for two days at 28°C. Bacteria were pelleted at 7000g and resuspended in 5% sucrose with 500µl Silvett L-77. Inflorescences of T0 plants were submerged in this media under slight agitation for 30 seconds and placed under a hood at 16°C. After two days plants were transferred to 23°C for seed ripening. These T1 seeds were germinated on media under selective pressure and transformants were singled out and propagated for further analysis.

D 3.11. Isolation of genomic DNA from *Arabidopsis*

Genomic DNA was isolated with the CTAB method (Rogers et al., 1988). Modifications are described. A small amount of fresh tissue (half a cotyledon to one leaf) was ground in 200µl 2xCTAB buffer (2 % Cetyltriethylammoniumbromid; 100 mM Tris-HCl (pH 8,0); 20 mM EDTA; 1,4 M NaCl; 1 % Polyvinylpyrrolidon) mixed thoroughly and incubated for at least one hour under agitation at 65°C. 200µl of CI (Chloroform:Isoamylalcohol, 24:1) was added, mixed thoroughly and centrifuged for 15 minutes. 150µl of the upper phase was transferred to a new 1.5 ml reaction tube, mixed with 200µl 2-Propanol and incubated for five minutes at RT. DNA is precipitated at 13000 x g, washed in 70% EtOH for 5 minutes at 13000 x g and air

dried until no traces of EtOH are left. It is not recommended to dry the pellet extensively. DNA is resuspended in an appropriate amount of H₂Odest (5-50µl).

D 3.12. Isolation of RNA from plants

RNA was isolated according to the TrizolR protocol from Invitrogen (Cat. No. 15596-026). TriReagentR from Molecular Research Center (TR 118) was used instead of Trizol. All material used was treated to prevent RNA contamination. 100mg of wild type, *elch* and 35S::ELCH plants was ground in liquid nitrogen and processed according to the manufactures instructions. The RNA was dissolved in 50µl of DEPC water and treated with RNase inhibitor from the Fermentas cDNA synthesis kit (Cat# K1612) and DNase from Ambion (Cat# 1906).

D 3.13. Reverse transcription

Equal amounts of RNA from *wild type*, *elch* and 35S::ELCH (approximately 8µg of total RNA) were used for first strand synthesis using the Invitrogen SuperScript™ First-Strand Synthesis System (Cat# 11904-018) according to the manufactures instructions. Primer IMZ004 was used to transcribe the ACT7 gene and CSP171 for transcription of the ELCH gene. CSP171 is complementary to the region that is deleted in *ELC-LIKE* and still intact in the *elch* mutant allele. As there is no intron in the ELCH gene RNA from all three lines was used in three separate reaction without reverse transcriptase. The “cDNA” of these reactions was used as negative control to determine whether there is genomic contamination in the isolated RNA.

D 3.14. Semiquantitative RT-PCR

To amplify the ACT7 gene as loading control and the ELCH fragment the following PCR conditions were used:

Initial denaturation	94°C/2min		
Denaturation	94°C/30sec		
Annealing	54°C/30sec	Annealing gradient:	58±5°C
Elongation	72°C/1min	Number of cycles:	18,19,21,23,30 (see Fi. B5 A)
End-elongation	72°C		

The volume of cDNA used for *wild type*, *elch* and *35S::ELCH* was adjusted in a way that the intensity of the *ACT7* control is approximately equal. The volume of cDNA used for *ACT7* and *wild type/ACT7* and *elc/ACT7* and *35S::ELCH* was kept equal.

D 3.15. Basic protein techniques (SDS-PAGE, Western blotting)

See “Molecular Cloning: A Laboratory Manual (Third Edition) By Joseph Sambrook, Peter MacCallum Cancer Institute, Melbourne, Australia; David Russell, University of Texas Southwestern Medical Center, Dallas”

D 3.16. Denaturing protein extraction

A plant sample (one to several leafs) were ground in Cracking buffer [60mM Tris/HCl, pH 8; 1% Mercaptoethanol; 1% SDS; 10% glycerol; 0,01% bromphenol-blue] and heated to 99°C for 10 minutes. Cell debris was pelleted and supernatend transferred to a fresh reaction tube. One to 15µl were used for SDS-PAGE.

D 3.17. Native protein extraction

Ubiquitin binding assay: All steps at 4°C. Four plants (4-5th leaf) from selection plates were ground in PPB [50 mM Phosphate buffer, 150mM NaCl; 0,5% NP40/CA630; 0,5mM DTT; 2,5% Complete] and centrifuged at 500 x g for one minute.

gel filtration: All steps at 4°C. Nine plants (4-5th leaf) from selection plates were ground in 600µl P150 [50 mM Phosphate buffer, 150mM NaCl]. 200 µl Complete-150 (one tablet Complete in 2ml P150) was added immediately. The homogenate was centrifuged at 16000 x g for two minutes. Supernatent was transferred to a fresh tube and centrifuged two more times for 37 and 5 minutes respectively. Each time a fresh tube was used.

Immunoprecipitation: All steps at 4°C. Protein was extracted from 0,3 to 1 g plant material. Plants were ground in 1.4 ml lysis buffer [50 mM TrisHCl (pH 8.0), 150 mM NaCl, 1% Triton X-100] complemented with 100µl protease inhibitor (one tablet Complete Protease Inhibitor in 2 ml lysis buffer) and 17.5µl 1 M DTT.

D 3.18. Ubiquitin binding assay

All steps at 4°C. Equal amounts of Ubiquitin- and Protein G agarose (approximately 70µl) were equilibrated. The beads were centrifuged at 500 x g and resuspended in 100µl PPB (repeat three times). 80 µl of PPB and 150 µl of native protein extract was added and incubated for 3 hours under slight agitation. Beads were centrifuged at 500 x g and resuspended carefully in 100 µl PPB (repeat three times). 50 µl cracking buffer was added, heated to 99°C for 10 minutes and used for SDS-PAGE. PAGE was performed using 12% polyacrylamide gels.

D 3.19. Size exclusion chromatography (gel filtration)

The Superose™ 6 10/300 GL column was equilibrated with two column volumes of P150. The column was then stepwise calibrated with 50µl of thyroglobulin (20mg/ml), 50µl β-amylase (16mg/ml), alcohol dehydrogenase (5mg/ml) and ovalbumin (20mg/ml). After washing with three column volumes of P150, 50µl of native protein extract was loaded and run under the same conditions like the standard (25ml, 0,35ml/min). Fractions of a volume of 0,4 ml were collected precipitated with trichloroacetic acid and resuspended in cracking buffer. The column was connected to a BioLogic DuoFlow™ FPLC machine from BioRad placed in a fridge at 4°C. PAGE was performed using 12% polyacrylamide gels.

D 3.20. Immunoprecipitation

All steps at 4°C if not indicated otherwise. For Immunoprecipitation a 1 ml aliquot of the native extract was used with 120 µl anti-HA MicroBeads (Miltenyi Biotec) according to the manufacturer's instructions with the following modifications: the column was rinsed five times with 200µl Wash Buffer 2, and the protein was eluted with 60 µl Elution Buffer heated to 95°C. The elution step was performed at RT. PAGE was performed using 12% polyacrylamide gels.

D 3.21. Antibody detection

Protein was blotted on Roti®-PVDF membranes from Roth (Cat# A147.1). Blots were blocked in 5% skimmed milk powder in PBT (PBS, 0,1% Tween®20). Primary antibody was incubated overnight at 4°C under agitation and washed three times in PBT. Secondary antibody was incubated for 90 minutes at RT and washed three times with PBT.

antibody	dilution
rat anti HA antibody	1:2000
mouse anti Ub antibody	1:1000-1500
mouse anti GFP antibody	1:2000
rabbit anti GFP antibody	1:2500
goat anti rat HRP	1:3000
goat anti mouse HRP	1:3000
goat anti mouse IRDye 680	1:3000
goat anti rabbit IRDye	1:3000

For detection the ECL™ System from Amersham Bioscience was used. Blots were placed between transparent foils and incubated with ECL™ Western Blotting Detection solution (RPN2109) according to the manufactures instructions. Hyperfilm ECL™ (RPN1674K) were exposed between 2 minutes and eight hours depending on signal strength. Films were developed by hand [eukobrom B/W paper developer (cat# 100294) and superfix plus rapid fixer (cat# 102760) from Tetenal] according to the manufactures instructions.

D 3.22. Silverstaining

For mass spectrometry compatible protein detection a silver staining protocol from Blum (Blum et al., 1987) was adopted. After PAGE the gel was fixed in 50% MeOH, 5% HAc for 20 minutes and washed in 50% MeOH for 10 minutes. Gel was washed in distilled water overnight, sensitized in 0,02% Natrium Thiosulphate for one minute and washed two times in water for one minute. For staining the gel was incubated at room temperature for 20 minutes in 0,15% silver nitrate/0,4% formalin. The gel was washed two times in distilled water for one minute and developed in 2% sodium carbonate/0,07% formalin until the staining was sufficient. Staining was stopped with 5% HAc. Bands were cut out and analyzed by Maldi-TOF mass spectrometry (Center for molecular medicin Cologne – Bioanalytical Laboratory).

D 3.23. Two colour western analysis

A method to detect two different proteins simultaneously with fluorescence marked antibodies. For detection the Odyssey Infrared Imaging System from Licor was used. The Odyssey scanner is equipped with two infrared channels for direct fluorescence

detection on membranes and discriminates the signals from two fluorescence marked antibodies. The blot was blocked in Rockland blocking solution for one hour. Mouse anti ubiquitin and rabbit anti GFP antibody were incubated overnight at 4°C under agitation in PBT (PBS, 0,2% Tween20, 5% skimmed milk powder. The blot was washed three times in PBT (0,2% Tween20). The blot was incubated with goat anti mouse IRDye 700 and goat anti rabbit IRDye 800 in PBT (PBS, 0,2% Tween20, 5% skimmed milk powder) at RT for 90 minutes. The blot was dried between Whatman paper in the dark and scanned with the Odyssey scanner. An overlay of the 700 and 800 nm channel was generated by the Licor software that also controls the scanner.

D 3.24. Image processing

All images were processed using Adobe Photoshop 6.0 software.

D 3.25. Sequence analysis

DNA and protein sequence analysis was performed using the Vector NTI® software from invitrogen™. Multiple sequence alignment was done using CLUSTALW from the NPS@ Web server. NPS@ is part of the Pôle Bioinformatique Lyonnais. For coiled coil domain analysis the COILS program was used (Lupas et al., 1991).

<http://www.invitrogen.com>

http://npsa-pbil.ibcp.fr/cgi-bin/npsa_automat.pl?page=npsa_clustalw.html

http://www.ch.embnet.org/software/COILS_form.html

E. Appendix

E 1. TSG101 has a size of 49 kDa on PAGE



Product Datasheet for ab83

Restrictions	Abcam is unable to supply ab83 to customers in: Japan
Product Name	TSG101 antibody [4A10]
Product type	Primary antibodies
Description	Mouse monoclonal [4A10] to TSG101
Immunogen	Fusion protein containing amino acids 167-374 of the TSG101 protein expressed in E. coli
Species Reactivity	Reacts with Human and Mouse Not yet tested in other species.
Specificity	This antibody recognizes the TSG-101 protein, the product of a recently identified tumor susceptibility gene the inactivation of which in mouse fibroblasts results in cell transformation and the ability of those cells to form tumors in nude mice
Tested applications	Immunocytochemistry, Immunofluorescence, Immunohistochemistry (Formalin/PFA-fixed paraffin-embedded sections), Immunoprecipitation, Western blot

Abreviews • WB (3 Abreviews)

Reviews by Abcam customers
(see 307)



Application notes	<p>Recommended dilutions</p> <p>ICC: Use at an assay dependent dilution. IF: Use at an assay dependent dilution. IHC-P: 1/100. Do not perform antigen retrieval. Wash thoroughly in 0.015M TBS (pH 7.6) and block with 20% normal rabbit serum. Incubate the antibody for 1 hr. Detect using biotinylated rabbit anti-mouse Ig followed by peroxidase conjugated streptavidin- biotin complex. IP: Use at an assay dependent dilution WB: 1/100 - 1/1000. Detects a band of approximately 47 kDa (predicted molecular weight: 43 kDa)</p> <p>Not tested in other applications. Optimal dilutions/concentrations should be determined by the end user.</p>
Cellular localization	Mainly cytoplasmic. Membrane-associated when active and soluble when inactive. Depending on the stage of the cell cycle, detected in the nucleus
Research areas	Nuclear Signaling >> Cell cycle >> Cell Differentiation Nuclear Signaling >> Cell cycle >> Cell Cycle Inhibitors >> Other Cell Biology >> Cell Cycle >> Cell Cycle inhibitors >> Other
Relevance	The protein encoded by this gene belongs to a group of apparently inactive homologs of ubiquitin-conjugating enzymes. The gene product contains a coiled-coil domain that interacts with stathmin, a cytosolic phosphoprotein implicated in tumorigenesis. The protein may play a role in cell growth and

differentiation and act as a negative growth regulator. In vitro steady-state expression of this tumor susceptibility gene appears to be important for maintenance of genomic stability and cell cycle regulation. Mutations and alternative splicing in this gene occur in high frequency in breast cancer and suggest that defects occur during breast cancer tumorigenesis and/or progression.

Database links	Entrez Gene	7251 (Human) 22088 (Mouse)	SwissProt	Q99816 (Human) Q61187 (Mouse)
	GeneCard	GC11M018466 (Human)	Unigene	532483 (Human) 241334 (Mouse)
	Omim	601387 (Human)		
Raised in	Mouse			
Clonality	Monoclonal			
Clone number	4A10			
Myeloma	NS1			
Isotype	IgG1			
Light chain type	kappa			
Purity	Protein G purified			
Storage buffer	PBS pH 7.4 w/o preservative			
Purification notes	Purified from ascites fluid by Protein G chromatography to at least 95% homogeneity as determined by SDS-PAGE.			
Form	Liquid			
Concentration	1.00 mg/ml			
Storage instructions	Aliquot and store at -20°C or -80°C. Avoid repeated freeze / thaw cycles.			
Supplier	Genetex (GTX70255)			

At Abcam, we have one centralized database to hold all of our product information, so that everything we know about this TSG101 antibody [4A10] is on this datasheet. But please do contact us if you would like any reassurance!



See below for TSG101 antibody [4A10] images, references, products related to ab83 and other tools.

TSG101 antibody [4A10] images:

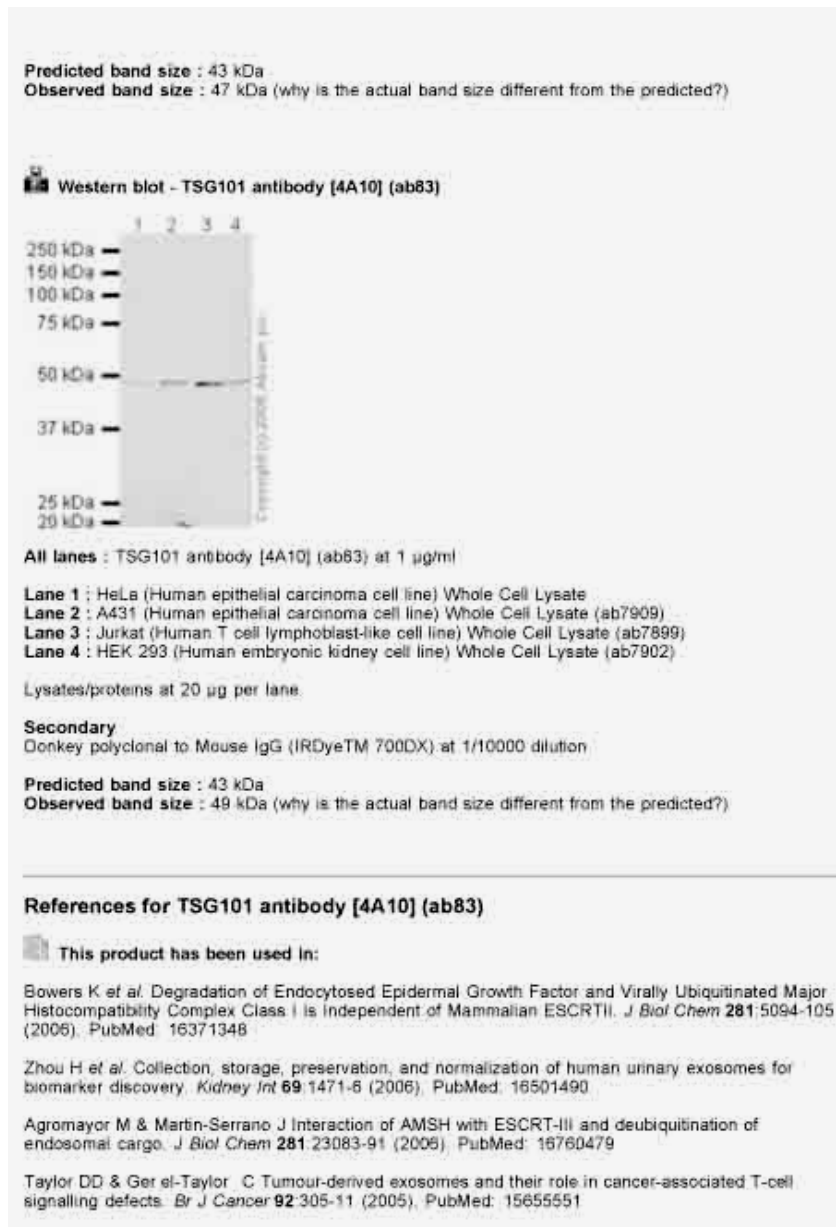
Western blot - TSG101 antibody [4A10] (ab83)



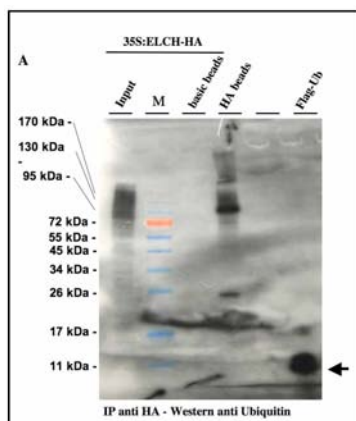
All lanes : TSG101 antibody [4A10] (ab83)

Lane 1 : 20ug HeLa cell extract

Lane 2 : 20ug HeLa cell extract from cells treated with TSG101 siRNA



E 2. SC8017 anti-Ubiquitin is specific for ubiquitin



E 3. Mass spectrometry data of ESCRT-I components

ELCH At3g12400 4487

MASCOT Mascot Search Results

Protein View

Match to: gi|18399596; Score: 183
 unknown protein [Arabidopsis thaliana]
 Nominal mass (M_r): 44859; Calculated pI value: 5.86
 NCBI BLAST search of gi|18399596 against nr
 Unformatted [sequence string](#) for pasting into other applications

Taxonomy: *Arabidopsis thaliana*
 Links to retrieve other entries containing this sequence from NCBI Entrez:
[gi|18399596](#) from *Arabidopsis thaliana*
[gi|18399597](#) from *Arabidopsis thaliana*
[gi|18399598](#) from *Arabidopsis thaliana*
[gi|18399599](#) from *Arabidopsis thaliana*
[gi|18399600](#) from *Arabidopsis thaliana*

Fixed modifications: Carbamidomethyl (C)
 Variable modifications: Oxidation (M)
 Cleavage by Trypsin: cuts C-term side of KR unless next residue is P
 Number of mass values searched: 46
 Number of mass values matched: 19
 Sequence Coverage: 49%

Matched peptides shown in **Bold Red**

```

1 MVPPFNPOQ VQGFSSALS QRPSSVPIE ESNKWLIRQH LLWLISYPS
51 LEPKASFRH NDRGVNLIQ ADGTIPMPFH GVTYINIPVIL WLESYFRHF
101 PCVIVYFAD HIKRKRPHAV TPGSLVSPY LQWVYFSSN LVDSVDSJA
151 AFARDPPLYS RRRPQPPPS PPTYVDSLS RPPSADQSLP RPPFPSPYGG
201 GVSRRVQVH HQQSSDDAA EVFRNAINK MVNVRSDLV SMRRAREEA
251 SEELSLQNL KRREDELTIQ LKEMVEEET LQQLQIISL NTDILDSVVR
301 ENQGFTRALY DLVDNATPC GDTLSQSLK CTALDAIED ATYSLKSPF
351 DGVVFPDYL RNVRLSREK FPHRATGSKV RAAQHEVQVA AIAGRLLS

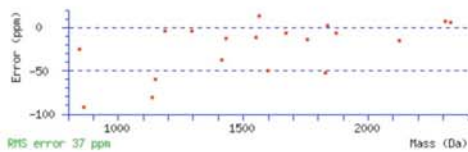
```

Show predicted peptides also

Sort Peptides By Residue Number Increasing Mass Decreasing Mass

Start	End	Observed	Mr(expt)	Mr(calc)	Delta	Miss	Sequence
2	22	2308.22	2307.21	2307.20	0.02	0	VPPFNPOQVQGFSSALSQR
23	34	1293.59	1292.58	1292.59	-0.01	0	GPSVPTTEENK
39	54	1839.00	1838.00	1837.99	0.00	0	QHLLNLISYFLEPK
55	64	1135.40	1134.40	1134.49	-0.09	0	TASFMHNGR
55	64	1151.42	1150.41	1150.48	-0.07	0	TASFMHNGR Oxidation (M)
99	114	1870.91	1869.90	1869.91	-0.01	0	HPPCVYVNTAGMIK Oxidation (M)
155	161	847.41	846.40	846.42	-0.02	0	DPLYSR
205	224	2330.14	2329.13	2329.12	0.01	0	VQVQVHQQQSDAAEVFK
231	243	1549.70	1548.69	1548.71	-0.02	0	MVENVRSDLVNR Oxidation (M)
231	243	1565.73	1564.72	1564.70	0.02	0	MVENVRSDLVNR 2 Oxidation (M)
245	261	1827.88	1826.88	1826.97	-0.10	1	AKAAEELSLQAGLK
247	261	1600.76	1599.75	1599.84	-0.09	0	EAAEELSLQAGLK
247	262	1756.92	1755.91	1755.94	-0.03	1	EAAEELSLQAGLKR
263	272	1186.64	1185.63	1185.64	-0.00	1	REDELMIQLK
308	326	2124.94	2123.94	2123.97	-0.03	0	NLVLDVONAFEGDITLTK
348	361	1670.81	1669.80	1669.81	-0.01	0	SFGQGVVFPDQYLK
369	374	863.34	862.33	862.41	-0.09	0	EQFTHR
382	395	1414.69	1413.69	1413.74	-0.05	0	AAQHEVQVAIAGR
382	395	1430.72	1429.72	1429.73	-0.02	0	AAQHEVQVAIAGR Oxidation (M)

No match to: 1102.48, 1218.56, 1222.61, 1250.61, 1317.69, 1329.68, 1342.71, 1465.70, 1476.75, 1588.87, 1730.99, 1822.96, 1884.92, 2082.99, 2138.96, 2209.14, 2313



LOCUS NP_566423 398 aa linear PLN 04-NOV-2005
 DEFINITION unknown protein [Arabidopsis thaliana].
 ACCESSION NP_566423
 VERSION NP_566423.1 GI:18399596
 DBSOURCE REFSEQ: accession NM_112075.2
 KEYWORDS
 SOURCE Arabidopsis thaliana [thale cress]
 ORGANISM Arabidopsis thaliana
 Eukaryota; Viridiplantae; Streptophyta; Embryophyta; Tracheophyta;
 Spermatophyta; Magnoliophyta; eudicotyledons; core eudicotyledons;
 rosids; eurosids II; Brassicales; Brassicaceae; Arabidopsis.
 COMMENT PROVISIONAL REFSEQ: This record has not yet been subject to final
 NCBI review. The reference sequence was derived from AT3G12400.lf.
 Method: conceptual translation.
 FEATURES
 source 1..398
 /organism="Arabidopsis thaliana"
 /db_xref="taxon:3702"
 /chromosome="3"
 /ecotype="Columbia"
 Protein 1..398
 /product="unknown protein"
 /calculated_mol_wt=44595
 Region 41..2134
 /region_name="Ubiquitin-conjugating enzyme E2, catalytic
 domain homologues"
 /note="UBC2"
 /db_xref="CDD:47542"
 CDS 1..398
 /locus_tag="AT3G12400"
 /coded_by="NM_112075.2:56..1252"
 /gc_component="chloroplast"
 /go_process="protein modification; protein transport;
 ubiquitin cycle"
 /note="tumour susceptibility gene 101 (TSG101) family
 protein, contains Pfam profile PF05743: Tumour
 susceptibility gene 101 protein (TSG101); similar to Tumor

ELCH At3g12400 4493

MASCOT Mascot Search Results

Protein View

Match to: gi|18399596; Score: 213
unknown protein [Arabidopsis thaliana]Nominal mass (Mr): 44859; Calculated pI value: 5.86
NCBI BLAST search of gi|18399596 against nr
Unformatted [sequence string](#) for pasting into other applicationsTaxonomy: [Arabidopsis thaliana](#)
Links to retrieve other entries containing this sequence from NCBI Entrez:
[gi|22136968](#) from [Arabidopsis thaliana](#)
[gi|15810487](#) from [Arabidopsis thaliana](#)
[gi|21593307](#) from [Arabidopsis thaliana](#)
[gi|12321968](#) from [Arabidopsis thaliana](#)
[gi|15795197](#) from [Arabidopsis thaliana](#)Fixed modifications: Carbamidomethyl (C)
Variable modifications: Oxidation (M)
Cleavage by Trypsin: cuts C-term side of KR unless next residue is P
Number of mass values searched: 38
Number of mass values matched: 18
Sequence Coverage: 46%Matched peptides shown in **Bold Red**

```

1  MVPPSPNPQQ VQQFLSSALS QRGPPSSVPE ESNKGLIRQH LLNLISSTPS
51  LEPKTAAPMR HDGRSVNLLQ ADGTIPMPFH GVTYNIPIII WLESYPRHP
101  KCVYVNPAD DMIKRPRIHV TPGGLVLEPY LQHWYTPSN LVDLVSDLSA
151  AFARDPPLYS RRRPQPPPS PPTVYDSSLR RPPGADQSLR RFPFSPVGG
201  GVSRRVQVHV HHQQSDDAE EVFKRNAINK MVMVHSDLV SMRRAREAEA
251  EELLSLQAGL KRREDELNIG LKEMVEEKET LEQQLIISM NTDILDSWVR
301  ENQGRTRNLV DLVDNAFEC GDTLSKQMLE CTALDLAIED AIYELDRSFQ
351  DGVVFPQYL RNVRLSRQ FFRATGSKV RAAGMEVQA AIAGLHS

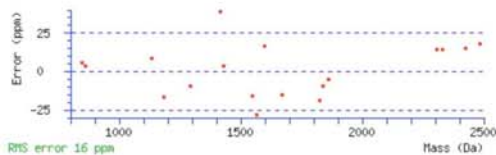
```

Show predicted peptides also

Sort Peptides By Residue Number Increasing Mass Decreasing Mass

Start - End	Observed	Mr(expt)	Mr(calco)	Delta	Miss	Sequence
2 - 22	2308.24	2307.23	2307.20	0.03	0	VPPSPNPQQVQQFLSSALSQR
23 - 34	1293.58	1292.58	1292.59	-0.01	0	GPSSVPTESNK
23 - 38	1861.94	1860.93	1860.94	-0.01	1	GPSSVPTESNGLIR
39 - 54	1838.98	1837.98	1837.99	-0.02	0	QHLNLISSYPLEPK
55 - 64	1135.50	1134.50	1134.49	0.01	0	TASFMNDGR
155 - 161	847.44	846.43	846.42	0.00	0	DPPLYSR
205 - 224	2330.16	2329.15	2329.12	0.03	0	VQVQVHHQQSDDAEVEFK
205 - 225	2486.27	2485.27	2485.22	0.05	1	VQVQVHHQQSDDAEVEFK
231 - 243	1549.69	1548.68	1548.71	-0.03	0	MVMVHSDIVSMR Oxidation (M)
231 - 243	1565.67	1564.66	1564.70	-0.04	0	MVMVHSDIVSMR 2 Oxidation (M)
245 - 261	1827.95	1826.94	1826.97	-0.03	1	AREAEELLSLQGLK
247 - 261	1600.87	1599.86	1599.84	0.03	0	EAEAEELLSLQGLK
263 - 272	1186.62	1185.62	1185.64	-0.02	1	REDELNIGL
327 - 347	2428.20	2427.19	2427.15	0.04	0	QMLECTALDLAIEDAIYSLDK Oxidation (M)
348 - 361	1670.79	1669.78	1669.81	-0.03	0	SPQDGVVFPDQYLR
369 - 374	863.42	862.41	862.41	0.00	0	EQFFHR
382 - 395	1414.80	1413.79	1413.74	0.05	0	AAQMEVQVAIAGR
382 - 395	1430.75	1429.74	1429.73	0.01	0	AAQMEVQVAIAGR Oxidation (M)

No match to: 852.39, 1021.51, 1037.53, 1102.47, 1317.66, 1342.72, 1619.77, 1821.97, 1868.87, 1884.91, 1893.91, 2038.18, 2139.00, 2196.06, 2209.16, 2442.18, 2663.



```

LOCUS       NP_566423             398 aa             linear   PLN 04-NOV-2005
DEFINITION unknown protein [Arabidopsis thaliana].
ACCESSION   NP_566423
VERSION     NP_566423.1  GI:18399596
DBSOURCE    REFSEQ: accession NM_112075.2
KEYWORDS    .
SOURCE      Arabidopsis thaliana (thale cress)
ORGANISM    Arabidopsis thaliana
             Eukaryota; Viridiplantae; Streptophyta; Embryophyta; Tracheophyta;
             Spermatophyta; Magnoliophyta; eudicotyledons; core eudicotyledons;
             rosids; eurosids II; Brassicales; Brassicaceae; Arabidopsis.
COMMENT     PROVISIONAL REFSEQ: This record has not yet been subject to final
             NCBI review. The reference sequence was derived from AT3G12400.lip.
             Method: conceptual translation.
FEATURES             Location/Qualifiers
     source          1..398
                     /organism="Arabidopsis thaliana"
                     /db_xref="taxon:3702"
                     /chromosome="3"
                     /scotype="Columbia"
     Protein         1..398
                     /product="unknown protein"
                     /calculated_mol_wt=44585
     Region          41..134
                     /region_name="Ubiquitin-conjugating enzyme E2, catalytic
                     domain homologues"
                     /note="UBCc"
                     /db_xref="CDD:47542"
     CDS             1..398
                     /locus_tag="AT3G12400"
                     /coded_by="NM_112075.2:56..1252"
                     /gc_component="chloroplast"
                     /gc_process="protein modification; protein transport;
                     ubiquitin cycle"
                     /note="tumour susceptibility gene 101 (TSG101) family
                     protein, contains Pfam profile PF05743: Tumour
                     susceptibility gene 101 protein (TSG101); similar to Tumour
                     susceptibility gene 101 protein (Swiss-Prot:Q99816) (Homo

```

ELCH At3g12400 4692

MASCOT Mascot Search Results

Protein View

Match to: gi|18399596; Score: 192
unknown protein [Arabidopsis thaliana]Nominal mass (M_r): 44859; Calculated pI value: 5.86
NCBI BLAST search of gi|18399596 against nr
Unformatted [sequence string](#) for pasting into other applicationsTaxonomy: Arabidopsis thaliana
Links to retrieve other entries containing this sequence from NCBI Entrez:
[gi|22136968](#) from Arabidopsis thaliana
[gi|15810489](#) from Arabidopsis thaliana
[gi|12321968](#) from Arabidopsis thaliana
[gi|15795159](#) from Arabidopsis thaliana
[gi|21593367](#) from Arabidopsis thalianaFixed modifications: Carbamidomethyl (C)
Variable modifications: Oxidation (M)
Cleavage by Trypsin: cuts C-term side of KR unless next residue is P
Number of mass values searched: 52
Number of mass values matched: 20
Sequence Coverage: 55%

Matched peptides shown in Bold Red

```

1  MVPPSPNQ VQFLSSALL QRPSSVPEY ESNKLIHQH LLNLISYPS
51  LEPKTASPMH NDRSIVNLLQ ADGTIPMPFH GVTYNIPVII WLESYPRHP
101 PCVTVNPEAD NIKRPHAMV TPGSLVSLPY LQNWVYPSN LVLDVSDLSA
151 AFARWPPPS RRKQPPPS PFTVYDSSLR RFGADQGLP RFPFSPFGG
201 GVSRRVQVHV HQQQSDAA EVFKRINAKN MVMVHSDLV SMKRAREAA
251 EELLSLQAGL KRREDELNIG LKEMVEKET LEQQLIISM NTDILDSWR
301 ENQKTKNLV DLVDNAFCG GPILSKQMLE CTALDLAIED AIYSLDRSFQ
351 DGVVFPDQL RNVKLSRQ FFRATGSKV RAAQMEVQVA AIAGRLHS

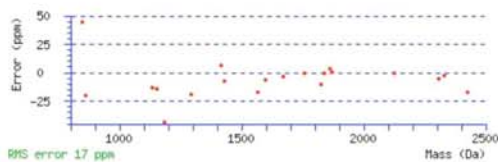
```

Show predicted peptides also

Sort Peptides By Residue Number Increasing Mass Decreasing Mass

Start - End	Observed	Mr (expt)	Mr (calc)	Delta	Miss	Sequence
2 - 22	2308.19	2307.19	2307.20	-0.01	0	VFPSPNQ VQFLSSALLSQ
23 - 34	1293.57	1292.56	1292.59	-0.03	0	GPSSVYERENK
23 - 38	1861.95	1860.94	1860.94	0.01	1	GPSSVYERENKLI
39 - 54	1839.00	1837.99	1837.99	-0.00	0	QHLNLISYPSLEPK
55 - 64	1135.48	1134.47	1134.49	-0.01	0	TASFMNDGR
55 - 64	1151.47	1150.47	1150.48	-0.02	0	TASFMNDGR Oxidation (M)
99 - 114	1870.92	1869.91	1869.91	0.00	0	HPPCVVNPATMIK Oxidation (M)
155 - 161	847.47	846.46	846.42	0.04	0	DPPLYR
205 - 224	2330.12	2329.11	2329.12	-0.01	0	VQVQVHVVHQSSDAAEVFK
231 - 243	1565.69	1564.68	1564.70	-0.03	0	MVMVHSDLVSMR 2 Oxidation (M)
245 - 261	1827.96	1826.96	1826.97	-0.02	1	AREAESELLSLQAGLK
247 - 261	1600.83	1599.83	1599.84	-0.01	0	EAESELLSLQAGLK
247 - 262	1756.94	1755.94	1755.94	-0.00	1	EAESELLSLQAGLKR
263 - 272	1186.59	1185.58	1185.64	-0.05	1	REDELNIGLK
308 - 326	2124.97	2123.97	2123.97	-0.00	0	NLVLDVDMNAFCGDTLSEK
327 - 347	2428.12	2427.11	2427.15	-0.04	0	QMLECTALDLAIEDAIYSLWK Oxidation (M)
348 - 361	1670.81	1669.80	1669.81	-0.01	0	SFQDGVVFPDQLYR
369 - 374	863.40	862.39	862.41	-0.02	0	EQFFHR
382 - 395	1414.76	1413.75	1413.74	0.01	0	AAQMEVQVAIAGR
382 - 395	1430.73	1429.72	1429.73	-0.01	0	AAQMEVQVAIAGR Oxidation (M)

No match to: 802.45, 807.43, 827.42, 852.39, 995.49, 1021.48, 1033.48, 1065.52, 1090.50, 1102.46, 1109.46, 1165.50, 1234.65, 1317.63, 1320.58, 1329.66, 1342.72.



LOCUS NP_566423 398 aa linear FLM 09-JUN-2006
DEFINITION unknown protein [Arabidopsis thaliana].
ACCESSION NP_566423
VERSION NP_566423.1 GI:18399596
DISOURCE REFSEQ: accession NM_112075.2
KEYWORDS .
SOURCE Arabidopsis thaliana (thale cress)
ORGANISM Arabidopsis thaliana
Eukaryota; Viridiplantae; Streptophyta; Embryophyta; Tracheophyta;
Spermatophyta; Magnoliophyta; eudicotyledons; core eudicotyledons;
rosids; eurosids II; Brassicales; Brassicaceae; Arabidopsis.
COMMENT PROVISIONAL REFSEQ: This record has not yet been subject to final
NCBI review. The reference sequence was derived from AT3G12400.1p.
Method: conceptual translation.
FEATURES
source
location/Qualifiers
1..398
/organism="Arabidopsis thaliana"
/db_xref="taxon:3702"
/chromosome="3"
/ecotype="Columbia"
Protein
1..398
/product="unknown protein"
/calculated_mol_wt=44585
Region
31..385
/region_name="Tsg101"
/note="Tumour susceptibility gene 101 protein (TSG101);
pfam05743"
/db_xref="CCD:45638"
CDS
1..398
/locus_tag="AT3G12400"
/coded_by="NM_112075.2:56..1252"
/go_component="chloroplast"
/go_process="protein modification; protein transport;
ubiquitin cycle"
/note="tumour susceptibility gene 101 (TSG101) family
protein, contains Pfam profile PF05743; Tumour

VPS28/1 At4g21560 4557


Mascot Search Results
Protein View

Match to: [gi|42572977](#); Score: 127
transporter [Arabidopsis thaliana]

Nominal mass (M_r): 23650; Calculated pI value: 5.21
 NCBI BLAST search of [gi|42572977](#) against nr
 Unformatted [sequence string](#) for pasting into other applications

Taxonomy: [Arabidopsis thaliana](#)
 Links to retrieve other entries containing this sequence from NCBI Entrez:

[gi|30685488](#) from [Arabidopsis thaliana](#)
[gi|15234509](#) from [Arabidopsis thaliana](#)
[gi|22531273](#) from [Arabidopsis thaliana](#)
[gi|30023672](#) from [Arabidopsis thaliana](#)
[gi|7268953](#) from [Arabidopsis thaliana](#)
[gi|4455264](#) from [Arabidopsis thaliana](#)
[gi|3080400](#) from [Arabidopsis thaliana](#)
[gi|13124598](#) from [Arabidopsis thaliana](#)
[gi|7485715](#) from [Arabidopsis thaliana](#)

Fixed modifications: Carbamidomethyl (C)
 Variable modifications: Oxidation (M)
 Cleavage by Trypsin: cuts C-term side of KR unless next residue is P
 Number of mass values searched: 25
 Number of mass values matched: 12
 Sequence Coverage: 57%

Matched peptides shown in **Bold Red**

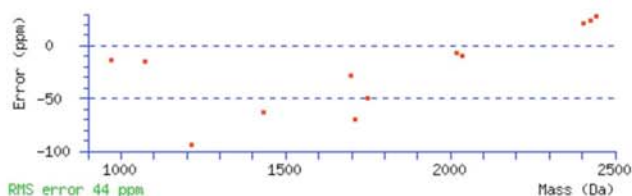
1 MEVKLW~~NDKR~~ **EREMYENFAE LYAIKATEK** LEKAYIRDLI SPSEYETECQ
 51 **KLIVHF**KTLASL**KDMVPNI** **ERFAETYKMD** CSAAVYRLVT SGVPATVEHR
 101 AAASASTSSS ASVVAECVQN FITSMDSLKLN**MVAVDQVYP** **LLS**DL**SASLN**
 151 **KLSILPPD**FE **GKIRK**EWLL RLSK**MGASDE** **LTEQ**QARQLH **FD**LESSYNSF
 201 **MAAL**PNAGN

Show predicted peptides also

Sort Peptides By Residue Number Increasing Mass Decreasing Mass

Start - End	Observed	Mr (expt)	Mr (calc)	Delta	Miss	Sequence
11 - 26	2018.98	2017.97	2017.98	-0.01	1	EREMYENFAELYAIK
11 - 26	2034.96	2033.96	2033.98	-0.02	1	EREMYENFAELYAIK Oxidation (M)
13 - 26	1749.75	1748.75	1748.83	-0.09	0	EMYENFAELYAIK Oxidation (M)
38 - 51	1698.71	1697.70	1697.75	-0.05	0	DLISPSEYETECQK
65 - 72	973.46	972.46	972.47	-0.01	0	DMVPNIER
65 - 78	1712.71	1711.70	1711.82	-0.12	1	DMVPNIERFAETYK
79 - 87	1072.44	1071.43	1071.45	-0.02	0	MDCSAAVYR
130 - 151	2406.31	2405.30	2405.25	0.05	0	LNMVAVDQVYPLLS DL SASLNK Oxidation (M)
152 - 162	1215.55	1214.54	1214.65	-0.11	0	LSILPPDFEGK
175 - 187	1435.56	1434.55	1434.64	-0.09	0	MGASDELTEQ QAR
188 - 209	2426.16	2425.16	2425.10	0.06	0	QLHF DL LESSYNSF MAAL PNAGN
188 - 209	2442.17	2441.17	2441.10	0.07	0	QLHF DL LESSYNSF MAAL PNAGN Oxidation (M)

No match to: 843.01, 1021.01, 1023.45, 1096.45, 1379.65, 1586.64, 1631.73, 1657.83, 1734.73, 1826.69, 1892.80, 1980.02,



LOCUS NP_974585 209 aa linear PLN 09-JUN-2006
 DEFINITION transporter [Arabidopsis thaliana].
 ACCESSION NP_974585
 VERSION NP_974585.1 GI:42572977
 DBSOURCE REFSEQ: accession NM_202856.1
 KEYWORDS .
 SOURCE Arabidopsis thaliana (thale cress)
 ORGANISM Arabidopsis thaliana
 Eukaryota; Viridiplantae; Streptophyta; Embryophyta; Tracheophyta;
 Spermatophyta; Magnoliophyta; eudicotyledons; core eudicotyledons;
 rosids; eurosids II; Brassicales; Brassicaceae; Arabidopsis.
 COMMENT PROVISIONAL REFSEQ: This record has not yet been subject to final
 NCBI review. The reference sequence was derived from AT4G21560.3p.
 Method: conceptual translation.
 FEATURES Location/Qualifiers

VPS28/1 At4g21560 4485

Mascot Search Results**Protein View**Match to: gi|42572977; Score: 79
transporter [Arabidopsis thaliana]Nominal mass (M_r): 23650; Calculated pI value: 5.21NCBI BLAST search of gi|42572977 against nr
Unformatted [sequence string](#) for pasting into other applications

Taxonomy: Arabidopsis thaliana

Links to retrieve other entries containing this sequence from NCBI Entrez:

[gi|3069488](#) from Arabidopsis thaliana
[gi|15233509](#) from Arabidopsis thaliana
[gi|22531273](#) from Arabidopsis thaliana
[gi|30023672](#) from Arabidopsis thaliana
[gi|7268957](#) from Arabidopsis thaliana
[gi|4352624](#) from Arabidopsis thaliana
[gi|3080408](#) from Arabidopsis thaliana
[gi|13124598](#) from Arabidopsis thaliana
[gi|7485715](#) from Arabidopsis thaliana

Fixed modifications: Carbamidomethyl (C)

Variable modifications: Oxidation (M)

Cleavage by Trypsin: cuts C-term side of KR unless next residue is P

Number of mass values searched: 42

Number of mass values matched: 8

Sequence Coverage: 42%

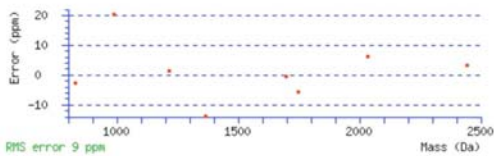
Matched peptides shown in **Bold Red**

1 MEVKLNDRK EREMYENFAE LYAIKATEK LEKAYIRDLI SPSEYETECQ
51 KLIVHFKTLS ASLKDMVPHI ERFAETYKMD CSAAYRRLVT SOVPATVEHR
101 AAASASTSSS ASVVAECVQN FITSMDSLK NMVAVDQVYP LLSDLASLN
151 KLSILPDPFE GKIKKEWLL KLSKMGASDE LTEQARQLH FDESSTNSP
201 MAALPNAGN

Show predicted peptides also**Sort Peptides By** Residue Number Increasing Mass Decreasing Mass

Start - End	Observed	Mr (expt)	Mr (calc)	Delta	Miss	Sequence
5 - 10	831.44	830.44	830.44	-0.00	1	LWDRK
11 - 26	2035.00	2033.99	2033.98	0.01	1	EREMYENFAELYAIK Oxidation (M)
13 - 26	1749.83	1748.82	1748.83	-0.01	0	EMYENFAELYAIK Oxidation (M)
38 - 51	1698.75	1697.74	1697.75	-0.00	0	DLISPSSEYETECQK
88 - 100	1365.73	1364.72	1364.74	-0.02	0	LVTSQVPAVTEHR
152 - 182	1215.66	1214.66	1214.65	0.00	0	LSILPDPFEK
165 - 171	991.56	990.55	990.53	0.02	1	MSGMLLR Oxidation (M)
188 - 209	2442.11	2441.10	2441.10	0.01	0	QLHFDLESYNSFMAALPNAGN Oxidation (M)

No match to: 807.40, 827.42, 949.49, 995.54, 1023.52, 1107.59, 1109.51, 1193.60, 1234.67, 1303.67, 1320.61, 1329.69, 1336.72, 1381.62, 1393.72, 1434.69, 1460.78,



LOCUS NP_974585 209 aa linear PLN 04-NOV-2005
 DEFINITION transporter [Arabidopsis thaliana].
 ACCESSION NP_974585
 VERSION NP_974585.1 GI:42572977
 DBSOURCE REFSEQ: accession NM_202856.1
 KEYWORDS .
 SOURCE Arabidopsis thaliana (thale cress)
 ORGANISM Arabidopsis thaliana
 Eukaryota; Viridiplantae; Streptophyta; Embryophyta; Tracheophyta;
 Spermatophyta; Magnoliophyta; eudicotyledons; core eudicotyledons;
 rosids; eurosids II; Brassicales; Brassicaceae; Arabidopsis.
 COMMENT PROVISIONAL REFSEQ: This record has not yet been subject to final
 NCBI review. The reference sequence was derived from AT4G21560.3p.
 Method: conceptual translation.
 FEATURES
 source Location/Qualifiers
 source 1..209
 /organism="Arabidopsis thaliana"
 /db_xref="taxon:3702"
 /chromosome="4"
 /ecotype="Columbia"
 Protein 1..209
 /product="transporter"
 /calculated_mol_wt=23363
 Region 18..>204
 /region_name="VPS28 protein"
 /note="VPS28"
 /db_xref="CDD:43914"
 CDS 1..209
 /locus_tag="AT4G21560"
 /coded_by="NM_202856.1:698..1327"
 /go_component="cellular component unknown"
 /go_function="transporter activity"
 /go_process="transport"
 /note="vacuolar protein sorting-associated protein 28
 family protein / VPS28 family protein, contains similarity
 to Swiss-Prot:Q02767 vacuolar protein sorting-associated
 protein VPS28 (Saccharomyces cerevisiae)"
 /db_xref="GeneID:828241"

VPS28/2 At4g05000 4557Ha

MASCOT Mascot Search Results

Protein View

Match to: gi|7267259; Score: 82
AT4g05000 [Arabidopsis thaliana]Nominal mass (M_r): 23714; Calculated pI value: 5.34NCBI BLAST search of gi|7267259 against nr
Unformatted [sequence listing](#) for pasting into other applications

Taxonomy: Arabidopsis thaliana

Links to retrieve other entries containing this sequence from NCBI Entrez:

[gi|5732073](#) from Arabidopsis thaliana[gi|2432912](#) from Arabidopsis thaliana[gi|13124615](#) from Arabidopsis thaliana

Fixed modifications: Carbamidomethyl (C)

Variable modifications: Oxidation (M)

Cleavage by Trypsin: cuts C-term side of KR unless next residue is P

Number of mass values searched: 25

Number of mass values matched: 8

Sequence Coverage: 47%

Matched peptides shown in **Red**

```

1 MEVFLWNDER EREMYENFAE LPAIKATEK LEKAYIRDLI NPSEYESEQ
51 KLIVHFKTIS ATLKDTVPPIR ERFADTFEED CPAALYRLVT SOLPAVVEHR
101 ATVAASTSNS ASIVAECVQN FITSMDSLK NNVAVDQVYP LLSDLASLN
151 KLSLPPDFE GKTMKKEWLS RLSKMGAADE LTEQQSRQLH FDLESSYNSF
201 MAALPRAGN

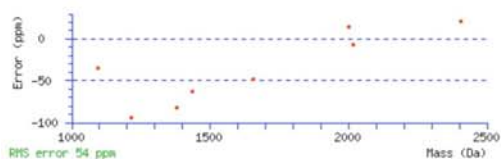
```

Show predicted peptides also

Sort Peptides By Residue Number Increasing Mass Decreasing Mass

Start - End	Observed	Mr (expt)	Mr (calc)	Delta	Miss	Sequence
11 - 26	2003.02	2002.02	2001.99	0.03	1	EREMYENFAELPAIK
11 - 26	2018.98	2017.97	2017.98	-0.01	1	EREMYENFAELPAIK Oxidation (M)
58 - 72	1657.83	1656.83	1656.90	-0.08	1	TLSATLKDTVPPIER
79 - 87	1096.45	1095.45	1095.48	-0.04	0	MCCPAALYR
88 - 100	1379.65	1378.64	1378.76	-0.11	0	LVTSGLPATVEHR
130 - 151	2406.31	2405.30	2405.25	-0.05	0	LNNVAVDQVYVFLLSDLASLNK Oxidation (M)
152 - 162	1215.55	1214.54	1214.65	-0.11	0	LSLPPDFEGR
175 - 187	1435.56	1434.55	1434.64	-0.09	0	MGADELTEQQSR

No match to: 843.01, 973.46, 1021.01, 1023.45, 1072.44, 1586.64, 1631.73, 1698.71, 1712.71, 1734.73, 1749.75, 1826.69, 1892.80, 1980.02, 2034.96, 2426.16, 2442.1



LOCUS CAB81042 209 aa linear PLN 16-APR-2005
DEFINITION AT4g05000 [Arabidopsis thaliana].
ACCESSION CAB81042
VERSION CAB81042.1 GI:7267259
DBSOURCE embi locus ATCHRIV14, accession AL161502.2
KEYWORDS
SOURCE Arabidopsis thaliana (thale cress)
ORGANISM Arabidopsis thaliana
Eukaryota; Viridiplantae; Streptophyta; Embryophyta; Tracheophyta;
Spermatophyta; Magnoliophyta; eudicotyledons; core eudicotyledons;
rosids; eurosids II; Brassicales; Brassicaceae; Arabidopsis.
REFERENCE 1 (residues 1 to 209)
AUTHORS EU Arabidopsis sequencing project.
TITLE Direct Submission
JOURNAL Submitted (10-MAR-2000) MIPS, at the Max-Planck-Institut fuer
Biochemie, Am Klopferspitz 18a, D-82152 Martinsried, FRG, E-mail:
lemcke@mips.biochem.mpg.de,mayer@mips.biochem.mpg.de Project
Coordinator: Mike Bevan, Molecular Genetics Department, Cambridge
Laboratory, John Innes Centre, Colney Lane, NR4 7UJ Norwich, UK,
E-mail: michael.bevan@bbsrc.ac.uk
COMMENT Information on performance of analysis and a more detailed
annotation of this entry and other sequences of chromosomes 3, 4
and 5 can be viewed at: <http://www.mips.biochem.mpg.de/proj/thal/>
this fragment has an overlap with ATCHRIV13 at the 5' end and an
overlap with ATCHRIV15 at the 3' end.
FEATURES
source
1..209
/organism="Arabidopsis thaliana"
/db_xref="taxon:3702"
/chromosome="4"
/ecotype="Columbia"
Protein
1..209
/name="AT4g05000"
Region
18..>204
/region_name="VPS28 protein"
/note="VPS28"
/db_xref="CDD:43914"
CDS
1..209
/gene="AT4g05000"
/coded_by="AL161502.2:95971..96600"
/note="contains similarity to S. cerevisiae vacuolar
protein sorting-associated protein VPS28 (GB:U39205)
similarity to
contains EST gb:AW032483.1, Z34723, AI996739.1"
/db_xref="GOA:Q9S9T7"
/db_xref="InterPro:IPR007143"
/db_xref="UniProtKB/Swiss-Prot:Q5S9T7"

VPS37/1 At3g53120 4556H1

MASCOT Mascot Search Results**Protein View**Match to: gi|15231750; Score: 119
unknown protein [Arabidopsis thaliana]Nominal mass (M_r): 24982; Calculated pI value: 6.86NCBI BLAST search of gi|15231750 against nr
Unformatted [sequence string](#) for pasting into other applicationsTaxonomy: [Arabidopsis thaliana](#)Links to retrieve other entries containing this sequence from NCBI Entrez:
[gi|6630732](#) from [Arabidopsis thaliana](#)

Fixed modifications: Carbamidomethyl (C)

Variable modifications: Oxidation (M)

Cleavage by Trypsin: cuts C-term side of KR unless next residue is P

Number of mass values searched: 48

Number of mass values matched: 14

Sequence Coverage: 50%

Matched peptides shown in **Bold Red**

```

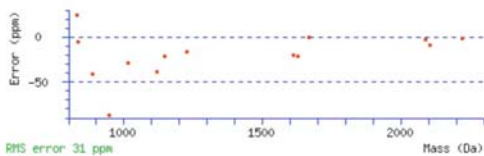
1 MFNFWGSKDQ QGGQSRPQEA SSQSPWYSPS LVSSPSSSRP QSSGQISAQV
51 SPGEAAGIIV FLKDKSVDEL RKLLSDRDAY QQFLSLDQV KVQNNIKDEL
101 RRRTLQLARD NLEKEPQIME LKQCRIRI TELATAQEL NLELRQKEEI
151 LKVTSPQLL KLGQAMNQQV DESEALQEK FLEKIDTAA FVGRYKLRKI
201 TYHRRALHL AAKTSNI

```

Show predicted peptides also**Sort Peptides By** Residue Number Increasing Mass Decreasing Mass

Start - End	Observed	Mr (expt)	Mr (calc)	Delta	Miss	Sequence
73 - 91	2224.18	2223.18	2223.18	-0.00	1	LLSDNDAYQQFLSLDQVK
78 - 91	1667.86	1666.86	1666.86	0.00	0	DAYQQFLSLDQVK
92 - 101	1228.64	1227.64	1227.66	-0.02	1	VQNNIKDEL
103 - 109	830.49	829.49	829.47	0.02	0	ETLQLAR
110 - 122	1614.78	1613.78	1613.81	-0.03	1	ENLEKEPQIMELR
110 - 122	1630.78	1629.77	1629.80	-0.03	1	ENLEKEPQIMELR Oxidation (M)
115 - 122	1015.49	1014.49	1014.52	-0.03	0	EPQIMELR
146 - 152	887.48	886.48	886.51	-0.04	1	QKKEILK
153 - 162	1148.59	1147.58	1147.60	-0.02	0	FYSPGSLHK
163 - 180	2090.95	2089.94	2089.95	-0.01	0	LQAMNQQVDESEALQEK
163 - 180	2105.93	2105.92	2105.94	-0.02	0	LQAMNQQVDESEALQEK Oxidation (M)
185 - 194	1121.54	1120.53	1120.58	-0.04	0	EIDTAAFPVK
198 - 204	946.44	945.43	945.51	-0.08	1	LRTTYHR
206 - 213	836.53	835.52	835.53	-0.00	0	ALIHIAAK

No match to: 831.47, 839.49, 960.44, 982.50, 983.52, 988.47, 990.54, 1058.48, 1074.47, 1078.47, 1090.47, 1106.49, 1107.55, 1176.60, 1215.59, 1265.55, 1303.57, 1



LOCUS NF_190880 217 aa linear PLN 09-JUN-2006
 DEFINITION unknown protein [Arabidopsis thaliana].
 ACCESSION NF_190880
 VERSION NF_190880.1 GI:15231750
 DBSOURCE REFSEQ: accession NM_115172.3
 KEYWORDS .
 SOURCE Arabidopsis thaliana (thale cress)
 ORGANISM Arabidopsis thaliana
 Eukaryota; Viridiplantae; Streptophyta; Embryophyta; Tracheophyta;
 Spermatophyta; Magnoliophyta; eudicotyledons; core eudicotyledons;
 rosids; eurosids II; Brassicales; Brassicaceae; Arabidopsis.
 COMMENT PROVISIONAL REFSEQ: This record has not yet been subject to final
 NCBI review. The reference sequence was derived from AT3G53120.jp.
 Method: conceptual translation.
 FEATURES
 Location/Qualifiers
 source 1..217
 /organism="Arabidopsis thaliana"
 /db_xref="taxon:3702"
 /chromosome="3"
 /ecotype="Columbia"
 Protein 1..217
 /product="unknown protein"
 /calculated_mol_wt=24809
 Region 62..>205
 /region_name="Modifier of rudimentary (Mod[r]) protein"
 /note="Mod_r"
 /db_xref="CDD:47084"
 CDS 1..217
 /locus_tag="AT3G53120"
 /coded_by="NM_115172.3:13..666"
 /go_component="chloroplast"
 /note="expressed protein"
 /db_xref="GeneID:824478"

VPS37/2 At2g36680 4556H2

MASCOT Mascot Search Results

Protein View

Match to: gi|42570370; Score: 102
unknown protein [Arabidopsis thaliana]Nominal mass (M_r): 25029; Calculated pI value: 6.62NCBI BLAST search of gi|42570370 against nr
Unformatted [sequence string](#) for pasting into other applicationsTaxonomy: [Arabidopsis thaliana](#)

Fixed modifications: Carbamidomethyl (C)

Variable modifications: Oxidation (M)

Cleavage by Trypsin: cuts C-term side of KR unless next residue is P

Number of mass values searched: 48

Number of mass values matched: 11

Sequence Coverage: 45%

Matched peptides shown in **Bold Red**

1 MFNFWGSKKQ QGQSRPSPE ASATPWYSPS LVTSFSSSRP QTSQIPIPHV
51 SPGEAAGIIA ILKDKSVDEL RRLLSKDAY QGFLHSLDQVTIQNNIR
101 RKETLHLARE NLEKEQIVE LRNQCRIIRT SELATAQEKL NELENQREEI
151 LKFYSPGSLI HRLQDAMNQV DEESEELQOK FMEKIDTAA FVQYKLLRS
201 KYHRRALHL AAWTSSIG

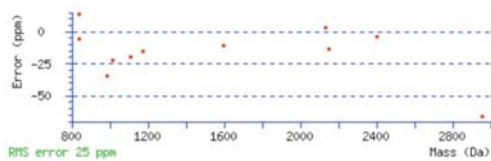
Show predicted peptides also

Sort Peptides By

 Residue Number
 Increasing Mass
 Decreasing Mass

Start - End	Observed	Mr (expt)	Mr (calc)	Delta	Miss	Sequence
73 - 97	2959.33	2958.32	2958.52	-0.20	1	LLSRDAYQFLHSLDQVTIQNNIR
78 - 97	2403.20	2402.19	2402.20	-0.01	0	DATQQFLHSLDQVTIQNNIR
103 - 109	839.49	838.48	838.47	0.01	0	ETLHLAR
110 - 122	1596.84	1595.83	1595.85	-0.02	1	ENLEKEQIVELR
115 - 122	983.52	982.51	982.54	-0.03	0	EPQIVELR
140 - 147	1015.49	1014.49	1014.51	-0.02	0	LNLENQR
153 - 162	1176.60	1175.59	1175.61	-0.02	0	FYSPGSLIHR
163 - 180	2133.97	2132.96	2132.95	0.01	0	LQDAMNQVDEESEELQOK
163 - 180	2149.93	2148.92	2148.95	-0.03	0	LQDAMNQVDEESEELQOK Oxidation (M)
185 - 194	1107.55	1106.54	1106.56	-0.02	0	DIDTAAFVQK
206 - 213	836.53	835.52	835.53	-0.00	0	ALHLAAK

No match to: 830.49, 831.47, 887.48, 946.44, 960.44, 982.50, 988.47, 990.54, 1058.48, 1074.47, 1078.47, 1090.47, 1106.49, 1121.54, 1148.59, 1215.59, 1228.64, 11



LOCUS NP_850268 218 aa linear PLN 09-JUN-2006
 DEFINITION unknown protein [Arabidopsis thaliana].
 ACCESSION NP_850268
 VERSION NP_850268.2 GI:42570370
 DBSOURCE REFSEQ: accession NM_179937.2
 KEYWORDS .
 SOURCE Arabidopsis thaliana (thale cress)
 ORGANISM Arabidopsis thaliana
 Eukaryota; Viridiplantae; Streptophyta; Embryophyta; Tracheophyta;
 Spermatophyta; Magnoliophyta; eudicotyledons; core eudicotyledons;
 rosids; eurosids II; Brassicales; Brassicaceae; Arabidopsis.
 COMMENT PROVISIONAL REFSEQ: This record has not yet been subject to final
 NCBI review. The reference sequence was derived from AT2G36680.lp.
 On Feb 17, 2004 this sequence version replaced gi:30686868.
 Method: conceptual translation.
 FEATURES
 Location/Qualifiers
 source 1..218
 /organism="Arabidopsis thaliana"
 /db_xref="taxon:3702"
 /chromosome="2"
 /ecotype="Columbia"
 Protein 1..218
 /product="unknown protein"
 /calculated_mol_wt=24856
 Region 62..>205
 /region_name="Modifier of rudimentary (Mod(r)) protein"
 /note="Mod_r"
 /db_xref="CDD:47084"
 CDS 1..218
 /locus_tag="AT2G36680"
 /coded_by="NM_179937.2:104..760"
 /go_component="chloroplast"
 /note="expressed protein"
 /db_xref="GeneID:818240"

Ig kappa chain constant region 4486a_seq

Mascot Search Results**Protein View**

Match to: **KAC_MOUSE**; Score: **86**
(P01837) Ig kappa chain C region

Nominal mass (M_r): **11942**; Calculated pI value: **5.23**

NCBI ELAST search of **KAC_MOUSE** against nr
Unformatted [sequence listing](#) for pasting into other applications

Taxonomy: **Mus musculus**

Fixed modifications: Carbamidomethyl (C)
Variable modifications: Oxidation (M)
Cleavage by Trypsin: cuts C-term side of KR unless next residue is P
Number of mass values searched: **51**
Number of mass values matched: **8**
Sequence Coverage: **87%**

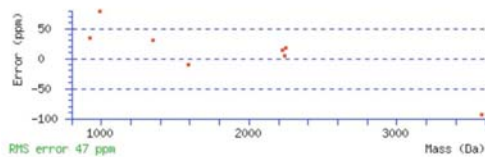
Matched peptides shown in **Bold Red**

1 ADAAPTYSIP PPSSEQLTSG GASVVCFLNN FYPKINVKM KIDGSRQNG
51 VLNSHTDQDS KDSYMSST LTLTKDEYER HNSYTCATHK KTSTSPIVKS
101 FNRNEC

Show predicted peptides also**Sort Peptides By** Residue Number Increasing Mass Decreasing Mass

Start	End	Observed	Mr (expt)	Mr (calc)	Delta	Miss	Sequence
1	34	3571.41	3570.40	3570.73	-0.33	0	ADAAPTYSIP PPSSEQLTSG GASVVCFLNN FYPK
40	47	990.58	989.57	989.49	0.08	1	WKIDGSR
42	61	2249.08	2248.07	2248.04	-0.04	1	IDGSRQNGVLSNWTQDSK
48	61	1591.72	1590.71	1590.73	-0.02	0	QNGVLSNWTQDSK
62	80	2227.04	2226.03	2226.00	0.03	1	DSTYMSSTLTLTKDEYER
62	80	2243.01	2242.01	2241.99	0.01	1	DSTYMSSTLTLTKDEYER Oxidation (M)
81	91	1347.62	1346.61	1346.57	0.04	0	HNSYTCATHK
100	106	926.41	925.40	925.37	0.03	1	FNRNEC

No match to: 1074.52, 1078.55, 1106.52, 1108.62, 1121.62, 1148.60, 1176.62, 1265.57, 1303.64, 1361.61, 1384.77, 1473.82, 1574.74, 1577.86, 1593.80, 1596.85, 1600



ID KAC_MOUSE STANDARD; PRT; 106 AA.
AC P01837;
DT 21-JUL-1986, integrated into UniProtKB/Swiss-Prot.
DT 21-JUL-1986, sequence version 1.
DT 18-APR-2006, entry version 51.
DE Ig kappa chain C region.
OS Mus musculus (Mouse).
OC Eukaryota; Metazoa; Chordata; Cranialia; Vertebrata; Euteleostomi;
OC Mammalia; Eutheria; Euarchontoglires; Glires; Rodentia; Sciurognathi;
OC Muroidea; Muridae; Murinae; Mus.
OX NCBI_TaxID=10090;
RN [1]
RP PROTEIN SEQUENCE (MOPC 21).
RX MEDLINE=73053310; PubMed=4638343;
RA Svasti J., Milstein C.;
RT "The complete amino acid sequence of a mouse kappa light chain.";
RL Biochem. J. 128:427-444(1972).

E 4. Mass spectrometry data of ELCH/ESCRT-I interacting proteins

UBA domain protein At5g53330 4486

MASCOT Mascot Search Results

Protein View

Match to: [gi|15809720](#); Score: 85
 AT5g53330/K19E1_13 [Arabidopsis thaliana]
 Nominal mass (M_r): 24247; Calculated pI value: 6.37
 NCBI BLAST search of [gi|15809720](#) against nr
 Unformatted [sequence](#) for pasting into other applications

Taxonomy: [Arabidopsis thaliana](#)
 Links to retrieve other entries containing this sequence from NCBI Entrez:
[gi|14190455](#) from [Arabidopsis thaliana](#)

Fixed modifications: Carbamidomethyl (C)
 Variable modifications: none
 Cleavage by Trypsin: cuts C-term side of KR unless next residue is P
 Number of mass values searched: 60
 Number of mass values matched: 9
 Sequence Coverage: 47%

Matched peptides shown in **Bold Red**

```

1 MDYDNRNKG GPSYRPMYG PPSTSPSPSS NHPMYGYPKI GGQTGPGQPF
51 FSPPERNSSF QNNTSPSSGI QIRVNLKPEY RITPPQLLRF RVGDIHRSSP
101 GFDFLEKRV LAGARKDND WSKFQSEWPF AKFHEPSPSS VQMQQVDHV
151 VHKITASGLN REAVNIIVAN YGDNPKVQE FANGFAIRE MGFPTNAVAD
201 ALFMPDNDTD KALAHLLHGS S

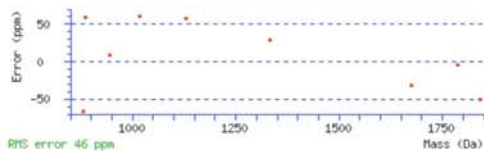
```

Show predicted peptides also

Sort Peptides By Residue Number Increasing Mass Decreasing Mass

Start - End	Observed	Mr (expt)	Mr (calc)	Delta	Miss	Sequence
40 - 56	1842.82	1841.81	1841.91	-0.09	0	IQQQTGPGQPF FSPPER
57 - 73	1788.85	1787.85	1787.86	-0.01	0	NSSPQNTSPSSG IGIR
74 - 81	1018.63	1017.62	1017.56	0.06	0	VNLKPEYR
82 - 91	1131.75	1130.75	1130.69	0.07	0	ITPPQLLRF
98 - 108	1332.66	1331.65	1331.61	0.04	0	SSPQDFGLER
109 - 116	887.57	886.56	886.51	0.05	1	KVLAEAK
124 - 132	946.47	945.46	945.46	0.01	0	FGSENPPAK
154 - 161	881.39	880.38	880.44	-0.06	0	YTASGLNR
162 - 177	1675.78	1674.77	1674.82	-0.05	0	REAVNIIVAN YGDNPVK

No match to: 926.41, 990.58, 1074.52, 1078.55, 1106.52, 1108.62, 1121.62, 1148.60, 1176.62, 1265.57, 1303.64, 1347.62, 1361.61, 1384.77, 1473.82, 1574.74, 1577.8



LOCUS AAL06788 221 aa linear PLN 30-SEP-2001
 DEFINITION AT5g53330/K19E1_13 [Arabidopsis thaliana].
 ACCESSION AAL06788
 VERSION AAL06788.1 GI:15809720
 DISOURCE accession AY054127.1
 KEYWORDS
 SOURCE Arabidopsis thaliana (thale cress)
 ORGANISM Arabidopsis thaliana
 Eukaryota; Viridiplantae; Streptophyta; Embryophyta; Tracheophyta;
 Spermatophyta; Magnoliophyta; eudicotyledons; core eudicotyledons;
 rosids; eurosids II; Brassicales; Brassicaceae; Arabidopsis.
 REFERENCE 1 (residues 1 to 221)
 AUTHORS Kim, C.J., Chen, H., Cheuk, R., Koesema, E., Meyers, M.C., Banh, J.,
 Bowser, L., Carninci, F., Dale, J.M., Goldsmith, A.D., Hayashizaki, Y.,
 Ishida, J., Jiang, P.X., Jones, T., Kamiya, A., Karlin-Neumann, G.,
 Kawai, J., Lam, B., Lee, J.M., Lin, J., Liu, S.X., Miranda, M.,
 Narusaka, M., Nguyen, M., Ouedera, C.S., Palm, C.J., Pham, P.K.,
 Quach, H.L., Sakurai, T., Satou, M., Seki, M., Southwick, A., Tang, C.C.,
 Toriumi, M., Yamada, K., Yamamura, Y., Yu, G., Yu, S., Shinozaki, K.,
 Davis, R.W., Theologis, A. and Ecker, J.R.
 TITLE Arabidopsis ORF clones
 JOURNAL Unpublished
 REFERENCE 2 (residues 1 to 221)
 AUTHORS Kim, C.J., Chen, H., Cheuk, R., Koesema, E., Meyers, M.C., Banh, J.,
 Bowser, L., Carninci, F., Dale, J.M., Goldsmith, A.D., Hayashizaki, Y.,
 Ishida, J., Jiang, P.X., Jones, T., Kamiya, A., Karlin-Neumann, G.,
 Kawai, J., Lam, B., Lee, J.M., Lin, J., Liu, S.X., Miranda, M.,
 Narusaka, M., Nguyen, M., Ouedera, C.S., Palm, C.J., Pham, P.K.,
 Quach, H.L., Sakurai, T., Satou, M., Seki, M., Southwick, A., Tang, C.C.,
 Toriumi, M., Yamada, K., Yamamura, Y., Yu, G., Yu, S., Shinozaki, K.,
 Davis, R.W., Theologis, A. and Ecker, J.R.
 TITLE Direct Submission
 JOURNAL Submitted (29-AUG-2001) Salk Institute Genomic Analysis Laboratory
 (SIGnAL), Plant Biology Laboratory, The Salk Institute for
 Biological Studies, 10010 N. Torrey Pines Road, La Jolla, CA 92037,
 USA
 COMMENT RIKEN Genomic Sciences Center (GSC) members carried out the
 collection and clustering of RAFL cDNAs (RAFL cDNA: 'RIKEN
 Arabidopsis Full-length cDNA') : Seki, M., Narusaka, M., Ishida, J.,
 Satou, M., Kamiya, A., Sakurai, T., Carninci, F., Kawai, J.,
 Hayashizaki, Y. and Shinozaki, K.
 The Salk, Stanford, FGEC (SSP) Consortium members carried out the
 sequencing and annotation of the RAFL cDNAs: Kim, C.J., Chen, H.,
 Cheuk, R., Koesema, E., Meyers, M.C., Shinn, P., Banh, J., Bowser, L.,
 Dale, J.M., Goldsmith, A.D., Jiang, P.X., Jones, T., Karlin-Neumann, G.,
 Lam, B., Lee, J.M., Lin, J., Liu, S.X., Miranda, M., Nguyen, M.,
 Ouedera, C.S., Palm, C.J., Pham, P.K., Quach, H.L., Southwick, A.,
 Tang, C.C., Toriumi, M., Yamada, K., Yamamura, Y., Yu, G., Yu, S.,
 Davis, R.W., Theologis, A., and Ecker, J.R.
 Kim, C.J. (SSP/Salk) and Seki, M. (RIKEN GSC) contributed equally to
 this work. Shinozaki, K. (RIKEN GSC) and Ecker, J.R. (SSP/Salk)

UBA domain protein At5g53330 4497H

MASCOT Mascot Search Results

Protein View

Match to: [gi|15809720](#); Score: 162
AT5g53330/K19E1_13 [Arabidopsis thaliana]

Nominal mass (M_r): 24247; Calculated pI value: 6.37
 NCBI BLAST search of [gi|15809720](#) against nr
 Unformatted [sequence string](#) for pasting into other applications

Taxonomy: [Arabidopsis thaliana](#)
 Links to retrieve other entries containing this sequence from NCBI Entrez:
[gi|14190455](#) from [Arabidopsis thaliana](#)

Fixed modifications: Carbamidomethyl (C)
 Variable modifications: Oxidation (M)
 Cleavage by Trypsin: cuts C-term side of KR unless next residue is P
 Number of mass values searched: 16
 Number of mass values matched: 10
 Sequence Coverage: 44%

Matched peptides shown in **Bold Red**

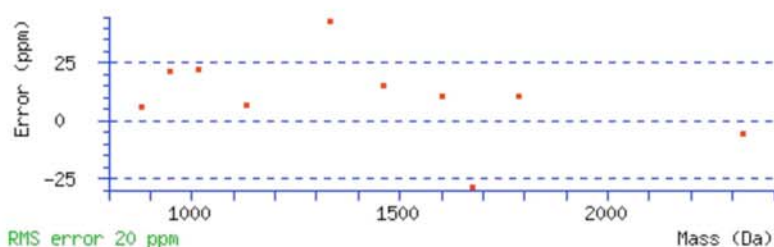
1 MDYDYRNKSG GPSYPRMYG PPSTSPSPSS NHPMYGYPKI GQQTGPGPQF
 51 FSPPERNSSF QHNTSPSSGI GIRVNLKPEY **RITPPPQLLP RVGDIHRSSF**
 101 **QDFDFGLERKV LAEAEKDNDP WSKFGSENPP AKFHEPSPSS VGQMVGVDHV**
 151 **VMKYTAGSLN REAVNIAVAN YGDNPTKVQE FANGFTAIRE MGFPTNAVAD**
 201 ALFMFDNDTD KALAHLLHGS S

Show predicted peptides also

Sort Peptides By Residue Number Increasing Mass Decreasing Mass

Start - End	Observed	Mr (expt)	Mr (calc)	Delta	Miss	Sequence
74 - 81	1018.59	1017.58	1017.56	0.02	0	VNLKPEYR
82 - 91	1131.70	1130.69	1130.68	0.01	0	ITPPPQLLPR
98 - 108	1332.68	1331.67	1331.61	0.06	0	SSFQDFGLER
98 - 109	1460.74	1459.73	1459.71	0.02	1	SSFQDFGLERK
110 - 123	1601.80	1600.79	1600.77	0.02	1	VLAEAEKDNDPWSK
117 - 132	1788.84	1787.83	1787.81	0.02	1	DNPDWSKFGSENPPAK
124 - 132	946.48	945.48	945.46	0.02	0	FGSENPPAK
133 - 153	2328.06	2327.05	2327.07	-0.01	0	FHEPSPSSVGQMVGVDHVVMK 2 Oxidation (M)
154 - 161	881.45	880.45	880.44	0.00	0	YTASGLNR
162 - 177	1675.78	1674.77	1674.82	-0.05	0	EAVNIAVANYGDNPTK

No match to: 904.34, 1729.86, 1794.77, 1798.78, 1826.78, 1852.91



LOCUS AAL06788 221 aa linear PLN 30-SEP-2001
 DEFINITION AT5g53330/K19E1_13 [Arabidopsis thaliana].
 ACCESSION AAL06788
 VERSION AAL06788.1 GI:15809720
 DBSOURCE accession AY054127.1
 KEYWORDS .
 SOURCE Arabidopsis thaliana (thale cress)
 ORGANISM Arabidopsis thaliana
 Eukaryota; Viridiplantae; Streptophyta; Embryophyta; Tracheophyta;
 Spermatophyta; Magnoliophyta; eudicotyledons; core eudicotyledons;
 rosids; eurosids II; Brassicales; Brassicaceae; Arabidopsis.
 REFERENCE 1 (residues 1 to 221)
 AUTHORS Kim,C.J., Chen,H., Cheuk,R., Koesema,E., Meyers,M.C., Banh,J.,
 Bowser,L., Carninci,P., Dale,J.M., Goldsmith,A.D., Hayashizaki,Y.,
 Ishida,J., Jiang,P.X., Jones,T., Kamiya,A., Karlin-Neumann,G.,
 Kawai,J., Lam,B., Lee,J.M., Lin,J., Liu,S.X., Miranda,M.,
 Narusaka,M., Nguyen,M., Onodera,C.S., Palm,C.J., Pham,P.K.,
 Quach,H.L., Sakurai,T., Satou,M., Seki,M., Southwick,A., Tang,C.C.,
 Toriumi,M., Yamada,K., Yamamura,Y., Yu,G., Yu,S., Shinozaki,K.,
 Davis,R.W., Theologis,A. and Ecker,J.R.
 TITLE Arabidopsis ORF clones
 JOURNAL Unpublished
 REFERENCE 2 (residues 1 to 221)
 AUTHORS Kim,C.J., Chen,H., Cheuk,R., Koesema,E., Meyers,M.C., Banh,J.,
 Bowser,L., Carninci,P., Dale,J.M., Goldsmith,A.D., Hayashizaki,Y.,
 Ishida,J., Jiang,P.X., Jones,T., Kamiya,A., Karlin-Neumann,G.,
 Kawai,J., Lam,B., Lee,J.M., Lin,J., Liu,S.X., Miranda,M.,
 Narusaka,M., Nguyen,M., Onodera,C.S., Palm,C.J., Pham,P.K.,
 Quach,H.L., Sakurai,T., Satou,M., Seki,M., Southwick,A., Tang,C.C.,
 Toriumi,M., Yamada,K., Yamamura,Y., Yu,G., Yu,S., Shinozaki,K.,
 Davis,R.W., Theologis,A. and Ecker,J.R.
 TITLE Direct Submission
 JOURNAL Submitted (29-AUG-2001) Salk Institute Genomic Analysis Laboratory
 (SIGnAL), Plant Biology Laboratory, The Salk Institute for
 Biological Studies, 10010 N. Torrey Pines Road, La Jolla, CA 92037,
 USA
 COMMENT RIKEN Genomic Sciences Center (GSC) members carried out the
 collection and clustering of RAFL cDNAs (RAFL cDNA : 'RIKEN
 Arabidopsis Full-Length cDNA') : Seki,M., Narusaka,M., Ishida,J.,
 Satou,M., Kamiya,A., Sakurai,T., Carninci,P., Kawai,J.,
 Hayashizaki,Y. and Shinozaki,K.

 The Salk, Stanford, PGEN (SSP) Consortium members carried out the
 sequencing and annotation of the RAFL cDNAs: Kim,C.J., Chen,H.,
 Cheuk,R., Koesema,E., Meyers,M.C., Shinn,P., Banh,J. Bowser,L.,
 Dale,J.M., Goldsmith,A.D., Jiang,P.X., Jones,T., Karlin-Neumann,G.,
 Lam,B., Lee,J.M., Lin,J., Liu,S.X., Miranda,M., Nguyen,M.,
 Onodera,C.S., Palm,C.J., Pham,P.K., Quach,H.L., Southwick,A.,
 Tang,C.C., Toriumi,M., Yamada,K., Yamamura, Y., Yu,G., Yu,S.,
 Davis,R.W., Theologis,A., and Ecker,J.R.

 Kim,C.J. (SSP/Salk) and Seki,M. (RIKEN GSC) contributed equally to
 this work. Shinozaki,K. (RIKEN GSC) and Ecker,J.R. (SSP/Salk)
 contributed equally to this work as PIs.
 Method: conceptual translation.
 FEATURES Location/Qualifiers
 source 1..221
 /organism="Arabidopsis thaliana"
 /db_xref="taxon:3702"
 /chromosome="5"
 /clone="U12482"
 /ecotype="Columbia"
 /note="This clone is in pUNI 51"
 Protein 1..221
 /product="AT5g53330/K19E1_13"
 CDS 1..221
 /coded_by="AY054127.1:1..666"
 /note="putative proline-rich cell wall protein"

VHA-a3 At4g39080 4491RE

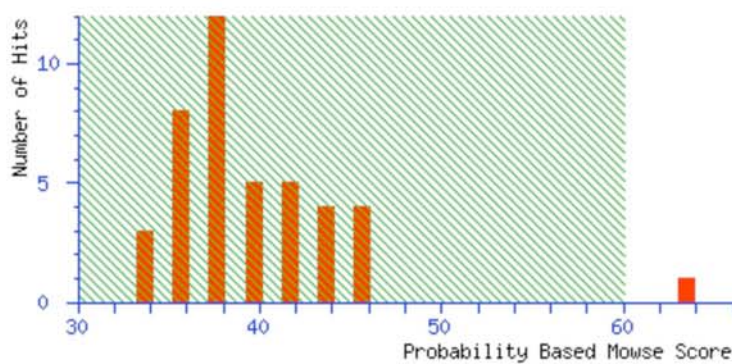


Mascot Search Results

User : ZBA
Email : zmmk-bioanalytik@uni-koeln.de
Search title : 4491
Database : NCBIInr 20060315 (3466531 sequences; 1190035678 residues)
Taxonomy : Arabidopsis thaliana (thale cress) (53264 sequences)
Timestamp : 8 Jun 2006 at 08:22:49 GMT
Top Score : 64 for [gi|18420373](#), ATPase [Arabidopsis thaliana]

Probability Based Mowse Score

Score is $-10 \cdot \log(P)$, where P is the probability that the observed match is a random event. Protein scores greater than 60 are significant ($p < 0.05$).



Concise Protein Summary Report

[Switch to full Protein Summary Report](#)

To create a bookmark for this report, right click this link: [Concise Summary Report \(4491\)](#)

Re-Search All

Search Unmatched

- [gi|18420373](#) **Mass:** 93344 **Total score:** 64 **Peptides matched:** 12
 ATPase [Arabidopsis thaliana]

[gi|7270891](#) **Mass:** 95726 **Total score:** 60 **Peptides matched:** 12
 putative proton pump [Arabidopsis thaliana]

[gi|21700881](#) **Mass:** 93633 **Total score:** 38 **Peptides matched:** 9
 At2g21410/F3K23.17 [Arabidopsis thaliana]

[gi|15226542](#) **Mass:** 93616 **Total score:** 38 **Peptides matched:** 9
 ATPase [Arabidopsis thaliana]
- [gi|34849893](#) **Mass:** 89768 **Total score:** 46 **Peptides matched:** 12
 At4g05190 [Arabidopsis thaliana]

[gi|7267279](#) **Mass:** 88387 **Total score:** 41 **Peptides matched:** 11
 kinesin-like protein [Arabidopsis thaliana]

[gi|30680014](#) **Mass:** 89766 **Total score:** 39 **Peptides matched:** 11
 ATK5; microtubule motor [Arabidopsis thaliana]
- [gi|15217502](#) **Mass:** 17362 **Total score:** 46 **Peptides matched:** 5
 unknown protein [Arabidopsis thaliana]

VHA-a3 At4g39080 4491UBQ

**(MATRIX)
(SCIENCE) Mascot Search Results****Protein View**Match to: [gi|18420373](#); Score: 54
ATPase [*Arabidopsis thaliana*]Nominal mass (M_r): 93344; Calculated pI value: 5.66
NCBI BLAST search of [gi|18420373](#) against nr
Unformatted [sequence string](#) for pasting into other applicationsTaxonomy: [Arabidopsis thaliana](#)
Links to retrieve other entries containing this sequence from NCBI Entrez:
[gi|16974583](#) from [Arabidopsis thaliana](#)
[gi|27363224](#) from [Arabidopsis thaliana](#)Fixed modifications: Carbamidomethyl (C)
Variable modifications: UBQ (K)
Cleavage by Trypsin: cuts C-term side of KR unless next residue is P
Number of mass values searched: 58
Number of mass values matched: 15
Sequence Coverage: 17%Matched peptides shown in **Bold Red**

```

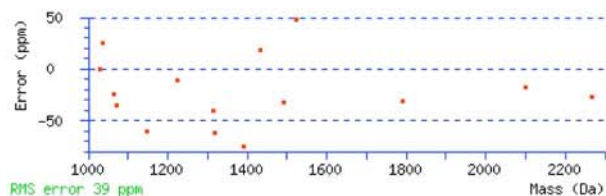
1 MAESGGGGC CPPMDLRSE TMQLVQLVLP MESAHLTVSY LGDGLVQVFK
1 DLNSEKSPFQ RTYAAQIKRC GEMARKIRFF RDQMSKAGVP AKEMQKEND
101 IDLDDVEVKL GELEAEIVEI NANNDKLRQ YNELMEYKLV LQKAGEFFSS
151 AHRSAADQQR ETESQQAGED LLESPLLQEE KSIDSTKQVK LGFLTGLVPR
201 EKSMVFERIL FRATRGNIFI RQTVIEEPIV DPNSGKAEK NVFFVYSGE
251 RAKSKILKIC EAFGANRYPF SEDLGRQAQM ITEVSGRLSE LKTTIDAGLG
301 QRNILLQTIG DKFELWNLKV RKEKAIYHTL NMLSLDVTKK CLVAEGWSPV
351 FASREIQDAL QRAAVDSNSQ VGSIFQVLR KESPPTYFR NKFTSAIQEI
401 VDAYGVARYQ EANPGVFTIV TFFFLFAVMF GDWGHGICIL LATMYLILKE
451 KKLASQKLGD IMEMAFGGRY VILMMSLFSI YTGLIYNEFF SIPFLFAPS
501 AYDCRDVSCS EATTIGLIK RDTYPPGLDP VWHGSRSELP FLNSLKMMS
551 ILLGVSQMNL GIIMSYFNAR FFKSSVINIF QFIPQMIFLN SLFGYLSVLI
601 IIKWCTGSQA DLYHVMIMYF LSPMDELGEN QLFPHQKTLQ LVLLFLALVS
651 VPCMLLPKPF ILKKQHEARH QGQAYAPLDE TDESLHVETN GGGSHGHEEF
701 EFSEIFVHQL IHTIEFVLGA VSNTASYLRL WALSLAHSEL SSVFYEKVLL
751 LAWGYNNPLI LIVGVLFVIF ATVGVLLVME TLSAFLHALR LHWVEFQNK
801 YEGDGYKFAF FTFIFTANED E

```

Residue Number Increasing Mass Decreasing Mass

Start - End	Observed	Mr (expt)	Mr (calc)	Delta	Miss	Sequence
51 - 61	1320.57	1319.57	1319.65	-0.08	1	DLNSEKSPFQR
51 - 61	1434.72	1433.72	1433.69	0.03	1	DLNSEKSPFQR UBQ (K)
57 - 68	1523.87	1522.86	1522.79	0.07	1	SFPQRTYAAQIK UBQ (K)
62 - 69	1064.56	1063.55	1063.58	-0.03	1	TYAAQIKR UBQ (K)
110 - 129	2268.12	2267.11	2267.18	-0.06	1	LGELEAEIVEINANNDKLRQ
191 - 200	1072.61	1071.61	1071.64	-0.04	0	LGFLTGLVPR
241 - 251	1316.61	1315.60	1315.66	-0.05	0	NVFFVYSGER
256 - 267	1391.64	1390.64	1390.74	-0.10	1	ILKICEAFGANR
259 - 267	1037.51	1036.50	1036.48	0.03	0	ICEAFGANR
259 - 276	2101.94	2100.93	2100.97	-0.04	1	ICEAFGANRYPFSEDLGR
293 - 302	1031.55	1030.54	1030.54	-0.00	0	TTIDAGLGR
363 - 379	1790.88	1789.88	1789.93	-0.05	0	AAVDSNSQVGSIFQVLR
380 - 389	1225.61	1224.60	1224.61	-0.01	1	TRKESPPTYFR
506 - 519	1493.70	1492.69	1492.74	-0.05	0	DVSCSEATTIGLIK
537 - 546	1147.57	1146.56	1146.63	-0.07	0	SELPFLNSLK

No match to: 827.40, 995.49, 1033.50, 1065.50, 1082.58, 1090.52, 1107.50, 1109.45, 1118.51, 1179.57, 1193.56, 1234.63, 1254.61, 1265.55, 1300.55, 1302.66, 1329.66, 1336.65, 1357.65, 1381.52, 1383.63, 1393.66, 1460.70, 1475.70, 1479.71, 1507.70, 1638.81, 1707.74, 1766.72, 1794.74, 1798.75, 1826.74, 1842.69, 1962.92, 1993.92, 2150.04, 2240.13, 2256.03, 2399.01, 2888.25, 2904.25, 3064.36, 3354.54



LOCUS NP_568051 821 aa linear PLN 09-JUN-2006
DEFINITION ATPase [*Arabidopsis thaliana*].
ACCESSION NP_568051
VERSION NP_568051.1 GI:18420373
DBSOURCE REFSEQ: accession NM_120068.3
KEYWORDS .
SOURCE Arabidopsis thaliana (thale cress)

```
ORGANISM Arabidopsis thaliana
          Eukaryota; Viridiplantae; Streptophyta; Embryophyta; Tracheophyta;
          Spermatophyta; Magnoliophyta; eudicotyledons; core eudicotyledons;
          rosids; eurosids II; Brassicales; Brassicaceae; Arabidopsis.
COMMENT  PROVISIONAL REFSEQ: This record has not yet been subject to final
          NCBI review. The reference sequence was derived from AT4G39080.lp.
          Method: conceptual translation.
FEATURES             Location/Qualifiers
     source           1..821
                    /organism="Arabidopsis thaliana"
                    /db_xref="taxon:3702"
                    /chromosome="4"
                    /ecotype="Columbia"
     Protein          1..821
                    /product="ATPase"
                    /calculated_mol_wt=92703
     Region           38..814
                    /region_name="V_ATPase I"
                    /note="V-type ATPase 116kDa subunit family; pfam01496"
                    /db_xref="CDD:41542"
     CDS              1..821
                    /locus_tag="AT4G39080"
                    /coded_by="NM_120068.3:85..2550"
                    /go_component="membrane"
                    /go_function="ATPase activity"
                    /go_process="proton transport"
                    /note="vacuolar proton ATPase, putative, similar to
                    Swiss-Prot:Q93050 vacuolar proton translocating ATPase 116
                    kDa subunit A isoform 1 (Clathrin-coated vesicle/synaptic
                    vesicle proton pump 116 kDa subunit, Vacuolar proton pump
                    subunit 1, Vacuolar adenosine triphosphatase subunit
                    Ac116) (Homo sapiens)"
                    /db_xref="GeneID:830063"
```

VHA-A At1g78900 4492

Mascot Search Results

Protein View

Match to: [gi|79321468](#); Score: 254
 VHA-A; ATP binding / hydrogen-transporting ATP synthase, rotational mechanism / hydrogen-transporti

Nominal mass (M_r): 69111; Calculated pI value: 5.11
 NCBI BLAST search of [gi|79321468](#) against nr
 Unformatted [sequence string](#) for pasting into other applications

Taxonomy: [Arabidopsis thaliana](#)
 Links to retrieve other entries containing this sequence from NCBI Entrez:
[gi|15219234](#) from [Arabidopsis thaliana](#)
[gi|30725440](#) from [Arabidopsis thaliana](#)
[gi|19698899](#) from [Arabidopsis thaliana](#)
[gi|16649079](#) from [Arabidopsis thaliana](#)
[gi|21553884](#) from [Arabidopsis thaliana](#)
[gi|27311967](#) from [Arabidopsis thaliana](#)
[gi|3834305](#) from [Arabidopsis thaliana](#)
[gi|2266990](#) from [Arabidopsis thaliana](#)
[gi|3334404](#) from [Arabidopsis thaliana](#)

Fixed modifications: Carbamidomethyl (C)
 Variable modifications: Oxidation (M)
 Cleavage by Trypsin: cuts C-term side of KR unless next residue is P
 Number of mass values searched: 28
 Number of mass values matched: 21
 Sequence Coverage: 41%

Matched peptides shown in **Bold Red**

```

1 MPAFYGGKLT TFEDEKESE YGYVRKVSQP VVVDGMAGA AMYELVRVGH
51 DNLIGEIIRL EGSATIQVY EETAGLTVND PVLRTHKPLS VELGPGILGN
101 IFDGIQRPLK TIARISGDVY IPRGVSVPAL DKDCLWEFQP NKFVEGDTIT
151 GGDLYATVFE NTLMNLHVAL PPDAMGKITY IAPAGQYSLK DTVIELEFQG
201 IKKSYMLQS WPVRTPRVA SKLAADTPLL TGQRVLDALF PSVLGGTCAI
251 PGAFGCGKTV ISQALSKEYSN SDAVVYVCGG ERGNEMAEVL MDFPQLTMTL
301 PDGRESVMK RTLVANTSN MPVAAREASI YTGITIAEYF RDMGYNVSM
351 ADSTSRWAEA LREISGRLAE MPADSGYPAY LAARLASFYE RAGKVKCLGG
401 PERNGSVTIV GAVSPGGDF SDPVTSATLS IVQVFWGLDK KLAQRKHFPS
451 VNWLIYSKY STALSFYEK FDPDFINIR KAREVLQRED DLNEIVQLVG
501 KDALAEGDKI TLETAKLLRE DYLAQNAFTP YDKFCFPYKS VMMRNIHF
551 YNLANQAVER AAGMDGQKIT YTLIKHRLGD LFYRLVSQKF EDPAEGEDTL
601 VEKFKLYDD LNAGFRALED ETR
  
```

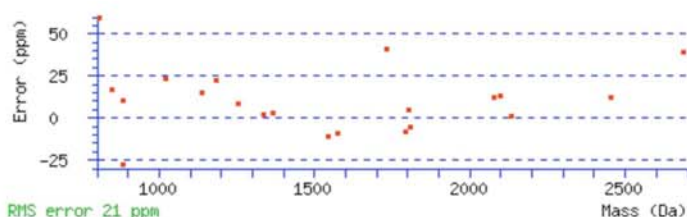
Show predicted peptides also

Sort Peptides By

Residue Number Increasing Mass Decreasing Mass

Start - End	Observed	Mr (expt)	Mr (calc)	Delta	Miss	Sequence
9 - 25	2080.96	2079.95	2079.93	0.03	1	L T T F E D E K E S E Y G Y V R
48 - 59	1335.74	1334.73	1334.73	0.00	0	V G H D N L I G E I I R
60 - 84	2690.46	2689.45	2689.34	0.10	0	L E G D S A T I Q V Y E E T A G L T V N D F V L R
115 - 123	1019.58	1018.57	1018.54	0.02	0	I S G D V Y I P R
124 - 132	885.48	884.47	884.50	-0.02	0	G V S V F A L D K
204 - 214	1367.68	1366.67	1366.67	0.00	0	S Y T M L Q S W F V R
223 - 234	1255.71	1254.70	1254.69	0.01	0	L A A D T P L L T G Q R
312 - 326	1545.79	1544.78	1544.80	-0.02	0	T T L V A N T S N M P V A A R
327 - 341	1733.94	1732.94	1732.87	0.07	0	E A S I Y T G I T I A E Y F R
368 - 384	1795.85	1794.85	1794.86	-0.01	0	L A E M P A D S G Y P A L A A R
368 - 384	1811.85	1810.85	1810.86	-0.01	0	L A E M P A D S G Y P A L A A R Oxidation (M)
460 - 479	2455.21	2454.21	2454.17	0.03	1	Y S T A L E S F Y E K F D P D F I N I R
471 - 479	1136.59	1135.58	1135.57	0.02	0	F D P D F I N I R
484 - 501	2097.15	2096.14	2096.11	0.03	1	E V L Q R E D D L N E I V Q L V G K
502 - 516	1574.81	1573.81	1573.82	-0.01	1	D A L A E G D K I T L E T A K
540 - 545	809.43	808.42	808.37	0.05	0	S V W M R
546 - 560	1801.94	1800.94	1800.93	0.01	0	N I H F Y N L A N Q A V E R
569 - 575	851.54	850.53	850.52	0.01	0	I T Y T L I K
578 - 584	883.48	882.47	882.46	0.01	0	L G D L F Y R
585 - 603	2134.06	2133.05	2133.05	0.00	1	L V S Q R F E D P A E G E D T L V E K
607 - 616	1183.60	1182.59	1182.57	0.03	0	L Y D D L N A G F R

No match to: 1415.65, 1689.75, 1826.81, 2508.41, 2902.42, 3353.69, 3652.84



LOCUS NP_001031299 623 aa linear PLN 04-NOV-2005
 DEFINITION VHA-A; ATP binding / hydrogen-transporting ATP synthase, rotational mechanism / hydrogen-transporting ATPase, rotational mechanism [Arabidopsis thaliana].
 ACCESSION NP_001031299
 VERSION NP_001031299.1 GI:79321468
 DBSOURCE REFSEQ: accession NM_001036222.1
 KEYWORDS .
 SOURCE Arabidopsis thaliana (thale cress)
 ORGANISM Arabidopsis thaliana
 Eukaryota; Viridiplantae; Streptophyta; Embryophyta; Tracheophyta; Spermatophyta; Magnoliophyta; eudicotyledons; core eudicotyledons; rosids; eurosids II; Brassicales; Brassicaceae; Arabidopsis.
 COMMENT PROVISIONAL REFSEQ: This record has not yet been subject to final NCBI review. The reference sequence was derived from AT1G78900.2p. Method: conceptual translation.
 FEATURES
 Location/Qualifiers
 source 1..623
 /organism="Arabidopsis thaliana"
 /db_xref="taxon:3702"
 /chromosome="1"
 /ecotype="Columbia"
 Protein 1..623
 /product="VHA-A; ATP binding / hydrogen-transporting ATP synthase, rotational mechanism / hydrogen-transporting ATPase, rotational mechanism"
 /calculated_mol_wt=68682
 Region 43..>85
 /region_name="ATP synthase alpha/beta family, beta-barrel domain"
 /note="ATP-synt_ab_N"
 /db_xref="CDD:42814"
 Region 88..>460
 /region_name="V/A-type ATP synthase catalytic subunit A"
 /note="V_A-ATPase_A"
 /db_xref="CDD:30000"
 Region 214..>498
 /region_name="Flagellum-specific ATPase/type III secretory pathway virulence-related protein"
 /note="ATPase_flagellum-secretory_path_III"
 /db_xref="CDD:30002"
 Region 478..>620
 /region_name="ATP synthase alpha/beta chain, C terminal domain"
 /note="ATP-synt_ab_C"
 /db_xref="CDD:40402"
 CDS 1..623
 /gene="VHA-A"
 /locus_tag="AT1G78900"
 /coded_by="NM_001036222.1:266..2137"
 /go_component="proton-transporting two-sector ATPase complex"
 /go_function="ATP binding; hydrogen-transporting ATP synthase activity, rotational mechanism; hydrogen-transporting ATPase activity, rotational mechanism"
 /go_process="proton transport"
 /note="similar to ATP synthase beta chain 2, mitochondrial [Arabidopsis thaliana] (TAIR:At5g08690.1); similar to ATP synthase beta chain, mitochondrial, putative [Arabidopsis thaliana] (TAIR:At5g08680.1); similar to ATP synthase beta chain 1, mitochondrial [Arabidopsis thaliana] (TAIR:At5g08670.1); similar to vacuolar H+-ATPase catalytic subunit [Pyrus communis] (GB:BAD90912.1); similar to vacuolar H+-ATPase catalytic subunit [Pyrus communis] (GB:BAD90911.1); similar to H+-exporting ATPase (EC 3.6.3.6), vacuolar, 69K chain - carrot (GB:XPXZV9); similar to V-ATPase catalytic subunit A [Prunus persica] (GB:AAL11505.1); similar to VATA_CITUN Vacuolar ATP synthase catalytic subunit A (V-ATPase A subunit) (Vacuolar proton pump alpha subunit) (V-ATPase 69 kDa subunit) (GB:Q9SM09); contains InterPro domain H+-transporting two-sector ATPase, alpha/beta subunit, C-terminal (InterPro:IPR000793); contains InterPro domain H+-transporting two-sector ATPase, alpha/beta subunit, N-terminal (InterPro:IPR004100); contains InterPro"
 /db_xref="GeneID:844228"

VHA-B At1g76030 4691H1

MASCOT Mascot Search Results

Protein View

Match to: gi|15222929; Score: 127
ATP binding / hydrogen-exporting ATPase, phosphorylative mechanism / hydrogen-transporting ATP syntNominal mass (M_r): 54188; Calculated pI value: 4.98
NCBI BLAST search of gi|15222929 against nr
Unformatted [sequence listing](#) for pasting into other applicationsTaxonomy: [Arabidopsis thaliana](#)

Links to retrieve other entries containing this sequence from NCBI Entrez:

[gi|21928027](#) from [Arabidopsis thaliana](#)[gi|20453110](#) from [Arabidopsis thaliana](#)[gi|27735259](#) from [Arabidopsis thaliana](#)

Fixed modifications: Carbamidomethyl (C)

Variable modifications: Oxidation (M)

Cleavage by Trypsin: cuts C-term side of KR unless next residue is P

Number of mass values searched: 84

Number of mass values matched: 22

Sequence Coverage: 57%

Matched peptides shown in **Bold Red**

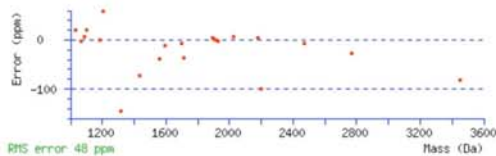
1 MGTNDLDIEE GTLEIGMEYR TVSGVAGPLV ILDKVKGPKY QEIVNIRLGD
51 GSTRRQVLVE VDGEKAVVQV FEQTSQIDNK FTTVQFTGEV LKTPVSLDML
 101 GRIFNOSKRP IDNSGPIPLP AYLDSIGSSI NPSREKTFPE HQQGISITID
 151 VMNSIARGQK IPLFRAAGLP HNEIAAQICR QAGLVKRLK TVDLEDHGE
 201 DNFAIVFAAM GVMETAQFF KRDFEENGSM ERVTLFLNLA NQPTFRIIT
 251 PRILATTAAY LAYECQKRVL VILTMSSYA DALREVSAAR EEVPGRRQTF
301 GYMTDLATL YERAGRIEGR KGSITQIPL TPNDITHP TPDLTGIIYE
351 QYIYDRLH HRIPIPIV LFLSRLKMS AIGEGKEDK HSDVSNQLYA
 401 NYAIKDVQA MKAVVGEAL SSEDLLLEF LDKFERKFM QGAYDRNIF
451 QSLDLAWTL RIFFBELLR IPAKTLDQFY SRDSTS

Show predicted peptides also

Sort Peptides By Residue Number Increasing Mass Decreasing Mass

Start - End	Observed	Mr (expt)	Mr (calc)	Delta	Miss	Sequence
37 - 47	1316.54	1315.53	1315.72	-0.19	1	GPKYQEVNIR
66 - 80	1563.74	1562.73	1562.79	-0.06	0	AVVQVFEVTSQIDNK
93 - 102	1088.58	1087.58	1087.57	0.01	0	TPVSLDMLGR
93 - 102	1104.59	1103.59	1103.56	0.02	0	TPVSLDMLGR Oxidation (M)
103 - 135	3454.47	3453.46	3453.74	-0.28	0	IFNCSGKPIDNPPILPEAVLDISGSSINPBER
136 - 157	2469.18	2468.17	2468.19	-0.02	0	TYPEMIQTGISTIDVNSIAR
161 - 180	2178.16	2177.15	2177.14	0.01	0	IPLFRAAGLPVNEIAAQICR
233 - 247	1715.87	1714.86	1714.93	-0.06	0	VTLFLNLANPTFIER
253 - 267	1702.82	1701.81	1701.83	-0.01	0	IALLTAAYLAYECGK
268 - 284	1904.00	1902.99	1902.99	0.00	0	HVLVILTMSSYADALR
298 - 313	1912.88	1911.87	1911.87	-0.00	0	GYPGYMTDLATYER
298 - 313	1928.87	1927.86	1927.87	-0.00	0	GYPGYMTDLATYER Oxidation (M)
363 - 376	1596.89	1595.88	1595.90	-0.02	0	QIYPPINVLPLSR
380 - 389	1065.53	1064.53	1064.53	-0.00	1	SAIGEGRTRK Oxidation (M)
389 - 406	2023.00	2021.99	2021.98	0.01	1	KIHSDVSNQLYANYAIGK
390 - 406	1894.90	1893.89	1893.89	0.01	0	DHSDVSNQLYANYAIGK
413 - 436	2772.32	2771.31	2771.39	-0.08	1	AVVGEALSSDLLLEFLDKFER
438 - 447	1187.55	1186.54	1186.54	-0.00	0	FVMQGYDTR
438 - 447	1203.62	1202.61	1202.54	0.07	0	FVMQGYDTR Oxidation (M)
448 - 465	2203.02	2202.01	2202.23	-0.22	1	NIPQSLDLAWTLRIIFR
471 - 482	1438.67	1437.66	1437.76	-0.10	1	IPAKTLDQFYR
475 - 482	1029.52	1028.51	1028.49	0.02	0	TLDQFYR

No match to: 809.50, 897.44, 918.42, 967.47, 973.52, 995.51, 999.45, 1036.54, 1070.52, 1074.54, 1095.55, 1109.51, 1128.59, 1136.68, 1141.53, 1157.57, 1172.34, 12



LOCUS NP_177729 486 aa linear PLN 09-JUN-2006
 DEFINITION ATP binding / hydrogen-exporting ATPase, phosphorylative mechanism / hydrogen-transporting ATP synthase, rotational mechanism / hydrogen-transporting ATPase, rotational mechanism [Arabidopsis thaliana].
 ACCESSION NP_177729
 VERSION NP_177729.1 GI:15222929
 DBSOURCE REFSEQ: accession NM_106251.2
 KEYWORDS .
 SOURCE Arabidopsis thaliana (thale cress)
 ORGANISM Arabidopsis thaliana
 Eukaryota; Viridiplantae; Streptophyta; Embryophyta; Tracheophyta; Spermatophyta; Magnoliophyta; eudicotyledons; core eudicotyledons; rosids; eurosids II; Brassicales; Brassicaceae; Arabidopsis.
 COMMENT PROVISIONAL REFSEQ: This record has not yet been subject to final NCBI review. The reference sequence was derived from AT1G76030.lp.
 Method: conceptual translation.
 FEATURES
 source 1..486
 /organism="Arabidopsis thaliana"
 /db_xref="taxon:3702"
 /chromosome="1"
 /ecotype="Columbia"
 Protein 1..486
 /product="ATP binding / hydrogen-exporting ATPase, phosphorylative mechanism / hydrogen-transporting ATP synthase, rotational mechanism / hydrogen-transporting ATPase, rotational mechanism"
 /calculated_mol_wt=53977
 Region 13..482
 /region_name="HtpB"
 /note="Archaeal/vacuolar-type H-ATPase subunit B [Energy production and conversion]; COG1156"
 /db_xref="COG:31356"

DET3 At1g12840 10610

Protein Identification Report



Sample 6 Hit 2

Protein Information

Protein name:	DET3 (DE-ETIOLATED 3) [Arabidopsis thaliana]
Alphalyse number:	ALPHA04960
GI-number:	gi 18391442
MW:	42593
pI:	5,4
Mascot score:	101
Sequence coverage:	41%

Analysis Information

- In-gel digestion, cleavage by Trypsin: cuts C-term side of KR unless next residue is P
- MS analysis method: MALDI-TOF peptide mass fingerprint and MALDI-TOF/TOF peptide sequencing
- Variable modifications: Carbamidomethyl (C), Oxidation (M)
- Database search program: Mascot version 1.9.03
- Peptide Tolerance: 60 ppm
- Allowed up to 1 miscleavage
- Database: NRDB (3946334 protein sequences)

Protein sequence

Matched peptides shown in bold underline

1 MTSRYWVSL PVKDSASSLW **NRLQEQISKH SFDTEVYRFN IPNLRVGTLD**
 51 SLLALGDDLL KSNSEVVEGVS **QKIRRQIBEL ERISGVESNA LITDGVVSDS**
 101 **YLTRFVWDEA** KYPTMSPLKE **VVDNIQSQVA** KIEDDLKVRV AEYNNIRGQL
 151 **NAINRKQSGS** LAVRDLSNLV KPEDIVESEH **LVTELLAVVEK YSQKDWLACY**
 201 **ETLTDYVUPR** SSKKLFEDNE **YALYTVLFT** RVADNFRFAA REKGFQVDF
 251 **EQSVEAQETR** KQELAKLVQD **QESLRSSLLQ** WCYTSYGEVF SSMHFCAVR
 301 **TPAESIMRYG** LPPAFLACVL **SPAVKSEKKV** RSLERLCDS TNSLYWKSEE
 351 DAGAMAGLAG DSETHPVVVF TINLA

Peptides used for identification

Start - End	Observed Mr(expt)	Mr(calc)	Delta	Miss	Sequence
14 - 22	1035,52	1034,51	1034,48	0,03	0 DSASSLWNR
30 - 38	1121,55	1120,55	1120,53	0,02	0 HSFDTEVYR (Ions score 3)
39 - 45	873,50	872,49	872,49	0,01	0 FNIPNLR (Ions score 7)
83 - 104	2292,22	2291,21	2291,16	0,05	0 ISGVESNALTVDGVVSDSYLTR
105 - 111	894,43	893,43	893,43	0,00	0 FVWDEAK
120 - 131	1329,66	1328,65	1328,69	-0,04	0 EVVDNIQSQVAK
148 - 155	885,51	884,50	884,48	0,02	0 GQLNAINR
148 - 156	1013,55	1012,54	1012,58	-0,04	1 GQLNAINRK (Ions score 2)
195 - 213	2246,19	2245,18	2245,07	0,11	1 DWLACYETLTDYVVPSSK
215 - 231	2095,04	2094,03	2094,03	0,00	0 LPEDNEYALYTVLFTTR
249 - 260	1438,64	1437,64	1437,64	0,00	0 DFEQSVEAQETR (Ions score 36)
267 - 275	1087,54	1086,53	1086,57	-0,03	0 LVQDQESLR
301 - 308	970,48	969,47	969,46	0,01	0 TPAESIMR Oxidation (M)
309 - 325	1802,92	1801,91	1801,98	-0,07	0 YGLPFAFLACVLSPAVK Carbamidomethyl (C)

E 5. Mass spectrometry data of VHA-a3-GFP interacting proteins

VHA-H At3g42050 10632

Protein Identification Report

Order 10632



Sample 6 Hit 1

Protein Information

Protein name:	ATP binding / hydrogen-transporting ATP synthase, rotational mechanism / hydrogen-transporting ATPase, rotational mechanism [Arabidopsis thaliana]
Alphalyse number:	ALPHA05216
GI-number:	gi 15228443
MW:	50253
pI:	6,58
Mascot score:	149
Sequence coverage:	37%

Analysis Information

- In-gel digestion, cleavage by Trypsin: cuts C-term side of KR unless next residue is P
- MS analysis method: MALDI-TOF peptide mass fingerprint and MALDI-TOF/TOF peptide sequencing
- Variable modifications: Carbamidomethyl (C), Oxidation (M)
- Database search program: Mascot version 1.9.03
- Peptide Tolerance: 60 ppm
- Allowed up to 1 miscleavage
- Database: NRDB (3946334 protein sequences)

Protein sequence

Matched peptides shown in bold underline

```

1 MDQAELSIEQ VLKRDIPWET YMNTKLVS AK GLQLRRYDK KPESARAQLL
51 DEDGPAYVHL FVSILRDIK EETVEYVLAL IYEMLSANPT RARLFHDESL
101 ANEDTYEPFL RLLWGNWFI QEKSCKILAW IISARPKAGN AVINGIDDV
151 LKGLVEWLCA QLKQPSHPTR GVPIAISCLS SLLEKEPVRS SFVQADGVKL
201 LVPLISPAST QSQIQLLYET CLCIWLLSY EPAIEYLATS RTMQRLTEVV
251 KHSTKEKVVV VVILTFRNLL PKGTFGAQMV DLGLPHIHS LKTQAWSDED
301 LLDALNQLLE GLKDKIKKLS SFDKYKQEV L LGHLDWNPMH KETNFWRENV
351 TCFEENDFQI LRVLLTILDT SSDPRSLAVA CFDISQFIQY HAAGRVIVAD
401 LKAKERVMKL INHENAETVK NAILCIQRLL LGAKYASFLQ A

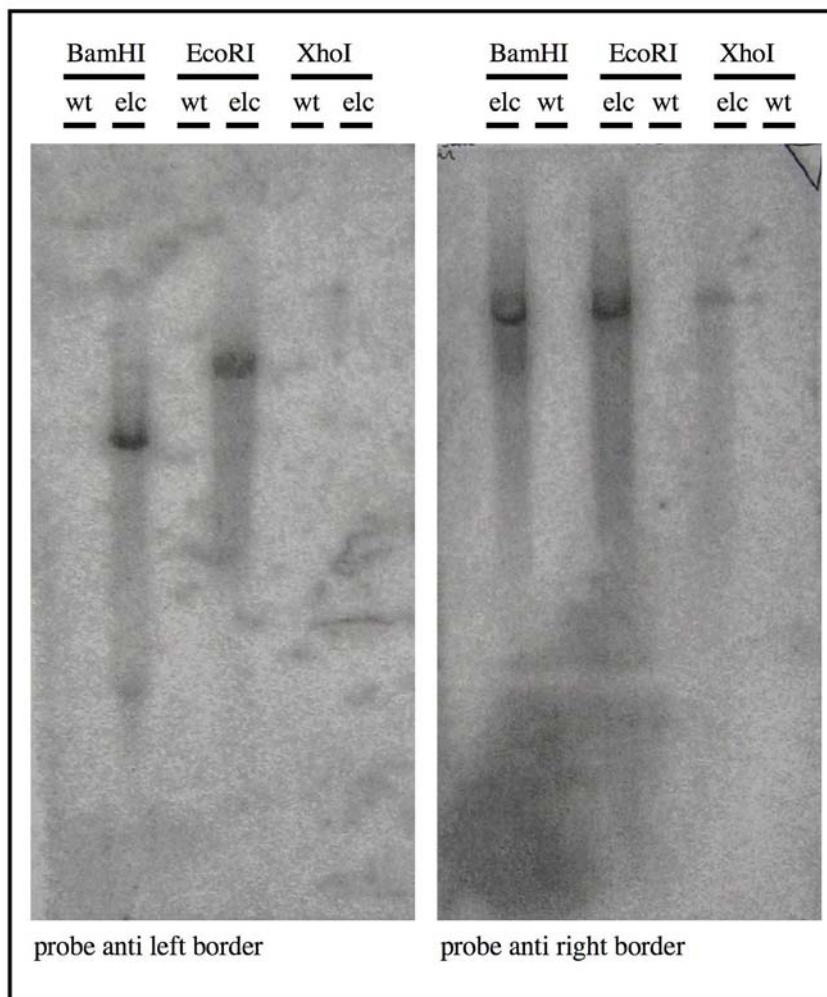
```

Peptides used for identification

Start - End	Observed Mr(expt)	Mr(calc)	Delta	Miss	Sequence
15 - 25	1413,63	1412,62	1412,63	-0,01	0 DIPWETYMNTK Oxidation (M)
94 - 111	2196,01	2195,00	2195,02	-0,01	0 LFHDESLANEDTYEPFLR
116 - 123	1021,50	1020,50	1020,50	-0,01	0 GNWFIQEK
138 - 152	1455,74	1454,74	1454,77	-0,04	0 AGNAVINGIDDV LK
171 - 184	1457,78	1456,77	1456,83	-0,06	0 GVPIAISCLSSLLK Carbamidomethyl (C)
190 - 199	1037,50	1036,49	1036,52	-0,03	0 SSFVQADGVK
261 - 267	847,55	846,54	846,53	0,01	0 VVILTFR
273 - 292	2150,11	2149,10	2149,14	-0,03	0 GTFGAQMVDLGLPHIHS LK Oxidation (M)
342 - 347	852,43	851,42	851,39	0,03	0 ETNFWR
348 - 362	1913,84	1912,83	1912,86	-0,03	0 ENVTCFEENDFQILR Carbamidomethyl (C) (Ions score 67)
363 - 375	1429,77	1428,76	1428,78	-0,02	0 VLLTILDTSSDPR (Ions score 12)
376 - 395	2254,15	2253,14	2253,10	0,04	0 SLAVACFDISQFIQYHAAGR Carbamidomethyl (C)
421 - 428	987,54	986,53	986,53	0,00	0 NAILCIQR Carbamidomethyl (C) (Ions score 12)

E 6. Number of *T-DNA* insertions in the used *elch* mutant line

Southern blotting and hybridisation was performed by a student of the University of Tübingen as part of a student practical laboratory course supervised by Dr. Swen Schellmann.



The *elch* mutant line harbours only one *T-DNA* insertion.

DNA from *wild type* and *elch* was digested with *EcoRI*, *BamHI* and *XhoI* and separated by agarose gelelectrophoresis. After southern blotting the DNA was hybridised with probes specific for *left* and *right border* of the *T-DNA*. The result indicates that only one *T-DNA* insertions causes the observed mutation and the phenotype

F. Literature

- Ahmed, S. U., Bar-Peled, M. and Raikhel, N. V.** (1997). Cloning and subcellular location of an Arabidopsis receptor-like protein that shares common features with protein-sorting receptors of eukaryotic cells. *Plant Physiol* **114**, 325-36.
- Albertson, R., Riggs, B. and Sullivan, W.** (2005). Membrane traffic: a driving force in cytokinesis. *Trends Cell Biol* **15**, 92-101.
- Arai, H., Terres, G., Pink, S. and Forgac, M.** (1988). Topography and subunit stoichiometry of the coated vesicle proton pump. *J Biol Chem* **263**, 8796-802.
- Babst, M.** (2005). A protein's final ESCRT. *Traffic* **6**, 2-9.
- Babst, M., Katzmann, D. J., Estepa-Sabal, E. J., Meerloo, T. and Emr, S. D.** (2002a). Escrt-III: an endosome-associated heterooligomeric protein complex required for mvb sorting. *Dev Cell* **3**, 271-82.
- Babst, M., Katzmann, D. J., Snyder, W. B., Wendland, B. and Emr, S. D.** (2002b). Endosome-associated complex, ESCRT-II, recruits transport machinery for protein sorting at the multivesicular body. *Dev Cell* **3**, 283-9.
- Babst, M., Odorizzi, G., Estepa, E. J. and Emr, S. D.** (2000). Mammalian tumor susceptibility gene 101 (TSG101) and the yeast homologue, Vps23p, both function in late endosomal trafficking. *Traffic* **1**, 248-58.
- Bache, K. G., Slagsvold, T., Cabezas, A., Rosendal, K. R., Raiborg, C. and Stenmark, H.** (2004). The growth-regulatory protein HCRP1/hVps37A is a subunit of mammalian ESCRT-I and mediates receptor down-regulation. *Mol Biol Cell* **15**, 4337-46.
- Bankaitis, V. A., Johnson, L. M. and Emr, S. D.** (1986). Isolation of yeast mutants defective in protein targeting to the vacuole. *Proc Natl Acad Sci U S A* **83**, 9075-9.
- Banta, L. M., Robinson, J. S., Klionsky, D. J. and Emr, S. D.** (1988). Organelle assembly in yeast: characterization of yeast mutants defective in vacuolar biogenesis and protein sorting. *J Cell Biol* **107**, 1369-83.
- Bethke, P. C., Hillmer, S. and Jones, R. L.** (1996). Isolation of Intact Protein Storage Vacuoles from Barley Aleurone (Identification of Aspartic and Cysteine Proteases). *Plant Physiol* **110**, 521-529.
- Bilodeau, P. S., Urbanowski, J. L., Winistorfer, S. C. and Piper, R. C.** (2002). The Vps27p Hse1p complex binds ubiquitin and mediates endosomal protein sorting. *Nat Cell Biol* **4**, 534-9.
- Bilodeau, P. S., Winistorfer, S. C., Kearney, W. R., Robertson, A. D. and Piper, R. C.** (2003). Vps27-Hse1 and ESCRT-I complexes cooperate to increase efficiency of sorting ubiquitinated proteins at the endosome. *J Cell Biol* **163**, 237-43.
- Bishop, N., Horman, A. and Woodman, P.** (2002). Mammalian class E vps proteins recognize ubiquitin and act in the removal of endosomal protein-ubiquitin conjugates. *J Cell Biol* **157**, 91-101.
- Bishop, N. and Woodman, P.** (2001). TSG101/mammalian VPS23 and mammalian VPS28 interact directly and are recruited to VPS4-induced endosomes. *J Biol Chem* **276**, 11735-42.
- Bowman, E. J. and Bowman, B. J.** (2000). Cellular role of the V-ATPase in *Neurospora crassa*: analysis of mutants resistant to concanamycin or lacking the catalytic subunit A. *J Exp Biol* **203**, 97-106.
- Chen, L., Shinde, U., Ortolan, T. G. and Madura, K.** (2001). Ubiquitin-associated (UBA) domains in Rad23 bind ubiquitin and promote inhibition of multi-ubiquitin chain assembly. *EMBO Rep* **2**, 933-8.
- Clague, M. J., Urbe, S., Aniento, F. and Gruenberg, J.** (1994). Vacuolar ATPase activity is required for endosomal carrier vesicle formation. *J Biol Chem* **269**, 21-4.

- Clough, S. J. and Bent, A. F.** (1998). Floral dip: a simplified method for *Agrobacterium*-mediated transformation of *Arabidopsis thaliana*. *Plant J* **16**, 735-43.
- Combet, C., Blanchet, C., Geourjon, C. and Deleage, G.** (2000). NPS@: network protein sequence analysis. *Trends Biochem Sci* **25**, 147-50.
- Dettmer, J., Hong-Hermesdorf, A., Stierhof, Y. D. and Schumacher, K.** (2006). Vacuolar H⁺-ATPase activity is required for endocytic and secretory trafficking in *Arabidopsis*. *Plant Cell* **18**, 715-30.
- Dettmer, J., Schubert, D., Calvo-Weimar, O., Stierhof, Y. D., Schmidt, R. and Schumacher, K.** (2005). Essential role of the V-ATPase in male gametophyte development. *Plant J* **41**, 117-24.
- Dobrzynski, J. K., Sternlicht, M. L., Farr, G. W. and Sternlicht, H.** (1996). Newly-synthesized beta-tubulin demonstrates domain-specific interactions with the cytosolic chaperonin. *Biochemistry* **35**, 15870-82.
- Edgar, B. A. and Orr-Weaver, T. L.** (2001). Endoreplication cell cycles: more for less. *Cell* **105**, 297-306.
- Feng, G. H., Lih, C. J. and Cohen, S. N.** (2000). TSG101 protein steady-state level is regulated posttranslationally by an evolutionarily conserved COOH-terminal sequence. *Cancer Res* **60**, 1736-41.
- Folkers, U., Berger, J. and Hulskamp, M.** (1997). Cell morphogenesis of trichomes in *Arabidopsis*: differential control of primary and secondary branching by branch initiation regulators and cell growth. *Development* **124**, 3779-86.
- Folkers, U., Kirik, V., Schobinger, U., Falk, S., Krishnakumar, S., Pollock, M. A., Oppenheimer, D. G., Day, I., Reddy, A. S., Jurgens, G. et al.** (2002). The cell morphogenesis gene *ANGUSTIFOLIA* encodes a CtBP/BARS-like protein and is involved in the control of the microtubule cytoskeleton. *Embo J* **21**, 1280-8.
- Forgac, M.** (1999). Structure and properties of the vacuolar (H⁺)-ATPases. *J Biol Chem* **274**, 12951-4.
- Frattoni, A., Orchard, P. J., Sobacchi, C., Giliani, S., Abinun, M., Mattsson, J. P., Keeling, D. J., Andersson, A. K., Wallbrandt, P., Zecca, L. et al.** (2000). Defects in TCIRG1 subunit of the vacuolar proton pump are responsible for a subset of human autosomal recessive osteopetrosis. *Nat Genet* **25**, 343-6.
- Futter, C. E., Pearse, A., Hewlett, L. J. and Hopkins, C. R.** (1996). Multivesicular endosomes containing internalized EGF-EGF receptor complexes mature and then fuse directly with lysosomes. *J Cell Biol* **132**, 1011-23.
- Galbraith, D. W., Harkins, K. R. and Knapp, S.** (1991). Systemic endopolyploidy in *Arabidopsis thaliana*. *Plant Physiology* **96**, 985-989.
- Garrus, J. E., von Schwedler, U. K., Pornillos, O. W., Morham, S. G., Zavitz, K. H., Wang, H. E., Wettstein, D. A., Stray, K. M., Cote, M., Rich, R. L. et al.** (2001). Tsg101 and the vacuolar protein sorting pathway are essential for HIV-1 budding. *Cell* **107**, 55-65.
- Geisler, M., Nadeau, J. and Sack, F. D.** (2000). Oriented asymmetric divisions that generate the stomatal spacing pattern in *Arabidopsis* are disrupted by the too many mouths mutation. *Plant Cell* **12**, 2075-86.
- Geisler, M., Yang, M. and Sack, F. D.** (1998). Divergent regulation of stomatal initiation and patterning in organ and suborgan regions of the *Arabidopsis* mutants too many mouths and four lips. *Planta* **205**, 522-30.
- Geuze, H. J., Slot, J. W., Strous, G. J., Lodish, H. F. and Schwartz, A. L.** (1983). Intracellular site of asialoglycoprotein receptor-ligand uncoupling: double-label immunoelectron microscopy during receptor-mediated endocytosis. *Cell* **32**, 277-87.
- Geyer, M., Yu, H., Mandic, R., Linnemann, T., Zheng, Y. H., Fackler, O. T. and Peterlin, B. M.** (2002). Subunit H of the V-ATPase binds to the medium chain of adaptor protein complex 2 and connects Nef to the endocytic machinery. *J Biol Chem* **277**, 28521-9.

- Giebel, B. and Wodarz, A.** (2006). Tumor suppressors: control of signaling by endocytosis. *Curr Biol* **16**, R91-2.
- Glotzer, M.** (2001). Animal cell cytokinesis. *Annu Rev Cell Dev Biol* **17**, 351-86.
- Herz, H. M., Chen, Z., Scherr, H., Lackey, M., Bolduc, C. and Bergmann, A.** (2006). vps25 mosaics display non-autonomous cell survival and overgrowth, and autonomous apoptosis. *Development* **133**, 1871-80.
- Hicke, L.** (2001). A new ticket for entry into budding vesicles-ubiquitin. *Cell* **106**, 527-30.
- Hirata, T., Iwamoto-Kihara, A., Sun-Wada, G. H., Okajima, T., Wada, Y. and Futai, M.** (2003). Subunit rotation of vacuolar-type proton pumping ATPase: relative rotation of the G and C subunits. *J Biol Chem* **278**, 23714-9.
- Hugdahl, J. D. and Morejohn, L. C.** (1993). Rapid and Reversible High-Affinity Binding of the Dinitroaniline Herbicide Oryzalin to Tubulin from *Zea mays* L. *Plant Physiol* **102**, 725-740.
- Hulskamp, M.** (2004). Plant trichomes: a model for cell differentiation. *Nat Rev Mol Cell Biol* **5**, 471-80.
- Hulskamp, M., Misera, S. and Jürgens, G.** (1994). Genetic dissection of trichome cell development in *Arabidopsis*. *Cell* **76**, 555-566.
- Ilgenfritz, H., Bouyer, D., Schnittger, A., Mathur, J., Kirik, V., Schwab, B., Chua, N. H., Jürgens, G. and Hulskamp, M.** (2003). The *Arabidopsis* STICHEL gene is a regulator of trichome branch number and encodes a novel protein. *Plant Physiol* **131**, 643-55.
- Johnson, L. M., Bankaitis, V. A. and Emr, S. D.** (1987). Distinct sequence determinants direct intracellular sorting and modification of a yeast vacuolar protease. *Cell* **48**, 875-85.
- Jordan, A., Hadfield, J. A., Lawrence, N. J. and McGown, A. T.** (1998). Tubulin as a target for anticancer drugs: agents which interact with the mitotic spindle. *Med Res Rev* **18**, 259-96.
- Jürgens, G.** (2005). Cytokinesis in higher plants. *Annu Rev Plant Biol* **56**, 281-99.
- Kane, P. M.** (1999). Introduction: V-ATPases 1992-1998. *J Bioenerg Biomembr* **31**, 3-5.
- Katzmann, D. J., Babst, M. and Emr, S. D.** (2001). Ubiquitin-dependent sorting into the multivesicular body pathway requires the function of a conserved endosomal protein sorting complex, ESCRT-I. *Cell* **106**, 145-55.
- Katzmann, D. J., Odorizzi, G. and Emr, S. D.** (2002). Receptor downregulation and multivesicular-body sorting. *Nat Rev Mol Cell Biol* **3**, 893-905.
- Katzmann, D. J., Stefan, C. J., Babst, M. and Emr, S. D.** (2003). Vps27 recruits ESCRT machinery to endosomes during MVB sorting. *J Cell Biol* **162**, 413-23.
- Kawasaki-Nishi, S., Bowers, K., Nishi, T., Forgac, M. and Stevens, T. H.** (2001). The amino-terminal domain of the vacuolar proton-translocating ATPase a subunit controls targeting and in vivo dissociation, and the carboxyl-terminal domain affects coupling of proton transport and ATP hydrolysis. *J Biol Chem* **276**, 47411-20.
- Kim, G. T., Shoda, K., Tsuge, T., Cho, K. H., Uchimiya, H., Yokoyama, R., Nishitani, K. and Tsukaya, H.** (2002). The *ANGUSTIFOLIA* gene of *Arabidopsis*, a plant CtBP gene, regulates leaf-cell expansion, the arrangement of cortical microtubules in leaf cells and expression of a gene involved in cell-wall formation. *Embo J* **21**, 1267-79.
- Kirik, V., Grini, P. E., Mathur, J., Klinkhammer, I., Adler, K., Bechtold, N., Herzog, M., Bonneville, J. M. and Hulskamp, M.** (2002). The *Arabidopsis* TUBULIN-FOLDING COFACTOR A gene is involved in the control of the alpha/beta-tubulin monomer balance. *Plant Cell* **14**, 2265-76.
- Klionsky, D. J. and Emr, S. D.** (1990). A new class of lysosomal/vacuolar protein sorting signals. *J Biol Chem* **265**, 5349-52.
- Klionsky, D. J., Nelson, H. and Nelson, N.** (1992a). Compartment acidification is required for efficient sorting of proteins to the vacuole in *Saccharomyces cerevisiae*. *J Biol Chem* **267**, 3416-22.

- Klionsky, D. J., Nelson, H., Nelson, N. and Yaver, D. S.** (1992b). Mutations in the yeast vacuolar ATPase result in the mislocalization of vacuolar proteins. *J Exp Biol* **172**, 83-92.
- Kluge, C., Seidel, T., Bolte, S., Sharma, S. S., Hanitzsch, M., Satiat-Jeunemaitre, B., Ross, J., Sauer, M., Gollack, D. and Dietz, K. J.** (2004). Subcellular distribution of the V-ATPase complex in plant cells, and in vivo localisation of the 100 kDa subunit VHA-a within the complex. *BMC Cell Biol* **5**, 29.
- Koncz, C., Martini, N., Mayerhofer, R., Koncz-Kalman, Z., Korber, H., Redei, G. P. and Schell, J.** (1989). High-frequency T-DNA-mediated gene tagging in plants. *Proc Natl Acad Sci U S A* **86**, 8467-71.
- Kostelansky, M. S., Sun, J., Lee, S., Kim, J., Ghirlando, R., Hierro, A., Emr, S. D. and Hurley, J. H.** (2006). Structural and functional organization of the ESCRT-I trafficking complex. *Cell* **125**, 113-26.
- Lenz, J. H., Schuchardt, I., Straube, A. and Steinberg, G.** (2006). A dynein loading zone for retrograde endosome motility at microtubule plus-ends. *Embo J* **25**, 2275-86.
- Lewis, S. A., Tian, G., Vainberg, I. E. and Cowan, N. J.** (1996). Chaperonin-mediated folding of actin and tubulin. *J Cell Biol* **132**, 1-4.
- Lu, Q., Hope, L. W., Brasch, M., Reinhard, C. and Cohen, S. N.** (2003). TSG101 interaction with HRS mediates endosomal trafficking and receptor down-regulation. *Proc Natl Acad Sci U S A* **100**, 7626-31.
- Lu, X., Yu, H., Liu, S. H., Brodsky, F. M. and Peterlin, B. M.** (1998). Interactions between HIV1 Nef and vacuolar ATPase facilitate the internalization of CD4. *Immunity* **8**, 647-56.
- Ludueno, R. F. and Roach, M. C.** (1991). Tubulin sulfhydryl groups as probes and targets for antimitotic and antimicrotubule agents. *Pharmacol Ther* **49**, 133-52.
- Lupas, A., Van Dyke, M. and Stock, J.** (1991). Predicting coiled coils from protein sequences. *Science* **252**, 1162-4.
- Martin, L., Fanarraga, M. L., Aloria, K. and Zabala, J. C.** (2000). Tubulin folding cofactor D is a microtubule destabilizing protein. *FEBS Lett* **470**, 93-5.
- Mathur, J. and Chua, N. H.** (2000). Microtubule stabilization leads to growth reorientation in Arabidopsis trichomes. *Plant Cell* **12**, 465-77.
- Mathur, J., Mathur, N. and Hulskamp, M.** (2002). Simultaneous visualization of peroxisomes and cytoskeletal elements reveals actin and not microtubule-based peroxisome motility in plants. *Plant Physiol* **128**, 1031-45.
- Mathur, J., Mathur, N., Kernebeck, B. and Hulskamp, M.** (2003). Mutations in actin-related proteins 2 and 3 affect cell shape development in Arabidopsis. *Plant Cell* **15**, 1632-45.
- Matsuoka, K., Higuchi, T., Maeshima, M. and Nakamura, K.** (1997). A Vacuolar-Type H⁺-ATPase in a Nonvacuolar Organelle Is Required for the Sorting of Soluble Vacuolar Protein Precursors in Tobacco Cells. *Plant Cell* **9**, 533-546.
- Mellman, I.** (1996a). Endocytosis and molecular sorting. *Annu Rev Cell Dev Biol* **12**, 575-625.
- Mellman, I.** (1996b). Membranes and sorting. *Curr Opin Cell Biol* **8**, 497-8.
- Morano, K. A. and Klionsky, D. J.** (1994). Differential effects of compartment deacidification on the targeting of membrane and soluble proteins to the vacuole in yeast. *J Cell Sci* **107** (Pt 10), 2813-24.
- Mulholland, J., Konopka, J., Singer-Kruger, B., Zerial, M. and Botstein, D.** (1999). Visualization of receptor-mediated endocytosis in yeast. *Mol Biol Cell* **10**, 799-817.
- Nacry, P., Mayer, U. and Jurgens, G.** (2000). Genetic dissection of cytokinesis. *Plant Mol Biol* **43**, 719-33.
- Nadeau, J. A. and Sack, F. D.** (2002). Control of stomatal distribution on the Arabidopsis leaf surface. *Science* **296**, 1697-700.
- Nebenfuhr, A., Frohlick, J. A. and Staehelin, L. A.** (2000). Redistribution of Golgi stacks and other organelles during mitosis and cytokinesis in plant cells. *Plant Physiol* **124**, 135-51.

- Nishi, T. and Forgac, M.** (2002). The vacuolar (H⁺)-ATPases--nature's most versatile proton pumps. *Nat Rev Mol Cell Biol* **3**, 94-103.
- Odorizzi, G., Babst, M. and Emr, S. D.** (1998). Fab1p PtdIns(3)P 5-kinase function essential for protein sorting in the multivesicular body. *Cell* **95**, 847-58.
- Otegui, M. and Staehelin, L. A.** (2000). Cytokinesis in flowering plants: more than one way to divide a cell. *Curr Opin Plant Biol* **3**, 493-502.
- Otegui, M. S., Mastronarde, D. N., Kang, B. H., Bednarek, S. Y. and Staehelin, L. A.** (2001). Three-dimensional analysis of syncytial-type cell plates during endosperm cellularization visualized by high resolution electron tomography. *Plant Cell* **13**, 2033-51.
- Paris, N. and Neuhaus, J. M.** (2002). BP-80 as a vacuolar sorting receptor. *Plant Mol Biol* **50**, 903-14.
- Patnaik, A., Chau, V. and Wills, J. W.** (2000). Ubiquitin is part of the retrovirus budding machinery. *Proc Natl Acad Sci U S A* **97**, 13069-74.
- Pearse, B. M. and Robinson, M. S.** (1990). Clathrin, adaptors, and sorting. *Annu Rev Cell Biol* **6**, 151-71.
- Pickart, C. M. and Rose, I. A.** (1985). Functional heterogeneity of ubiquitin carrier proteins. *J Biol Chem* **260**, 1573-81.
- Pineda-Molina, E., Belrhali, H., Piefer, A. J., Akula, I., Bates, P. and Weissenhorn, W.** (2006). The crystal structure of the C-terminal domain of Vps28 reveals a conserved surface required for Vps20 recruitment. *Traffic* **7**, 1007-16.
- Pornillos, O., Garrus, J. E. and Sundquist, W. I.** (2002). Mechanisms of enveloped RNA virus budding. *Trends Cell Biol* **12**, 569-79.
- Prescianotto-Baschong, C. and Riezman, H.** (2002). Ordering of compartments in the yeast endocytic pathway. *Traffic* **3**, 37-49.
- Qian, J., Yang, J., Zhang, X., Zhang, B., Wang, J., Zhou, M., Tang, K., Li, W., Zeng, Z., Zhao, X. et al.** (2001). Isolation and characterization of a novel cDNA, UBAP1, derived from the tumor suppressor locus in human chromosome 9p21-22. *J Cancer Res Clin Oncol* **127**, 613-8.
- Raymond, C. K., Howald-Stevenson, I., Vater, C. A. and Stevens, T. H.** (1992). Morphological classification of the yeast vacuolar protein sorting mutants: evidence for a prevacuolar compartment in class E vps mutants. *Mol Biol Cell* **3**, 1389-402.
- Razi, M. and Futter, C. E.** (2006). Distinct roles for Tsg101 and Hrs in multivesicular body formation and inward vesiculation. *Mol Biol Cell* **17**, 3469-83.
- Robinson, J. S., Klionsky, D. J., Banta, L. M. and Emr, S. D.** (1988). Protein sorting in *Saccharomyces cerevisiae*: isolation of mutants defective in the delivery and processing of multiple vacuolar hydrolases. *Mol Cell Biol* **8**, 4936-48.
- Rothman, J. E. and Schmid, S. L.** (1986). Enzymatic recycling of clathrin from coated vesicles. *Cell* **46**, 5-9.
- Rusinova, E., Borst, J. W., Kwaaitaal, M., Cano-Delgado, A., Yin, Y., Chory, J. and de Vries, S. C.** (2004). Heterodimerization and endocytosis of Arabidopsis brassinosteroid receptors BRI1 and AtSERK3 (BAK1). *Plant Cell* **16**, 3216-29.
- Samuels, A. L., Giddings, T. H., Jr. and Staehelin, L. A.** (1995). Cytokinesis in tobacco BY-2 and root tip cells: a new model of cell plate formation in higher plants. *J Cell Biol* **130**, 1345-57.
- Sancho, E., Vila, M. R., Sanchez-Pulido, L., Lozano, J. J., Paciucci, R., Nadal, M., Fox, M., Harvey, C., Bercovich, B., Loukili, N. et al.** (1998). Role of UEV-1, an inactive variant of the E2 ubiquitin-conjugating enzymes, in in vitro differentiation and cell cycle behavior of HT-29-M6 intestinal mucosecretory cells. *Mol Cell Biol* **18**, 576-89.
- Schiff, P. B., Fant, J. and Horwitz, S. B.** (1979). Promotion of microtubule assembly in vitro by taxol. *Nature* **277**, 665-7.

- Schnittger, A., Schobinger, U., Stierhof, Y. D. and Hulskamp, M.** (2002). Ectopic B-type cyclin expression induces mitotic cycles in endoreduplicating *Arabidopsis* trichomes. *Curr Biol* **12**, 415-20.
- Schumacher, K.** (2006). Endomembrane proton pumps: connecting membrane and vesicle transport. *Curr Opin Plant Biol*.
- Schumacher, K., Vafeados, D., McCarthy, M., Sze, H., Wilkins, T. and Chory, J.** (1999). The *Arabidopsis* *det3* mutant reveals a central role for the vacuolar H(+)-ATPase in plant growth and development. *Genes Dev* **13**, 3259-70.
- Segui-Simarro, J. M., Austin, J. R., 2nd, White, E. A. and Staehelin, L. A.** (2004). Electron tomographic analysis of somatic cell plate formation in meristematic cells of *Arabidopsis* preserved by high-pressure freezing. *Plant Cell* **16**, 836-56.
- Segui-Simarro, J. M. and Staehelin, L. A.** (2005). Cell cycle-dependent changes in Golgi stacks, vacuoles, clathrin-coated vesicles and multivesicular bodies in meristematic cells of *Arabidopsis thaliana*: A quantitative and spatial analysis. *Planta*, 1-14.
- Staehelin, L. A. and Hepler, P. K.** (1996). Cytokinesis in higher plants. *Cell* **84**, 821-4.
- Steinborn, K., Maulbetsch, C., Priester, B., Trautmann, S., Pacher, T., Geiges, B., Kuttner, F., Lepiniec, L., Stierhof, Y.-D., Schwarz, H. et al.** (2002a). The *Arabidopsis* PILZ group genes encode tubulin-folding cofactor orthologs required for cell division but not cell growth. *Genes and Development* **16**, 959-971.
- Steinborn, K., Maulbetsch, C., Priester, B., Trautmann, S., Pacher, T., Geiges, B., Kuttner, F., Lepiniec, L., Stierhof, Y. D., Schwarz, H. et al.** (2002b). The *Arabidopsis* PILZ group genes encode tubulin-folding cofactor orthologs required for cell division but not cell growth. *Genes Dev* **16**, 959-71.
- Stevens, T. H. and Forgac, M.** (1997). Structure, function and regulation of the vacuolar (H+)-ATPase. *Annu Rev Cell Dev Biol* **13**, 779-808.
- Strompen, G., Dettmer, J., Stierhof, Y. D., Schumacher, K., Jurgens, G. and Mayer, U.** (2005). *Arabidopsis* vacuolar H-ATPase subunit E isoform 1 is required for Golgi organization and vacuole function in embryogenesis. *Plant J* **41**, 125-32.
- Sze, H., Schumacher, K., Muller, M. L., Padmanaban, S. and Taiz, L.** (2002). A simple nomenclature for a complex proton pump: VHA genes encode the vacuolar H(+)-ATPase. *Trends Plant Sci* **7**, 157-61.
- Thompson, B. J., Mathieu, J., Sung, H. H., Loeser, E., Rorth, P. and Cohen, S. M.** (2005). Tumor suppressor properties of the ESCRT-II complex component Vps25 in *Drosophila*. *Dev Cell* **9**, 711-20.
- Tian, G., Huang, Y., Rommelaere, H., Vandekerckhove, J., Ampe, C. and Cowan, N. J.** (1996). Pathway leading to correctly folded beta-tubulin. *Cell* **86**, 287-96.
- Trowbridge, I. S., Collawn, J. F. and Hopkins, C. R.** (1993). Signal-dependent membrane protein trafficking in the endocytic pathway. *Annu Rev Cell Biol* **9**, 129-61.
- Urbanowski, J. L. and Piper, R. C.** (2001). Ubiquitin sorts proteins into the intraluminal degradative compartment of the late-endosome/vacuole. *Traffic* **2**, 622-30.
- Vaccari, T. and Bilder, D.** (2005). The *Drosophila* tumor suppressor *vps25* prevents nonautonomous overproliferation by regulating notch trafficking. *Dev Cell* **9**, 687-98.
- Valls, L. A., Hunter, C. P., Rothman, J. H. and Stevens, T. H.** (1987). Protein sorting in yeast: the localization determinant of yeast vacuolar carboxypeptidase Y resides in the propeptide. *Cell* **48**, 887-97.
- van der Bliek, A. M., Redelmeier, T. E., Damke, H., Tisdale, E. J., Meyerowitz, E. M. and Schmid, S. L.** (1993). Mutations in human dynamin block an intermediate stage in coated vesicle formation. *J Cell Biol* **122**, 553-63.
- Vitale, A. and Galili, G.** (2001). The endomembrane system and the problem of protein sorting. *Plant Physiol* **125**, 115-8.

-
- Vitale, A. and Raikhel, N. V.** (1999). What do proteins need to reach different vacuoles? *Trends Plant Sci* **4**, 149-155.
- Walker, J. D., Oppenheimer, D. G., Concienne, J. and Larkin, J. C.** (2000). SIAMESE, a gene controlling the endoreduplication cell cycle in *Arabidopsis thaliana* trichomes. *Development* **127**, 3931-40.
- Wilkins, M. R., Lindskog, I., Gasteiger, E., Bairoch, A., Sanchez, J. C., Hochstrasser, D. F. and Appel, R. D.** (1997). Detailed peptide characterization using PEPTIDEMASS--a World-Wide-Web-accessible tool. *Electrophoresis* **18**, 403-8.
- Winter, V. and Hauser, M. T.** (2006). Exploring the ESCRTing machinery in eukaryotes. *Trends Plant Sci* **11**, 115-23.
- Zambryski, P., Joos, H., Genetello, C., Leemans, J., Montagu, M. V. and Schell, J.** (1983). Ti plasmid vector for the introduction of DNA into plant cells without alteration of their normal regeneration capacity. *Embo J* **2**, 2143-2150.

Zusammenfassung

Innerhalb des Sekretorischen Systems von Hefen und Tieren reguliert der Endosomal Sorting Complex Required for Transport (ESCRT) wichtige Aufgaben. Dazu gehört die Sortierung von Biosynthese-Produkten und die Regulation von Plasma Membran Rezeptoren. Das Ziel meiner Doktorarbeit war die Untersuchung des ELCH Proteins aus *Arabidopsis* welches Ähnlichkeit zu Vps23p und TSG101 aufweist. Diese Proteine bilden die Kernkomponenten des ESCRT-I Komplexes in Hefen und Tieren. Ich konnte zeigen, dass die Ubiquitinbindung und Komplexbildung zwischen *Arabidopsis*, Hefen und Tieren konserviert ist. Dies stützt die These, dass die ESCRT vermittelte Proteinsortierung eine allgemeine Strategie eukaryontischer Organismen ist. Mit ELCH bzw. ESCRT-I interagierende Proteine wurden durch Immunoprecipitation und anschließender Massenspektrometrie identifiziert. Mit dieser Vorgehensweise wurde ein Protein mit Ubiquitin-Assoziierter Domäne, sowie mehrere Untereinheiten der vakuolären ATPase isoliert. Die VHA-a3 Untereinheit der vakuolären ATPase wurde genauer auf eine mögliche Modifizierung mit Ubiquitin untersucht da Mono-Ubiquitinierung das Erkennungssignal des ESCRT Proteinsortierungsweges ist. Mittels Infrarot Fluoreszenz konnte gezeigt werden das VHA-a3 mono-ubiquitiniert wird was darauf hindeutet das dieses Protein von den ESCRT Komplexen sortiert wird. Die vakuoläre ATPase ist, ähnlich wie die ESCRT Komplexe, an der Sortierung von Biosynthese-Produkten und der Regulation von Plasma Membran Rezeptoren beteiligt. Eine Interaktion zwischen einem ESCRT Komplex und der V-ATPase konnte bisher nicht gezeigt werden.

Eine T-DNA Insertion im ELCH Gen von *Arabidopsis* führt dazu, dass eine geringe Anzahl von Zellen mehr als einen Zellkern aufweisen. Da mehrkernige Zellen auf Zellteilungsdefekte hinweisen, wurden Trichome, Blattepidermiszellen und Stomata auf unvollständige Zellwände untersucht. Diese konnten in Stomata und Blattepidermiszellen nachgewiesen werden, nicht aber in Trichomen. Zellteilungsdefekte wurden bisher nicht in *vps23* Mutanten beobachtet, sie erinnern jedoch an mehrkernige Zellen welche in TSG101 mutanten Zelllinien vorhanden sind. Ferner sind *Arabidopsis* Linien, die Mutationen in der Untereinheit E der vakuolären ATPase aufweisen, embryonal lethal. Sie zeigen Zellteilungsdefekte, sowie eine gestörte Vakuolen Morphologie (Strompen et al., 2005). Obwohl Mutationen in *ELCH*, *TSG101* und *VHA-E* ähnliche Phänotypen hervorrufen, konnte bisher nicht ermittelt werden warum Störungen des ESCRT Systems oder der vakuolären ATPase zu Zellteilungsdefekten führen. Genetische Analysen mit der *tubulin-folding cofactor A* (*tfc-a*) Mutante legen nahe,

dass ELCH die Zellteilung durch Regulation von Mikrotubuli beeinflusst. Zellteilung in Pflanzen ist im hohen Maße von einer pflanzenspezifischen Struktur, dem Phragmoplast abhängig. Dessen Hauptbestandteile sind Mikrotubuli und Vesikel. Störungen im Zusammenspiel dieser Komponenten können mit hoher Wahrscheinlichkeit zu den beobachteten Zellteilungsdefekten führen.

Erklärung

Ich versichere, dass ich die von mir vorgelegte Dissertation selbständig angefertigt, die benutzten Quellen und Hilfsmittel vollständig angegeben und die Stellen der Arbeit – einschließlich Tabellen, Karten und Abbildungen –, die anderen Werken im Wortlaut oder dem Sinn nach entnommen sind, in jedem Einzelfall als Entlehnung kenntlich gemacht habe; dass diese Dissertation noch keiner anderen Fakultät oder Universität zur Prüfung vorgelegen hat; dass sie – abgesehen von unten angegebenen Teilpublikationen – noch nicht veröffentlicht worden ist sowie, daß ich eine solche Veröffentlichung vor Abschluß des Promotionsverfahrens nicht vornehmen werde. Die von mir vorgelegte Dissertation ist von Prof. Dr. Martin Hülskamp betreut worden.

Christoph Spitzer

Veröffentlichungen

The *Arabidopsis elch* mutant reveals functions of an ESCRT component in cytokinesis
Christoph Spitzer, Swen Schellmann, Aneta Sabovljevic, Mojgan Shahriari, Channa Keshavaiah,
Nicole Bechtold, Michel Herzog, Stefan Müller, Franz-Georg Hanisch, and Martin Hülskamp
Development 2006 **133**: 4679-4689.

Lebenslauf

Persönliche Angaben:

Nachname, Vorname: Spitzer, Christoph
Geburtsdatum: 09.04.1975
Geburtsort: Lünen (NRW)
Eltern: Vater : Spitzer Peter
Mutter: Spitzer Irene, geb. Harder
Staatsangehörigkeit: deutsch
Familienstand: ledig
Anschrift: 50674 Köln
Rathenauplatz 6

Schulausbildung:

1981 – 1984 Grundschule Nörvenich (NRW)
1984 – 1992 Gymnasium am Wirteltor in Düren (NRW)
1992 – 1995 Deutsche Schule London (GB)

Hochschulausbildung:

Oktober 1995 – Februar 1996 Mathematik Studium in Köln

Wehrdienst:

März 1996 – Juli 1997

Hochschulausbildung:

Oktober 1997 – Oktober 1998 Geographie Studium in Köln
Oktober 1998 – Oktober 2001 Biologie Studium in Köln
Oktober 2001 – Oktober 2002 Diplomarbeit am Botanischen Institut der
Universität zu Köln AG Hülskamp
05. September 2002 Diplomprüfung in Biologie
Oktober 2002 – Januar 2007 Doktorarbeit am Botanischen Institut der
Universität zu Köln AG Hülskamp

Vortrag im Rahmen eines Workshops auf dem Arabidopsis meeting 2004 in Berlin

Titel: *Vacuolar protein degradation in plants: a conserved Vps23 dependent pathway?*
